AMINO ACIDS IN COPPER DEPOSITION

AMINO ACIDS AS ADDITIVES IN COPPER ELECTRODEPOSITION

by

Robert James Gale

A thesis submitted to the Faculty of Graduate Studies and Research in partial fulfilment of the requirements for the degree of Doctor of Philosophy.

From the Physical Chemistry Laboratory under the supervision of Professor C.A.Winkler.

McGill University,
Montreal, Canada.

August, 1972

Department of Chemistry

R.J.Gale

Ph.D.

AMINO ACIDS AS ADDITIVES IN COPPER ELECTRODEPOSITION

ABSTRACT

The addition agent behaviours of cystine and methionine were studied by radioisotopic and galvanostatic overpotential measurements. There appeared to be major discrepancies between the extents of surface coverages estimated from overpotential increments by simple site-blocking theory and from occlusion rates determined by radioisotopic techniques. The mean rate of adsorption of methionine corresponded closely to the mean rates of occlusion during electrodeposition in the c.d. range 0.25 - 3 A dm^{-2}. There was a maximum in its occlusion rate at ≈ 5 A dm^{-2}. Exchange reactions in the absence and presence of oxygen indicated Cu(I) complexes to be the major species adsorbed. The rates of occlusion of cystine indicated a rapid, reversible reduction to cysteine and its subsequent occlusion as Cu(I) complex. Morphologies of the deposits for various conditions are described and a mechanism suggested for initiation of pyramidal deposition.

Cu(II) and Cu(I) complexes of some related amino acids were prepared and their characterizations attempted, with a view to assessing the likelihood that they might function as effective addition agents.

ACKNOWLEDGEMENTS

I am pleased to acknowledge the award of a demonstratorship by McGill University during 1968 and the award of Scholarships during the period 1969-1972 by the National Research Council of Canada.

I am also grateful to Dr.G.Donnay (Crystallography Department, McGill University) for the use of facilities, and for considerable personal assistance, that enabled x-ray diffraction experiments to be made with cupric penicillamine disulphide complexes; and to Dr.R.St.J.Manley of the Pulp and Paper Institute, McGill University, who very kindly provided the electron microscope photographs. I also acknowledge gratefully the assistance of Mr.J.Klinger during the acid-base studies. Finally, I am indebted to Julia Mary, my wife, for typing the manuscript of this thesis.

TABLE OF CONTENTS

PAGE

INTRODUCTION

At present, the deposition of copper from cupric sulphate-sulphuric acid baths is widely used for electroplating, electroforming, electrowinning and refining, and for the manufacture of copper powder. Historically, these applications resulted from a number of classical investigations of copper deposition, including those of Grotthus in 1806, and of Faraday in 1832, the first commercial electroplating operations by Bessemer, De la Rue, and the Elkingtons in the 1830s (1,2), Jacobi's electrotyping patent of 1840 (3), and the commencement of electrochemical copper refining in 1869 by James Elkington. About the year 1845, it was observed that "bright copper" electrodeposits were obtained (4) whenever a large number of wax moulds, which had been phosphorized with a solution of phosphorus in carbon bisulphide, were put into acid copper baths. Soon, addition agents or additives were added purposely to the electrodeposition baths to improve the surface smoothness, the brightness, the hardness, and the grain size of deposits, or to increase the limiting current density and to reduce dendritic formations.

Usually, the choice of suitable addition agents has been made empirically. Many hundreds of addition agents

have now been studied, patented, and applied to the deposition of copper. Originally, colloidal materials were found to offer the greatest promise as addition agents (4,5) and the reducing properties of the additive (6), or its ability to form complexes with the metal ions were regarded as mainly responsible for its beneficial effects. These early attempts to establish precise classification of additives in terms of molecular properties such as structure and functional groups were invariably unsuccessful (7). Discordant effects, often revealed by substances with slight structural differences, support the notion that highly selective interactions are involved in these processes. This is illustrated by the relative large differences displayed by similar amino acids in their abilities to increase the cathodic polarisation (8,9), or to modify internal stresses of deposits (10). The data to be presented in this thesis will provide further evidence for the high degree of specificity to be encountered in the behaviour of sulphur-containing amino acids as addition agents. In general, each system and additive has to be evaluated on an individual basis. There is still no simple theory that can correlate satisfactorily the remarkable specificities and addition agent abilities of certain organic compounds with their molecular structures. Indeed, it is currently acknowledged that relatively little is

understood of the way in which addition agents may be involved in the consecutive steps during the electrocrystallisation of metals at solid electrodes (11,12). This is hardly surprising, perhaps, when it is realized that even the basic aspects of electrodeposition mechanisms in the absence of additives are controversial. For example, there is yet no unequivocal resolution of such problems as the relative extents to which deposition of reduced metal ions occurs at the growth sites, from either the solution phase directly or by diffusion as ad-atoms on the crystal plane surfaces (13-18). Similarly, little progress has been made in understanding the factors that govern the morphology of crystals formed by electrocrystallisation.

Absolute quantitative measures for all of the manifold physical properties of the electrodeposit, and perhaps for those of the electrolyte too, would be required to assess fully the efficacy of a compound as an addition agent. Together with the range of operating conditions, possibilities of chemical changes that may occur and effects due to trace impurities that may be present, these total to a formidable set of variables. Accordingly, the most convenient way to categorize addition agents is by reference to their prime function in operation. The major industrial uses of addition agents in copper electroplating are for leveling and brightening electrodeposits, and

theories to account for these effects have been developed, as outlined later. It is not possible, within the limited scope of this thesis, to survey all the practical and theoretical aspects pertaining to the use of addition agents in acid copper deposition, but the reader may be referred to excellent review articles by Kardos and Foulke (19) and Kruglikov (20), and to the many references mentioned therein, which treat the definitions, terminologies, and effects of additives on leveling and brightening. Theories to account for electrocrystallisation and for the behaviour of additives (inhibitors) upon morphologies of electrodeposits are to be found in the textbooks of Raub and Müller (12), Bockris and Razumney (14), and Fischer (21).

Little is known regarding the dependence of addition agent action on parameters such as current density, bulk concentration of additive, temperature and pH of the electrolyte, etc., because few quantitative determinations have been made of actual surface concentrations of additives during electrodeposition. Extremely low concentrations of addition agents are often sufficient to achieve the modification(s) that is required to the deposit or to the deposition process and, therefore, the concentrations are difficult to measure. In part, this thesis seeks to provide analytical data, from which estimates might be

made of the rates and extents of adsorption of some amino acid addition agents at copper electrodes in acid copper sulphate electrolytes. Both open-circuit and electrodeposition conditions were employed. For particular systems, the data are applied to examine effects produced by these addition agents on cathodic polarisations and on deposit morphologies, in terms of the appropriate theories that were available.

LEVELING AND BRIGHTENING ACTIONS

Leveling and brightening phenomena are fundamentally associated with those parameters which determine the current distribution and the processes of crystal growth on an electrode. This is because, broadly speaking, the current distribution at the surface will control the local growth rates of the electrodeposit. The current distribution which would result if polarisation were considered to be absent at a metallic electrode is known as the primary current distribution (PCD). If the counter-electrode is at a distance such that the equipotential lines of the electric field are able to become independent of the shape of the electrode profile, the PCD will depend directly on the profile shape (19,20,22). Dirichlet boundary conditions then apply and the local current, i, in the solution near

the electrode is determined by

$$i = -\chi \left| \frac{d\psi}{dn} \right|$$

where χ is the electrolytic conductivity and $|d\psi/dn|$ is the magnitude of the local potential gradient (n is the outwardly directed normal to the equipotential surface at the given point). The PCD is identical on different sized electrodes having a specific geometrical configuration.

Depending on the experimental conditions, the heterogeneous electrodeposition reaction must produce at an electrode, to varying degrees, overpotentials due to charge transfer, diffusion, reaction, and crystallisation, as well as resistance polarisation (23). As a consequence, the actual current distribution that prevails, called the secondary current distribution (SCD), becomes a function of the nature of the cathodic polarisation and the species discharged, the magnitude of the current density, the scale of the roughness profile, and whether or not additives are present. Variations in local current efficiencies and non-uniformities arising from polycrystallinity may also influence the SCD. The former is particularly important during the deposition of nickel, owing to the concurrent evolution of hydrogen; it is of relatively little significance during the deposition of copper. If the

sizes of individual crystals can be neglected relative to other roughness factors, an experimental leveling rate of a saw-tooth groove may be determined in comparison with a so-called "natural" or "geometrical" leveling rate, to obtain a figure for the micro-throwing power of a particular electrolyte. The term geometrical leveling is used to describe the leveling obtained from a uniform current density distribution.

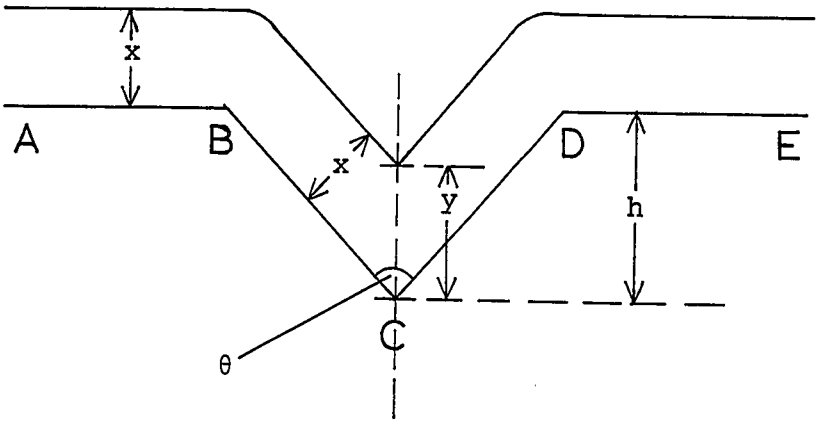

In the diagram, a uniform deposit of thickness x covers the surfaces, AB and DE, and walls, BC and CD, of a groove section, ABCDE (the treatment neglects effects at the sharp edges B, C, and D). The deposit thickness, y, at the

bottom of the groove is related to the thickness x by

$$y = x/\sin\frac{\theta}{2}$$

Consequently, a groove of depth h will disappear completely when the deposit thickness becomes x' if

$$y' = x' + h$$

$$\text{i.e. } x' = h/[(1/\sin\tfrac{\theta}{2}) - 1]$$

"True" leveling is said to occur when the current density effective in the groove, BCD, is greater than on the surface edges, AB and DE. The micro-throwing power, P, may be defined by the expression

$$P = \frac{y'}{x'} \sin\frac{\theta}{2}$$

For P>1, true leveling will occur. However, deviations from the theoretical leveling expressions are commonplace. Attempts to measure true leveling are discussed in depth by Kruglikov (20).

Two theories have been advanced to explain the action of leveling additives: (i) Adsorption theory, according to which the additive is preferentially adsorbed on micropeaks of a rough cathode, so that metal deposition

is inhibited there, and the current density, hence rate of deposition, becomes relatively higher in the microrecesses. The general theoretical basis for adsorption of organic compounds at electrodes can be found in the textbooks of Conway (24), Gileadi (25), and Damaskin, Petrii, and Batrakov (26). Beacom and Riley (27), and others (19), have provided evidence for adsorption at preferred sites using radioisotopic techniques. For example, nickel foils were plated to thicknesses in the range 0.0005-0.0025 in. on grooved cathodes (depth, h = 0.030in., included angle of groove, $\theta = 90°$), from a Watts type nickel plating bath containing the radioactive leveler, sodium allyl sulphonate-^{35}S (27). When autoradiographic film was then exposed to the flattened foils, darker bands appeared on the autoradiograms in places corresponding to the originally more elevated ridges of the cathode profile. (ii) Diffusion theory, based on the observation that leveling additives are often occluded and consumed fairly rapidly at the cathode. The SCD necessary for leveling is thought to arise from non-uniformities in the thickness and composition of the diffusion layer immediately adjacent to the cathode. The rate of consumption of additive is supposedly greater at thin sections of the diffusion layer i.e. at "peaks" on the surface, and diffusion of additive from micro-recesses towards regions of lower concentration at micro-

peaks results in a relatively higher SCD, hence more deposition, in the microrecesses. Inhibition by adsorbed additive at the micropeaks may complement this mechanism.

It is well established that the leveling and the brightening actions of additives are not correlative. Often applied in conjunction with leveling agents, brighteners usually decrease the degree of leveling. Effective copper brighteners e.g. thiourea, sulphonated acetylthiourea, acetylcyanamide etc., increase the specular reflectance of the surface by reducing the sub-microscopic irregularities on the crystal planes. A quantitative geometrical condition for surface brightness is (28)

$$\lambda\alpha = 2H \cos \theta$$

where λ is the wavelength of the light incident on the surface at angle θ to the normal, α a constant $\simeq 0.1$, and H is the height of the surface protrusions. For a mirror-like brightness, the protrusions should be about 1/20 the wavelength of light i.e. for λ = 500 nM, H $\simeq$ 25 nM.

Randomization of crystal growth and grain refinement (decrease of crystal size) are thought to be contributory factors to brightening action. Grain refining has been attributed to increased nucleation on the mid-planes of crystallographic faces, brought about when inhibitors are

adsorbed on the edges, kinks, grain boundaries, etc.. Highly specific mechanisms, invoking current-density-sensitive, site-sensitive, or shape-sensitive adsorption (29), seem most probable when strong brightening occurs with additives present in low concentrations (10^{-5}M). Diffusional disparities, as postulated in leveling action, could be responsible for the action of those brighteners that are used in much higher concentrations (e.g. thiourea, coumarin).

ADSORPTION IN ELECTRODEPOSITION

Few quantitative determinations have been made of the adsorption of organic substances during electrodeposition (19,26). Highly sensitive analytical techniques are required since extremely low concentrations of additives are able to cause profound changes in the electro-crystallisation processes. For example, Bockris et al (30) have shown that bulk concentrations of as little as 10^{-9} M n-decylamine were able to modify the morphological growth forms on a copper single crystal at a deposition current density of 5 mA cm^{-2}. Ideally, the surface coverages of a single species should be measured during electrodeposition. In practice, data have to be interpreted carefully for, as Kardos and Foulke caution (19), the

additive may be electrolytically and/or chemically decomposed into two or more products with different adsorptivities. Gileadi, Duic, and Bockris (31) have emphasized the usefulness of electrochemical and radioisotopic methods in combination to investigate the surface coverages of species adsorbed at electrodes. Radioisotopic analytical techniques are invaluable in addition agent studies because of their high sensitivity and non-interference with the electrodeposition conditions. Certain electrochemical methods are sufficiently sensitive to determine fractional monolayer quantities of adsorbed compounds, but they often involve electrolytic reduction of the additive. In the presence of excess metal ions, such as are found in electroplating solutions, it may not be possible to distinguish from the total reduction reactions that occur the faradaic yield due to reduction of the additive. If decomposition of an additive is suspected, double radioactive tagging with two-channel counting (e.g. ^{14}C and ^{3}H) can sometimes be used to trace the ultimate disposition of various fragments of the additive molecule.

The electrocapillary method applied to the adsorption of neutral additives, at ideally polarised liquid metal electrodes such as mercury, provides the thermodynamically soundest approach to studying adsorption at electrode-

solution interfaces (24,25,26). At constant temperature and pressure, the Gibbs-Lippmann equation has the form

$$d\sigma = -q_m dE - \sum_i \Gamma_{i,l}\, d\mu_{i,l}$$

where $d\sigma$ is the change in surface tension, $\Gamma_{i,l}$ is the surface excess quantity of component i in the liquid phase, $d\mu_{i,l}$ is the change in the chemical (electrochemical) potential of component i in the liquid phase, q_m is the surface excess charge on the metal electrode, and E is the electrode potential. From the fundamental electrocapillary equation, it follows immediately that

$$-\left(\frac{\partial\sigma}{\partial E}\right)_{\mu_i,T,P} = q_m$$

$$-\left(\frac{\partial^2\sigma}{\partial E^2}\right)_{\mu_i,T,P} = \left(\frac{\partial q_m}{\partial E}\right)_{\mu_i,T,P} = C$$

The electrode potential at which $(\partial\sigma/\partial E)_{\mu_i,T,P} = 0$ is the potential of zero charge (PZC), sometimes denoted E_z. The PZC will be a function of the nature of the metal and of any adsorption of specifically adsorbed ions and/or oriented additive dipoles. The metal-solution potential difference is not necessarily zero at the PZC when $q_m = 0$ on account of adsorbed solvent or additive dipoles, chemisorbed ions, and other factors.

The second derivative of the interfacial tension with respect to the electrode potential is called the differential capacity, C. It is found experimentally that neutral additive molecules reduce the surface tension most at the peaks of the "bell-shaped" electrocapillary curves (σ versus E) i.e. at potentials at or near the PZC. The maximum adsorption is often slightly negative to the PZC, but depends on the nature of the additive molecule. On mercury, for example, aliphatic molecules have their adsorption maxima at potential values negative to the PZC, while aromatic molecules have their adsorption maxima on the positive side. The PZC was displaced to positive values by adsorption of aliphatics and to negative values by aromatics (25).

At solid electrodes, the adsorption behaviour of an organic compound also can be influenced by the metallographic history and the surface heterogeneity of the metal. If the electrodes are non-polarized, the surface coverages may be modified by competitive adsorption of reaction intermediates, gases, water molecules, or ions. Of course, the capillary electrometer cannot be used to study the adsorption of organic additives at solid electrodes and, generally, the number and precision of experimental techniques that are available for such studies are considerably restricted. The major experimental methods

with their limitations are described in references (24) and (26).

For the present study, the simplest radioisotopic procedure was chosen to try to establish the nature, the quantities, and the behaviour of species that are adsorbed on polycrystalline copper foils, or which affect the cathodic reactions during copper deposition from an acid copper sulphate electrolyte with added amino acids. To use this method, the electrode must be placed in an electrolyte with a radioactive additive, withdrawn at an appropriate time, and washed to remove residual electrolyte. On removal of the electrode the adsorption conditions are disturbed and when the electrode is washed, traces of the adsorbate may be lost. The precision of this technique is therefore limited (26). However, it was considered to be adequate for the purposes intended. Generally, fewer assumptions are needed for interpretation of data so obtained than for those from measurements of the usual electrochemical parameters.

In some respects, gelatin would have been an interesting addition agent with which to make the present studies. It was one of the earliest additives used to harden copper electrodeposits and its behaviour has been studied perhaps more extensively than that of any other addition agent (e.g. 32-40). In recent years, however,

it has come into disfavour for practical applications because its degradation products cause brittleness of the deposits (1,41). Moreover, it is not readily available in radioactive form. On the other hand, cystine and methionine have been shown to behave as cathode polarizing agents during copper electrodeposition in much the same way as gelatin (42), and cystine, at least, has found practical application as a nickel brightener (43), while its reduction product, cysteine, has been used in the electrodeposition of rhenium (44), and manganese and manganese-molybdenum alloys (45). Because of their availability with various radioisotopes and their relatively simple molecular structures, cystine and methionine were chosen for much of the present work.

While no studies of the adsorption of cystine or methionine at copper electrodes were found in the chemical literature, Pradac and Koryta (46) have measured the coverage-time curves of cystine-^{35}S (bulk concentration 10^{-4} M in N H_2SO_4) on pre-heated platinum and gold electrodes. Their investigations, by radioisotope and cyclic voltammetry techniques, were instigated because previous attempts by others to establish a standard reduction-oxidation potential for the cystine/cysteine couple at these solid electrodes had been unsuccessful. They found that the extent of open-circuit adsorption on

Pt increased slowly, to reach about 2×10^{-10} mole cm^{-2} in 15 minutes (a factor of 3.0 was assumed for the surface roughness). The corresponding coverage figure for gold was slightly lower than for platinum, but the adsorption occurred much more rapidly. No desorption of the radioisotope ^{35}S was found from either platinum or gold at 0.4 - 0.65 V versus normal hydrogen electrode (NHE) in a cystine-free, deaerated electrolyte. They concluded that cystine probably dissociates to cysteine, which then forms a strong chemisorption bond to platinum and a weaker bond to gold.

Disparities between the potential of the cystine/cysteine couple and the theoretical Nernst relation have been summarized by Leyko (47), and Cater and Silver (48). The reaction,

$$2RSH \rightleftharpoons RSSR + 2H^+ + 2e$$

would give, replacing activities by concentrations,

$$E = E_0 + \frac{RT}{2F} \ln \frac{[RSSR][H^+]^2}{[RSH]^2}$$

Leyko was unable to account for the potentiometric behaviour of a cystine/cysteine system at copper electrodes if a cysteine-cupric cysteinate equilibrium were assumed,

similar to a cysteine-mercuric cysteinate couple proposed by earlier workers for measurements at mercury electrodes. Determination of the cystine/cysteine standard potential from heats of combustion data gave a value +0.025 V vs. NHE (49). This is in good agreement with the results from a recent kinetic technique which similarly does not rely upon solid electrodes. It involves, instead, analyses of the thiol-disulphide exchange between glutathione (GSH) and cystine or oxidised-glutathione (GSSG) and cysteine. From knowledge of the standard oxidation-reduction potential of GSSG/GSH, a value of +0.02 V vs. NHE was computed for the cystine/cysteine standard potential (50). Hence, cysteine may be oxidised to cystine by cupric ion in aqueous solution and the cuprous ion so formed may then complex with cysteine, under certain experimental conditions, in the reaction

$$2Cu^{2+} + 4RS^{-} \rightleftharpoons RSSR + 2RSCu$$

A polarographic investigation of cuprous cysteinate complexes in ammoniacal medium by Kolthoff and Stricks (51) indicated that the formation of complexes between cuprous cysteinate and cuprous ions might be feasible [Cu^{+}(RSCu) etc.], but that complexes between cuprous cysteinate and cysteine should not be possible.

Miller and Teva (52) have studied the reduction reactions of cystine by potential sweep oscillopolarography. They suggested that mercury cysteinate was formed slowly from cystine by a surface process, the rate of which was controlled by the reactions

$$RSSR + Hg \rightleftharpoons (RS)_2Hg$$

$$(RS)_2Hg + Hg \rightleftharpoons 2RSHg$$

On the other hand, a fast diffusion controlled reaction occurred between mercury and cysteine to form the cysteinate,

$$RSH + Hg \rightleftharpoons RSHg + H^+ + e$$

To resolve the potentiometric behaviour of the cystine/cysteine couple at solid electrodes, it is necessary that the electrode processes and the identities of complex species, such as those postulated above, be determined for the experimental conditions.

As a means of investigating the adsorption behaviour of additives under conditions of copper electrodeposition, the determination of occluded material should indicate the extent to which an additive is irreversibly adsorbed to the electrode. If, however, the additive

species undergoes electrochemical reaction at the surface, both the reactant itself (the additive) and products of the reaction have to be monitored, since they may either be occluded or diffuse back into the bulk electrolyte. Slight amounts of additive may also be occluded into deposits by mechanical trapping in crevices, holes, or grain boundaries (53).

Kochergin and Khonina (54) have used the radioisotopic technique to measure the amounts of ^{35}S occluded in copper deposits from the additives cystine-^{35}S and thiourea-^{35}S as functions of the temperature and current density. The electrolyte comprised 0.534 g L^{-1} cystine in $CuSO_4.5H_2O$ (200 g L^{-1}) and H_2SO_4 (50 g L^{-1}) at 40°C. The temperature dependence experiments showed that sulphur was occluded preferentially at about 50°C in the range 20 - 80°C, but no explanation for this result was suggested. The sulphur content of the electrodeposited copper was found to decrease, from 0.06 to 0.02% by weight, with increase of the current density, from 1.2 to 7.5 A dm^{-2}. A marked decrease in ^{35}S or ^{14}C radioisotopic content of deposits with increasing current density has often been noted (e.g.(12),(55)).

POLARISATION IN THE PRESENCE OF ADDITIVES

Despite numerous studies of changes in the polarisation caused by the presence of additives at an electrode during deposition, the manner by which the polarisation becomes modified is still a matter of great interest (8,9,19,20,42,56). For a particular current density, many organic compounds which are effective as addition agents increase the cathodic polarisation above that obtained in the pure electrolyte. Lahousse and Heerman (57) have recorded cathodic overpotential plots for the steady state and transient galvanostatic depositions of copper with a number of thiocompounds, including methionine and cystine. As previous data had already shown (9,42,58), both of these additives strongly influenced the current density/overpotential characteristics and the surface roughness of copper deposits on polycrystalline foils. At bulk concentrations of 2×10^{-6} M, however, the additives were found to lower slightly the overpotentials from those found in the absence of additives. Of the additives tested, only methionine had, at all concentrations, normal forms for the transient curves i.e. curves similar in form to those obtained in the absence of additive. It was suggested, therefrom, that methionine bonds to the surface more weakly than does cystine.

Various approaches have been taken in attempts to correlate the surface coverage of an addition agent to the magnitude of the polarisation increment, $|\Delta\eta|$. Volk and Fischer (59) have determined differential capacities at electrodes during nickel deposition with the additives 2-butyn-1,4-diol and 2-propyn-1-ol. The strongest decrease of differential capacity, thus the strongest increase of surface coverage, occurred at the lowest current densities. Kruglikov (20) states that, in general, $|\Delta\eta|$ should decrease with increasing current density for a constant thickness of the diffuse layer, but that exceptions are known to this behaviour. He suggests that the decrease in surface coverages at high current densities may be caused by desorption of the additive due to the negative potentials, or to its consumption by occlusion, electrochemical reduction, etc.. An attempt has been made by Kruglikov et al (60) to account for the rate at which thiourea is occluded at a copper rotating disc electrode by applying the concept of a simple blocking action of the adsorbed additive.

This theory has been developed by Sukava and his colleagues (61,62) to correlate the $|\Delta\eta|$ values and the additive adsorbability. They proposed that if a fraction, θ, of the surface becomes blocked by the additive, the true current density, i, will be increased on the uncovered surface to

$$i' = \frac{i}{(1 - \theta)}$$

The assumption is then made that the measured overpotential, η, is made up entirely of the charge-transfer overpotential for cupric ion discharge and that the latter obeys the Tafel equation for the experimental conditions i.e. the contribution of the mean outer Helmholtz plane potential, ψ_1, is neglected. For conditions of high ionic strength, such as prevail generally in acid copper sulphate electrolytes, ψ_1 will be small and will vary little at high values of η (24). In the absence of additive

$$\eta = a - b \ln i$$

In the presence of additive

$$\eta' = a - b \ln i'$$

$$\Delta\eta = b \ln[1/(1 - \theta)]$$

or $$\theta = 1 - \exp[-\Delta\eta/b]$$

If the experimentally determined Tafel slope, b, remains constant in the absence and presence of an inert additive, it seems reasonable to assume that, for liquid metal electrodes, the kinetic parameters of the metal charge-transfer reaction remain uninfluenced by the

addition agent. For example, the transfer coefficient was found to be unaltered for the discharge of Zn(II) at a hanging zinc amalgam electrode in the presence of n-amyl alcohol (63).

Sukava and Chu (61) have measured $|\Delta\eta|$ for a series of straight-chain, carboxylic acid additives during copper deposition from acid copper sulphate electrolytes and have calculated the θ values based on the above expressions. They have then proceeded to deduce standard free energies of adsorption by application of a Langmuir isotherm,

$$\frac{\theta}{(1 - \theta)} = c \cdot \exp\left(\frac{-\Delta G^0_a}{RT}\right)$$

in which θ is the fractional surface coverage, c is the bulk concentration of additive, and ΔG^0_a is the standard free energy of adsorption. Adsorption of each additive molecule was considered to displace n water molecules adsorbed at the electrode surface

$$A_{soln.} + n\ H_2O_{ads.} \rightleftharpoons A_{ads.} + n\ H_2O_{soln.}$$

Straight line plots passing through the origin were obtained from Bockris-Swinkels isotherm plots of $f(\theta)$ against c when n was taken to be 2. Typical net free energies of adsorption at 25° calculated from this model

are -3.8 Kcal $mole^{-1}$ for propanoic acid, -5.6 Kcal $mole^{-1}$ for pentanoic acid, -7.4 Kcal $mole^{-1}$ for heptanoic acid, and -6.3 Kcal $mole^{-1}$ for hexanedioic acid.

This treatment does not attempt to take into account certain considerations that may have important and seriously complicating effects on the adsorption behaviour. (i) Since adsorption equilibrium for the additive may not always be achieved under deposition conditions, if diffusion, or occlusion, or a slow chemical reaction controls the adsorption mechanism, the kinetics of the adsorption process might require detailed examination; (ii) it might not be true, as the model assumes, that all of the surface sites at polycrystalline copper are equivalent for adsorption of the additive and for nucleation by discharged cations; and (iii) in certain regions, the form of the adsorption isotherm for the additive during deposition might be strongly potential dependent. In view of these possible complications, it would seem desirable that the validity of the blocking theory should be examined by applying simultaneously some other experimental method to estimate surface coverages by an additive during electrodeposition (e.g. differential capacity, in situ radioisotopic techniques, etc.). This would seem to be particularly relevant in view of the observation that the blocking theory indicated increased values for θ with

increasing current density (61,62), whereas other methods have often indicated the opposite trend, namely lower coverages at higher current densities. These issues will be discussed later in relation to experimental data for methionine and cystine, where surface coverages by these additives, estimated from experimentally determined occlusion rates, are compared with coverages calculated from $|\Delta\eta|$ values with the straightforward blocking approximation.

MORPHOLOGY AND ELECTROCRYSTALLISATION THEORIES

Observations and measurements of the morphological characteristics of deposits are of fundamental importance in electrodeposition theory, as a reflection of the manner in which the structure of the deposit depends upon the conditions of electrolysis. Experimental data show that the morphology of the deposit may depend on the nature of the metal, the current density, the substrate epitaxy, the types of anions and cations present in the electrolyte, and the influence of additives when these are present (14,18,21,24,30,64-74). The morphologies produced from purified acid copper electrolytes with increase of current density usually progress through stages of layer and ridged-type growths, pyramidal growths, platelets and

truncated pyramids, cubic blocks, and finally to polycrystalline topographies (e.g. 18,30,66,67,71,74,75,76). Additionally, spiral forms are often observed which are thought to arise from screw dislocations present in the crystal lattice (77,78), as well as whiskers, powders, and dendrites which are formed under special conditions of deposition.

The early general theories of crystal growth proposed by Kossel, developed by Stranski, and utilised to discuss electrolytic crystal growth (79), have provided a framework for the development of electrocrystallisation theories by many workers, including Volmer (80), Conway and Bockris (14,81), and Pangarov (82).

In the classical model for crystallisation the growth of flat crystals is ensured by surface diffusion of the species over the atomic planes and their incorporation at kink sites. For metal deposition by this mechanism, an ion is discharged at a flat portion of a crystal face and the so-called ad-atom is then transported by diffusion to a ledge or crystal step where it is incorporated into the lattice. A kink site is sometimes called the half-crystal position and although an atom there has only one-half of the coordination number of an atom in the bulk of the crystal, the energy for an atom in this latter position, from coordination considerations alone,

is equivalent to that for the energy at the kink site. This is because the factor 1/2 arises when considering the net nearest neighbour interactions of atoms in the bulk crystal, as each bond is considered twice (24). In support of this model for electrocrystallisation, Conway and Bockris (81) have attempted to determine the relative activation energies for cation discharge at various sites of a metal surface. Figure 1 depicts a solvated cation attempting to discharge at (a) a plane surface, (b) an edge, and (c) a kink site. It is apparent that, of these three sites, displacement of water molecules of solvation should occur more readily, and the cation approach an atom of the surface more easily, for direct transfer of the cation to the planar surface site (a). However, as the figure illustrates, sites (d) and (e), which have not been considered energetically in previous calculations, possibly are even more accessible to approach by a solvated cation undergoing discharge at an atom of the crystal surface. A discharge mechanism at such sites would support an alternative model that has been proposed to account for electrocrystallisation, in which cations are assumed to undergo simultaneous discharge and lattice incorporation at the half-crystal positions. It should be borne in mind that these a priori models neglect entirely any role that adsorbed solvent molecules or anions may have at the surface.

FIGURE 1

Illustration of cation discharge at various surface sites.

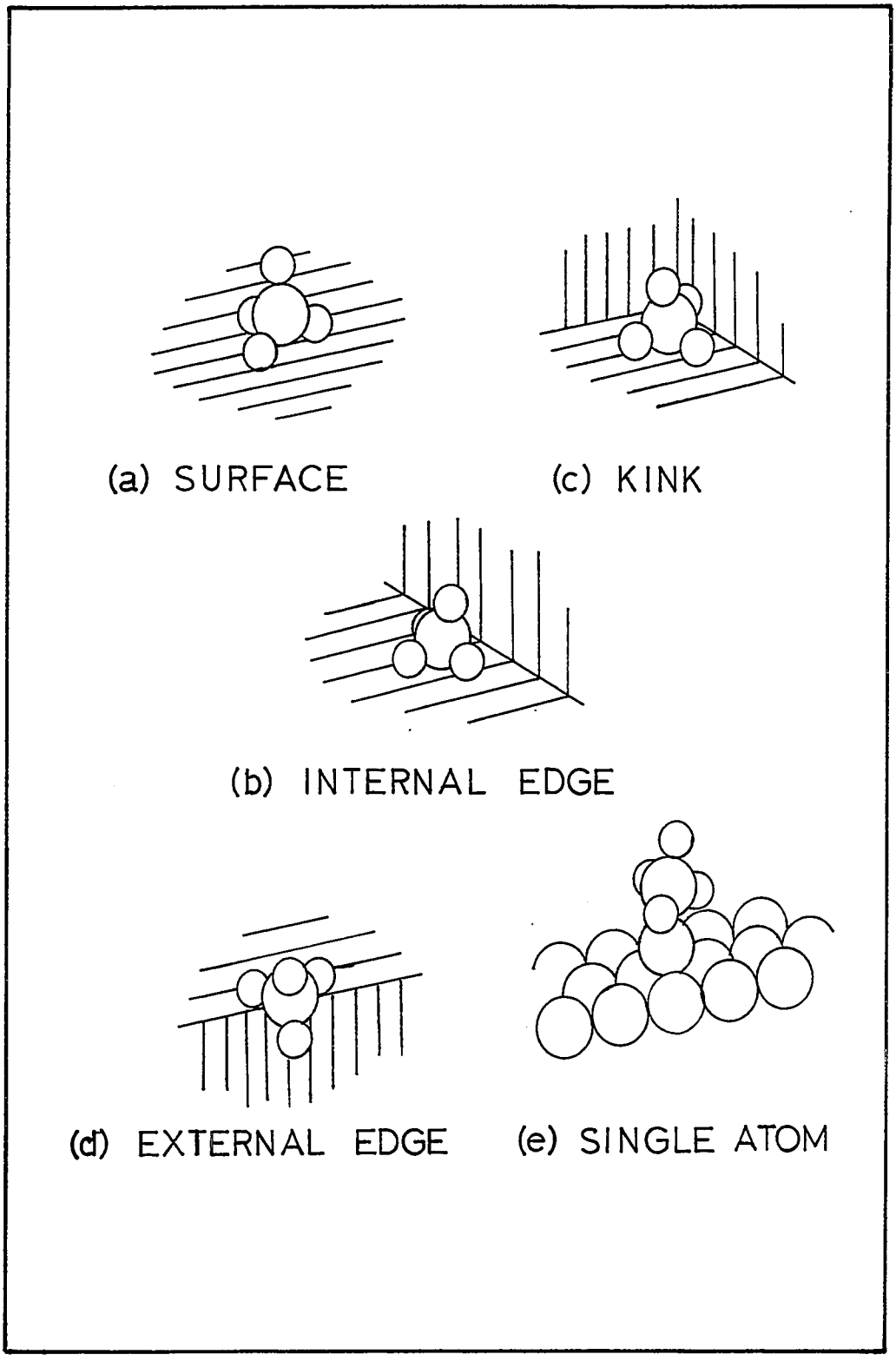
(a) SURFACE
(c) KINK
(b) INTERNAL EDGE
(d) EXTERNAL EDGE
(e) SINGLE ATOM

The latter may be able to facilitate electron transfer by the donor-bridge mechanism i.e. a mechanism similar to the outer-sphere complex electron path for homogeneous electron transfer reactions between solvated metal ions.

Unlike the crystallisation of ionic salts, the growth rates of crystals in electrodeposits are always controlled through the input of electrical energy. Thus, two considerations of Strickland-Constable (83) are applicable to electrocrystallisation; (i) theories that involve restrictions of the crystal growth due to surface diffusion mechanisms, or lattice energy requirements, may frequently be unable to describe adequately the high crystal growth rates observed during electrodeposition; (ii) the growth rate of a flat crystal face will depend only on the rate of initiation of new layers. Whatever the model chosen for electrocrystallisation, it might be expected that, as the current density is increased, a stage will be reached, possibly heralded by the onset of pyramid forms, when the surface diffusion or lateral growth processes are superseded by outward growth or, effectively, random deposition at all sites. Much of the experimental evidence has been interpreted with an emphasis on "lateral" rather than on "vertical" growth processes, whereas morphological observations have indicated that the range of current densities for practical copper deposition is conducive mainly to outward growth of

the crystals, exemplified by pyramids, cubes, blocks, etc..

Bockris et al (30) were the first to measure the growth rates of layers and pyramids. They used {100} faces of copper single crystals and highly purified 0.25 M $CuSO_4$, 0.1 M H_2SO_4 electrolyte. At 5 mA cm^{-2}, the horizontal growth rates of the visible layers were $\simeq 2\times10^{-6}$ cm s^{-1} and those for the sides of pyramids were $\simeq 1\times10^{-6}$ cm s^{-1}. From the horizontal growth rates of the layers (macrosteps), which are generally thought to arise from a bunching action of atomic microsteps, it was calculated that the majority of the crystal growth occurred on the plane areas between the layers. The distances between the macrosteps decreased as the concentration of an additive (n-decylamine) in the solution was increased[†]. The number of pyramids increased from about 10^5 to about 10^6 per cm^2 when the current density was increased from 15 to 20 mA cm^{-2}. It was suggested that the pyramids were initiated when the substrate orientation approached the perfect (100) plane, because then an insufficient number of microsteps would be available as nucleation sites.

On the other hand, Jenkins (76) has emphasized that

[†]Footnote: Fischer and collaborators (75) have proposed that the formation of growth layers from microsteps needs the presence of traces of adsorbable foreign material.

preparation of a nominal crystallographic face is not likely to be more accurate than ±0.1°, and that this small amount of disorientation produces about 10^5 and about 10^7 atomic steps per cm along the [111] and [321] axes, respectively. The formation of pyramids has been observed on copper (100) planes from perchlorate (76) and sulphate (18) electrolytes at current densities in the range, 4-400 μA cm^{-2}. Even at 4 μA cm^{-2}, the pyramids present were calculated to account for approximately 20% of the total volume of material deposited. From consideration of current density/overpotential data for the {111} and {321} faces, it was argued that as the degree of sensitivity to their microstep densities was minimal, the most likely mechanism for crystal growth was direct addition of atoms to random sites. Jenkins proposed, further, that there was no evidence that structural defects played a significant role in either the crystal growth or dissolution processes of these experiments. However, i-η curves at these low current densities were slightly sensitive to the substrate orientation and to the metallographic preparation of the single crystals. Hayashi et al (84) have reported that the concentration of free acid in the electrolytes and the magnitude of the current density can influence the relative cathodic overpotentials at different crystallographic faces.

It should be emphasized that if incorporation of a discharged cation occurs in more or less random manner, as Jenkins has suggested, flat crystal faces must result provided each arriving cation is eventually located in an atomic "monolayer in formation" on the substrate. At 5 mA cm^{-2}, the mean growth rate of atoms at an ideal (100) lattice plane may be estimated as roughly 20 atoms $site^{-1}$ s^{-1} (d_{100} = 0.3615nM), if all atoms in the plane are taken to be equivalent sites. The horizontal growth rate of pyramids reported by Bockris et al (30), $\simeq 1\times10^{-6}$ cm s^{-1}, would represent about 28 atoms $site^{-1}$ s^{-1} of direct, random discharge, which indicates that discharged atoms may not be particularly mobile after arrival at a site on a pyramid. This calculation assumes that pyramids have epitaxy similar to that of the substrate, and this has yet to be studied experimentally. It is interesting to note that pyramids formed in the c.d. range 4-400 μA cm^{-2} (18,78) were found to decrease in size with increase in c.d.. One possible interpretation of this observation is that the increase in c.d. makes the initiation of pyramidal forms increasingly competitive with their growth.

Recent observations of morphologies produced on {100} faces of copper single crystals indicate that pyramid formation occurs at current densities and overpotentials only slightly in excess of the reversible potential. This

perhaps implies that the surface diffusion processes are slow in these systems. No direct experimental measurements are available for the rates of surface diffusion during electrocrystallisation processes. An unresolved problem is whether the pyramidal growths on copper are a consequence of two-dimensional or three-dimensional nucleation. Undoubtedly, much more experimental evidence is needed before even the predominant atomic movements of discharged cations can be correlated with theoretical approaches.

EXPERIMENTAL AND RESULTS

PRELIMINARY EXPERIMENTS

Stabilities of cystine and methionine

It is well known that organic additives in practical electroplating baths must be replenished from time to time, owing to their occlusion or co-precipitation into the metallic deposits (4,19). In some cases, their decomposition may make it necessary to remove decomposition products for continued satisfactory operation of the process. In certain instances, the transformed species are thought to enhance the particular addition agent function sought. Because of these considerations, it seemed desirable to examine the

stabilities of cystine and methionine prior to more detailed investigations of their behaviours as addition agents. Not only were their stabilities to undesirable electrochemical oxidation or reduction a point at issue, but also their stabilities to chemical changes that might occur during storage of electrolytes to which they had been added.

Degradation in storage

Previous studies have shown that cystine is fairly stable to air oxidation in solution with cupric ion and H_2SO_4 (85,86), although cysteic acid or other intermediate oxidation products will accumulate in these solutions over extended periods of storage. For example, about 5% of cystine was lost after 200 days exposure to pure oxygen at 38° from a solution comprising 1.600 g L-cystine in 320 ml 5N H_2SO_4 with 10^{-4} M Cu^{2+} (85). In the present studies no chemical changes for cystine dissolved in the standard electrolyte were found to arise from storage (0-4 weeks), as might be revealed by precipitates, odours, or irreproducibility in polarisation measurements.

Alternatively, selenocystine [D,L-3,3'-diselenobis (2-aminopropanoic acid)] at 5.0×10^{-4} M under comparable conditions yielded a reddish-orange precipitate after short periods of storage, which (i) gave a positive test for Se

in organic matter (87); (ii) extracted into CS_2 and recrystallised as a light red-brown stain; and (iii) changed to grey when oven heated to 130°. From these observations, it is reasonable to conclude that it was the red amorphous variety of elemental selenium produced by acid hydrolysis of the additive. In comparison, hydrolysis of selenocystine by 6M HCl at 110° yields the black vitreous allotrope of selenium (88).

Methionine solutions of concentration 2×10^{-4} M in 1M H_2SO_4, or in the standard electrolyte, developed a slight odour reminiscent of an alkyl sulphide after a few days. The odour increased in intensity with storage time. All experiments with methionine were therefore made promptly after the preparation of its solutions, to minimise its degradation and possible contamination by the products therefrom.

ADSORPTION AND OCCLUSION OF CYSTINE AND METHIONINE ON COPPER

As an essential preliminary to any attempt to describe their addition agent actions quantitatively, measurements were made of the quantities of cystine and methionine adsorbed on open circuit, and during copper deposition. The rate of adsorption of cystine on copper foils was also determined, since it was of interest to

compare this value with its rates of adsorption on platinum and gold electrodes, reported previously as relatively slow processes (46). A further point of interest for a particular additive was the relation between its initial rate of adsorption and its mean rate of occlusion during deposition at various current densities, since little is known about the relation between these two rates.

Apparatus and method

A standard electrolyte was made to contain 125 g L^{-1} $CuSO_4 \cdot 5H_2O$ (analar grade, twice recrystallised from triple distilled water), 100 g L^{-1} conc. H_2SO_4 (analar grade, redistilled), and triple distilled water.

To study the adsorption and occlusion of cystine and methionine, thin copper foils (1.0 cm × 1.0 cm × 0.004 cm; Fisher Scientific Co.) were suspended in 150 ml beakers open to the air and containing fresh, unstirred 50 ml portions of the electrolytes to which the radioactive additives had been added. When the cell was on open circuit, only adsorption of additive on the foil occurred, whereas occlusion of additive in the electrodeposit became possible when the foil was a cathode during flow of current through the cell. For occlusion experiments, the cathode was located between two copper anodes of polycrystalline sheet, 1 cm × 10 cm, each

at a distance of 2 cm from the cathode. Before they were used the cathode foils were degreased, etched in HNO_3/H_2SO_4, washed thoroughly in triple distilled water, and finally rinsed with standard electrolyte. The anodes were similarly treated between each experiment.

The electrolytes were prepared to have a nominal radioactivity of 50 μC L^{-1} (unless otherwise noted), with one of : L-methionine (methyl-^{14}C), D,L-methionine-2-^{14}C, D,L-cystine-3-^{14}C (all from Int. Chem. and Nucl. Corp.), D,L-cystine-1-^{14}C (New England Nucl. Co.), or L-cystine-^{35}S (Amersham Searle Corp.). They were diluted as required with D,L-methionine or L-cystine (Fisher Scientific Co.). Bulk concentrations of additives were weighed to better than ± 2 %. One supplier quoted nominal total activity as ± 5 %. However, transfer of the radioactive compounds, usually < 1 mg quantities, could introduce error larger than this in the radioactivity measurements.

After each experiment the foil was rinsed for about 20 seconds in 1 litre of distilled water, dried in air at room temperature, and its radioactivity determined with a windowless β-proportional counter (Baird-Atomic Scaler-timer, model 135) with constant geometry and settings. The foil samples were counted three times on each surface and the count rates shown in tabulated data and figures refer to the mean values per cm^2. The count rates for the amounts

of adsorption were not significantly influenced by any moderate extent to which the foils were rinsed after the immersion period. For example, two foil samples with adsorbed cystine had count rates of 77 and 51 counts per minute (CPM) after the usual rinse procedure and yielded count rates of 81 and 42 CPM, respectively, after being washed for 1 minute in running distilled water.

Some of the foils were dissolved in 2.0 ml portions of nitric acid (10 % by volume), after which was added 10.0 ml of a solution containing 2,5-diphenyloxazole (5.0 g L^{-1}), napthalene (100 g L^{-1}), and 1,4-dioxane to a total volume of 1 litre (all liquid scintillation grade chemicals). Samples of the solutions were then counted in a Beckman liquid scintillation counter, model LS 150, that had been calibrated against solutions similarly prepared from non-radioactive foils, to which known amounts of the appropriate radioactive electrolyte were added by microburette. The Gilmont microburette used for these experiments had a total capacity of 0.2 ml and delivered 0.01 ml amounts with better than ± 10 % reproducibility. The print-out of data from the liquid counter provided 2σ standard deviation errors (95.5 % confidence limit) for the samples and the counter was regularly checked for consistency of operation against standard ^{14}C samples. Typical calibration data for the liquid counter are given

in Table I. The least-squares gradient used for calibration with methionine was 4125 CPM (liquid) ≡ 1.0×10^{-8} mole cm^{-2} (data in tables and figures for the count rates have been corrected for their background intensities). Prepared radioactive solutions of cystine and methionine of various radioisotopes and from various suppliers revealed a reproducibility in count rates better than ± 25 %, when data were normalised for their radioactivity contents. All surface concentration values were calculated for apparent (geometrical) areas of the foils, and with the assumption that no degradation of additive occurred. Although the currents used for deposition of copper on the foils could be maintained to about ± 2 %, undetermined error is introduced by lack of data for the true surface areas of the electrodes. To determine the surface area (e.g. by the B.E.T. method, by measurements of the double-layer capacity, or by determinations of the adsorptions of hydrogen, oxygen, or organic compounds on the metal, etc.) it is necessary to make various assumptions and approximations and, generally, one particular method will predict areas that differ from those found by another method. Moreover, the surface comprises crystallites, crevices, etc. and if these are preferred sites for deposition, the definition of the true surface area is further complicated, especially during the deposition reaction. It is obvious, of course, that the true

TABLE I

CALIBRATION OF LIQUID SCINTILLATION COUNTER

Total methionine concn.: 2.0×10^{-4} M (in standard electrolyte)

Radioisotope: L-methionine (methyl-^{14}C)

Electrolyte added (ml)	CPM*	2σ
2.0×10^{-4} M methionine, 50 μC L^{-1}		
0.002	93.0	(7.0 %)
0.004	194.5	(5.0 %)
0.006	247.0	(5.0 %)
0.008	334.6	(5.0 %)
0.010	401.6	(3.0 %)
0.002	117.6	(7.0 %)
0.005	334.5	(5.0 %)
0.01	565.3	(3.0 %)
0.02	947.7	(3.0 %)
0.03	1566.0	(2.0 %)
0.04	1839.0	(2.0 %)
0.05	2279.1	(1.5 %)
0.06	2745.3	(1.5 %)
0.08	3297.1	(1.5 %)
0.10	4027.0	(1.5 %)
2.0×10^{-3} M methionine, 500 μC L^{-1}		
0.01	5014.0	(3.0 %)
0.02	10225.0	(2.0 %)
0.03	14500.0	(2.0 %)
0.04	16851.0	(2.0 %)
0.05	20895.0	(1.5 %)
0.06	25431.0	(1.5 %)
0.07	27659.0	(1.5 %)
0.08	28043.0	(1.5 %)
0.09	33306.0	(1.5 %)
0.10	38690.0	(1.5 %)

* Corrected for background

area will be larger than the geometrical area[†].

From samples counted as foils and as solutions of foils, it was possible to calibrate the count rates observed with the foil samples for both adsorption on open circuit and for occlusion during electrodeposition. The data, shown in Figures 2 and 3, indicate that the counting results for the foils and for the solutions were in fair agreement for both the adsorption and occlusion experiments.

Some adsorption experiments were made under purified nitrogen in the cell, with the apparatus depicted in Figure 4. The gas train comprised two Fisher-Milligan gas scrubbers, containing ammonium meta-vanadate solutions to remove oxygen, and a third gas scrubber containing standard electrolyte to adjust the moisture content of the gas, and to remove any possible spray from the second scrubber. The gas issuing from the cell again was passed through a gas scrubber containing meta-vanadate solution and finally through a water bubbler, to prevent any back-diffusion of air into the cell. The solutions to remove oxygen were each prepared from 2 g ammonium meta-vanadate boiled with 25 ml

---

[†]Footnote: The absence of ideal polarizability may introduce difficulties in the measurement of areas for some metals on open circuit. It is difficult, for example, to find a surface active substance which is adsorbed on silver, because of its high exchange current (26).

FIGURE 2

Relation between counts made on copper foils and on solutions made from foils, after adsorption of radioactive cystine and methionine.

O - 1.0×10^{-4} M cystine (in standard electrolyte)

Radioisotope: D,L-cystine-1-^{14}C, 50 $\mu C\ L^{-1}$.

X - 2.0×10^{-4} M methionine (in standard electrolyte)

Radioisotope: D,L-methionine-2-^{14}C, 50 $\mu C\ L^{-1}$.

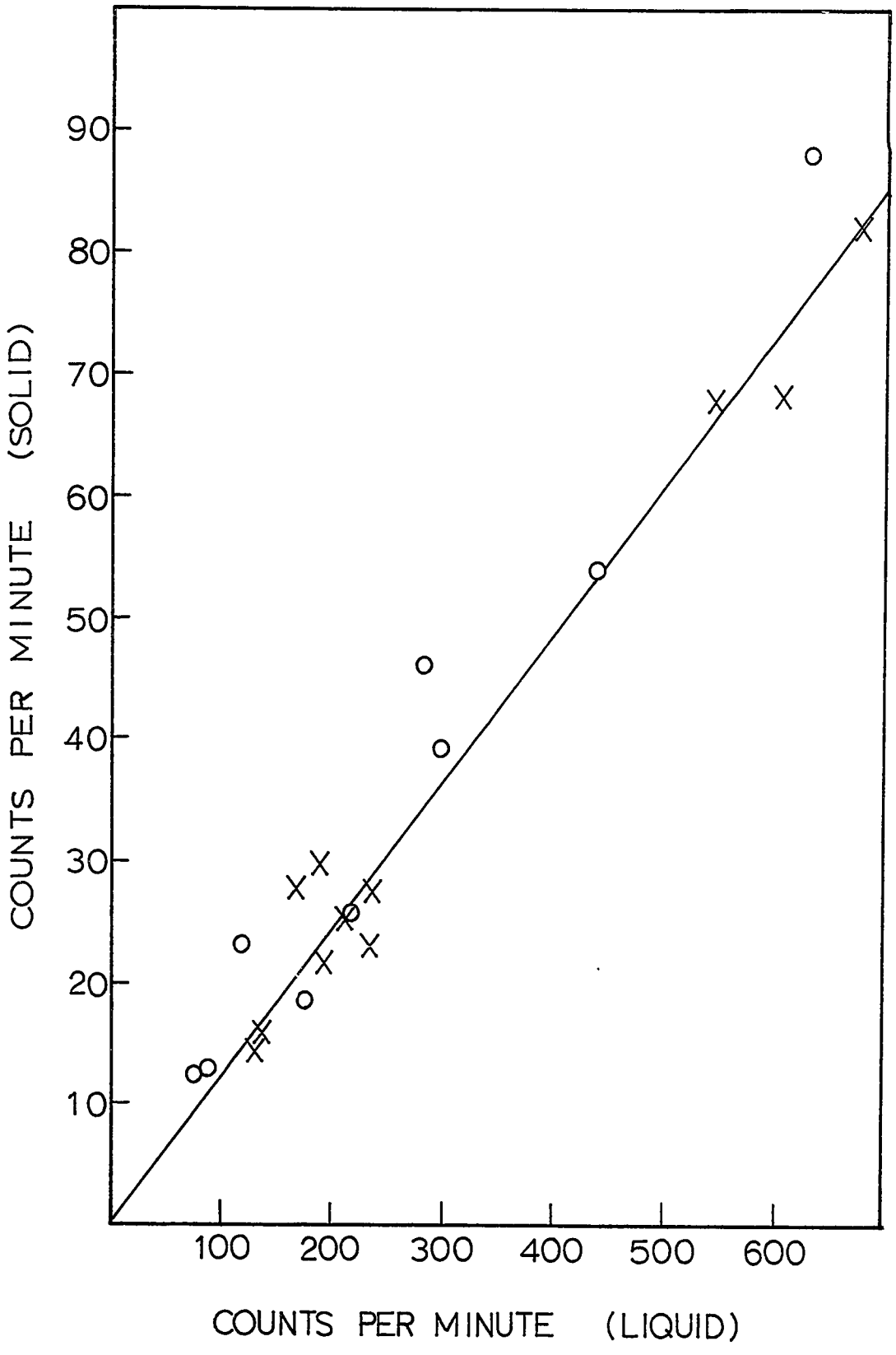
90
80
70
60
50
40
30
20
10
COUNTS PER MINUTE (SOLID)
100
200
300
400
500
600
COUNTS PER MINUTE (LIQUID)

FIGURE 3

Relation between counts made on copper foils and on solutions made from foils, after occlusion of radioactive cystine and methionine.

O - 1.0×10^{-4} M cystine (in standard electrolyte)

Radioisotope: D,L-cystine-1-^{14}C, 50 μC L^{-1}.

○ - 2.0×10^{-4} M methionine (in standard electrolyte)

Radioisotope: L-methionine (methyl-^{14}C), 50 μC L^{-1}.

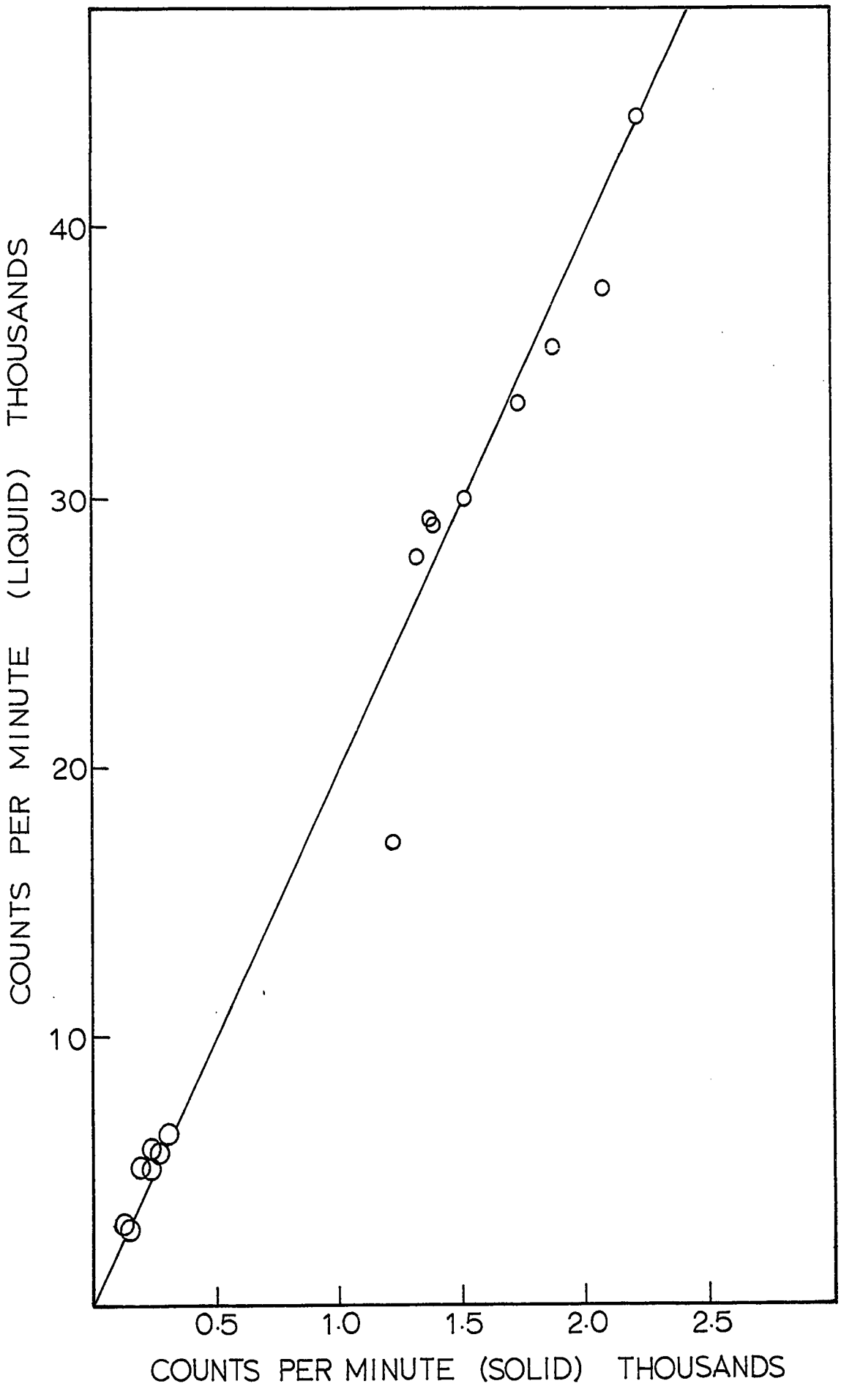
COUNTS PER MINUTE (LIQUID) THOUSANDS
40
30
20
10
0·5
1·0
1·5
2·0
2·5
COUNTS PER MINUTE (SOLID) THOUSANDS

FIGURE 4

Schematic diagram of apparatus for adsorption experiments in purified nitrogen.

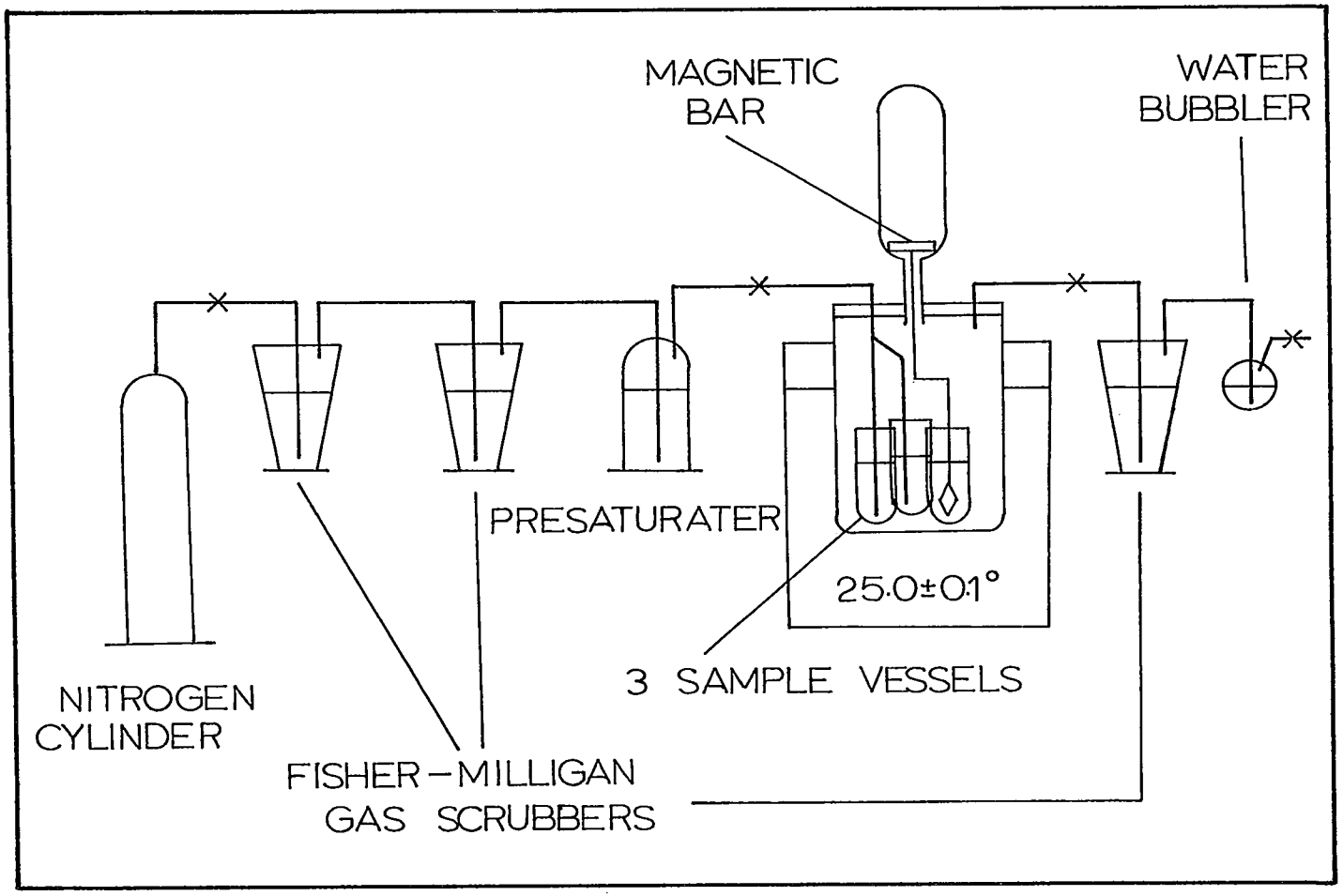
MAGNETIC
BAR
WATER
BUBBLER
PRESATURATER
25.0±0.1°
3 SAMPLE VESSELS
NITROGEN
CYLINDER
FISHER–MILLIGAN
GAS SCRUBBERS

conc. HCl, diluted to 200 ml, and added to 25 g amalgamated zinc metal, in accordance with the suggestion of Meites (89). Copper foil samples were prepared as in the previous experiments and then suspended in the cell in 50 ml deaerated 1M H_2SO_4 solution for at least two hours, while solutions of 50 ml standard electrolyte (non-radioactive) and 50 ml of electrolyte containing radioactive additive were flushed with streams of purified nitrogen gas. The samples were attached to a glass rod and magnetic bar arrangement that could be moved with the aid of a magnet, so that they could be immersed into the appropriate solutions as required without opening the apparatus. The cell assembly was immersed in a thermostat at 25.0 ± 0.1°C for all experiments.

Adsorption of methionine on copper

Data are shown in Table II and Figure 5 for the adsorption of methionine-2-^{14}C on copper foils, with no current flowing, from 2.0×10^{-4} M methionine in the standard electrolyte. (The data shown in the figure for cystine will be discussed later.) The approximate mean rate of adsorption during the first seven minutes was 1.4×10^{-12} mole cm^{-2} s^{-1}. The amount of adsorption then remained constant temporarily at about 5.4×10^{-10} mole cm^{-2}, but increased again after a period of about one hour, as shown in Table III. The

TABLE II

ADSORPTION OF METHIONINE ON COPPER FOILS

Total methionine concn.: 2.0×10^{-4} M (in standard electrolyte)

Total radioactivity: 50 $\mu C\ L^{-1}$ (D,L-methionine-2-^{14}C)

Immersion period $(seconds)^{1/2}$	Surface coverage, θ (mole cm^{-2}) $\times 10^{10}$				
	CPM* (Copper foils)	θ	CPM* (Solutions of copper foils)	2σ	θ
3.2	4.7	0.9	-		-
5.5	7.1	1.4	-		-
7.7	10.8	2.2	86.2	(7.0 %)	2.1
11.0	13.4	2.7	99.8	(7.0 %)	2.4
13.4	17.5	3.5	156.9	(5.0 %)	3.8
15.5	18.0	3.6	140.5	(5.0 %)	3.4
17.3	22.1	4.4	-		-
24.5	24.0	4.8	-		-
30.0	27.8	5.6	196.6	(5.0 %)	4.8
34.6	27.9	5.6	-		-
38.7	28.2	5.6	193.7	(5.0 %)	4.7
42.4	24.8	5.0	-		-
49.0	23.9	4.8	173.0	(5.0 %)	4.2
60.0	26.9	5.4	-		-

* Corrected for background

FIGURE 5

Adsorption of methionine and cystine on copper foils.

X - 2.0×10^{-4} M methionine (in standard electrolyte)

Radioisotope: D,L-methionine-2-^{14}C, 50 μC L^{-1}.

O - 1.0×10^{-4} M cystine (in standard electrolyte)

Radioisotope: D,L-cystine-1-^{14}C, 50 μC L^{-1}.

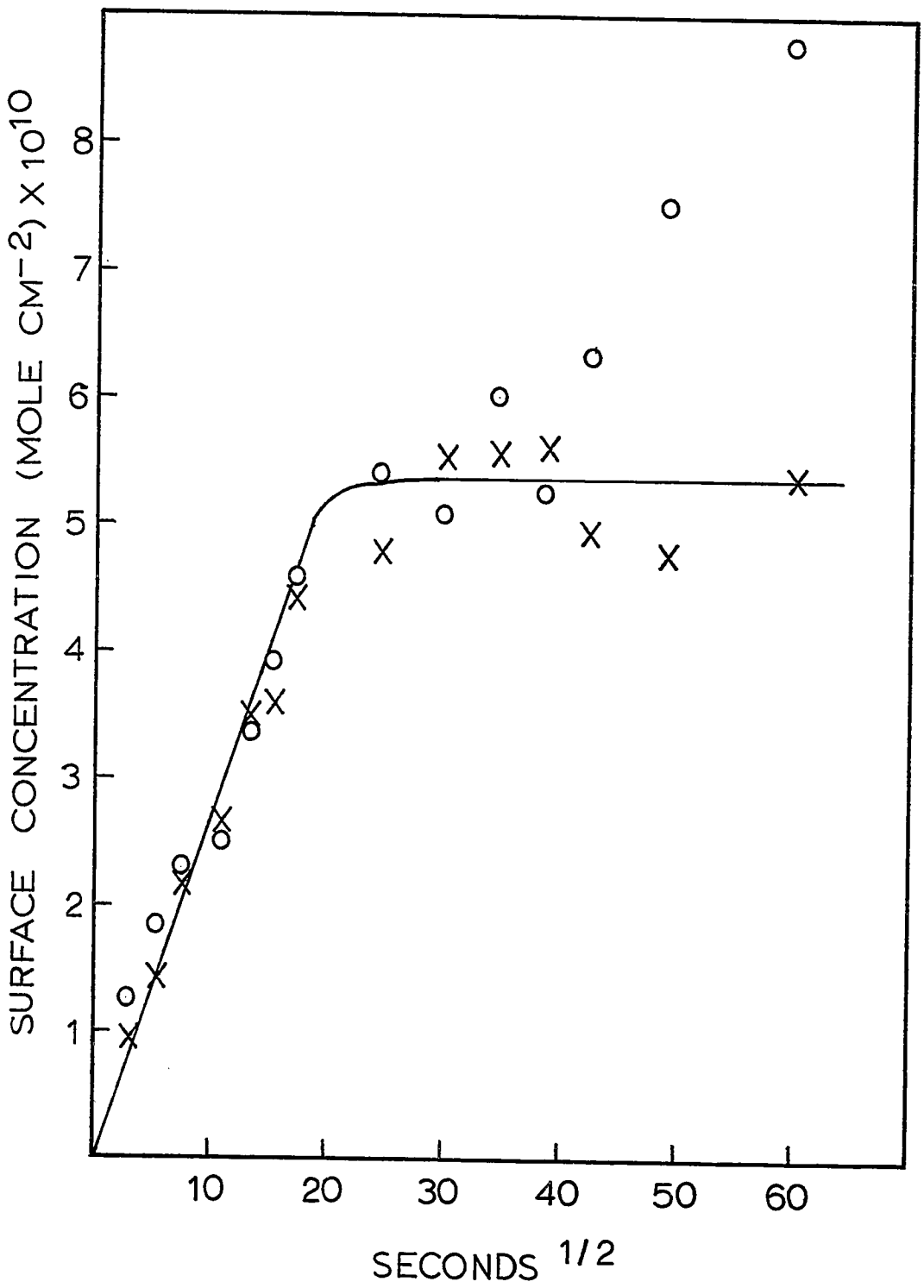
SURFACE CONCENTRATION (MOLE CM^{-2}) X 10^{10}
1
2
3
4
5
6
7
8
10
20
30
40
50
60
SECONDS $^{1/2}$

TABLE III

ADSORPTION OF METHIONINE ON COPPER FOILS

Total methionine concn.: 2.0×10^{-4} M (in standard electrolyte)

Total radioactivity: 50 μC L^{-1} (L-methionine (methyl-^{14}C))

Immersion period (min)	Surface coverage, θ (mole cm^{-2}) × 10^{10}				
	CPM* (copper foils)	θ	CPM* (solutions of copper foils)	2σ	θ
30	27.6	5.7	237.6	(5.0 %)	5.8
120	52.9	10.7	-		-
150	68.4	13.6	605.6	(3.0 %)	14.7
180	67.8	13.5	545.9	(3.0 %)	13.2
240	82.3	16.4	676.1	(3.0 %)	16.4
300	80.4	16.0	757.2	(3.0 %)	18.4

* Corrected for background

adsorbed radioisotope, on foils that had been immersed for 30 minutes in an electrolyte containing radioactive methionine, was sufficiently strong to resist significant desorption for as long as six hours when the foils were washed in distilled water and immersed in the standard electrolyte with no additive present (Table IV).

Experiments also were made in which foils that had been immersed for 30 minutes in an electrolyte containing radioactive methionine, were washed in distilled water and immersed for various periods in electrolyte containing non-radioactive methionine of equal bulk concentration in the standard electrolyte. The data in Table V and Figure 6 show that an exchange reaction occurred to decrease the radioactivity of the foils. There was a reproducible temporary decrease in the exchange rate after roughly 50 % of the adsorbed methionine had exchanged and some radioactivity remained even after four hours.

When these experiments were repeated with solutions of L-methionine (methyl-^{14}C) of similar concentrations, which had been flushed thoroughly with purified nitrogen, the rate of adsorption was increased generally, but the data were very scattered (Table VI). This scattering could be accounted for if traces of oxygen were able to modify the adsorption processes. It is possible that there were slight leaks in the apparatus or that traces of oxygen might have

TABLE IV

DESORPTION OF METHIONINE FROM COPPER FOIL

Adsorption (30 minutes)

Total methionine concn.: 2.0×10^{-4} M (in standard electrolyte)

Total radioactivity: 50 μC L^{-1} (L-methionine (methyl-^{14}C))

Desorption

Standard electrolyte - no additive present.

Desorption period (min)	Residual surface coverage, θ (mole cm^{-2}) $\times 10^{10}$
10	5.3
60	4.6
180	4.7
360	5.7

TABLE V

EXCHANGE OF METHIONINE FROM COPPER FOILS

Adsorption (30 minutes)

Total methionine concn.: 2.0×10^{-4} M (in standard electrolyte)

Total radioactivity: 50 μC L^{-1} (L-methionine (methyl-^{14}C))

Desorption

Total methionine concn.: 2.0×10^{-4} M (non-radioactive, in standard electrolyte)

Desorption period $(\text{seconds})^{1/2}$	Residual surface coverage, θ (mole cm^{-2}) × 10^{10}				
	CPM* (copper foils)	θ	CPM* (Solutions of copper foils)	2σ	θ
0	27.6	5.5	237.6	(5.0 %)	5.8
3.2	-	-	225.9	(5.0 %)	5.5
7.7	-	-	225.2	(5.0 %)	5.5
11.0	-	-	214.5	(5.0 %)	5.2
13.4	-	-	217.9	(5.0 %)	5.3
17.3	-	-	186.5	(5.0 %)	4.5
24.5	27.9	5.6	168.9	(5.0 %)	4.1
34.6	15.9	3.2	142.5	(5.0 %)	3.5
42.4	14.4	2.9	132.1	(5.0 %)	3.2
57.4	17.7	3.5	151.7	(5.0 %)	3.7
60.0	19.2	3.8	136.6	(5.0 %)	3.3
73.3	13.7	2.7	104.6	(7.0 %)	2.5
84.9	6.5	1.3	53.3	(7.0 %)	1.3
94.9	4.4	0.9	48.2	(10 %)	1.2
103.9	6.8	1.4	68.8	(7.0 %)	1.7
112.2	4.1	0.8	39.6	(10 %)	1.0
120.0	6.0	1.2	37.1	(10 %)	0.9
134.2	4.2	0.8	48.3	(7.0 %)	1.2

* Corrected for background

FIGURE 6

Exchange of radioactive methionine from copper foils.
Standard electrolyte containing non-radioactive methionine (2.0×10^{-4} M).
Radioisotope: L-methionine (methyl-^{14}C).

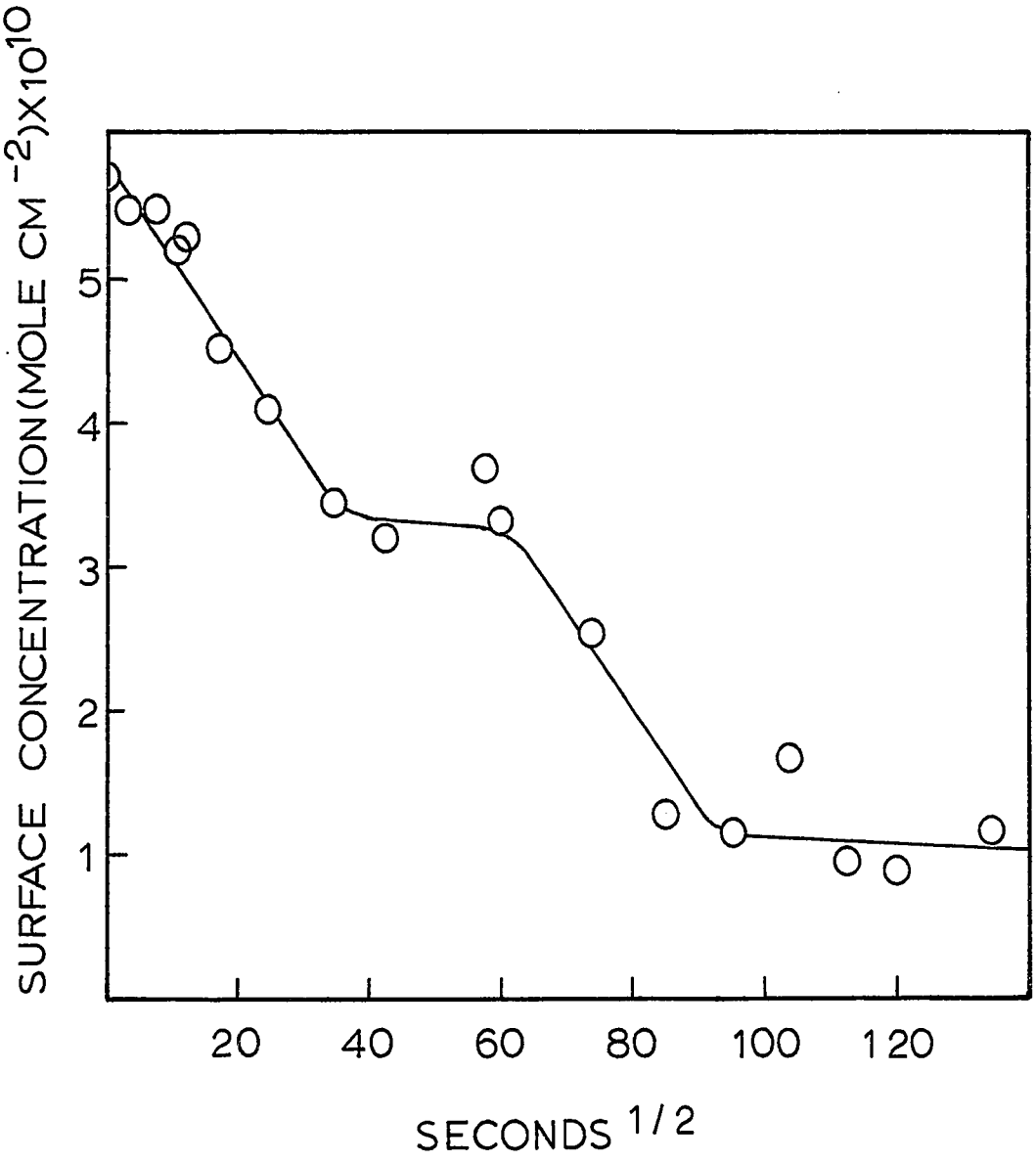
SURFACE CONCENTRATION (MOLE CM $^{-2}$) X 10^{10}
1
2
3
4
5
20
40
60
80
100
120
SECONDS $^{1/2}$

TABLE VI

ADSORPTION OF METHIONINE ON COPPER FOILS IN SOLUTIONS FLUSHED WITH PURIFIED NITROGEN

Total methionine concn.: 2.0×10^{-4} M (in standard electrolyte)

Total radioactivity: 50 μC L^{-1} (L-methionine (methyl-^{14}C))

Immersion period (min)	Surface coverage, θ (mole cm^{-2}) × 10^{10}		
	CPM* (Solutions of copper foils)	2σ	θ
0.5	297.6	(5.0 %)	7.2
1	429.2	(3.0 %)	10.4
2	352.5	(5.0 %)	8.6
5	168.1	(5.0 %)	4.1
10	905.6	(3.0 %)	22.0
20	331.7	(5.0 %)	8.0
30	424.2	(3.0 %)	10.3
"	544.6	(3.0 %)	13.2
"	478.1	(3.0 %)	11.6
"	567.5	(3.0 %)	13.8
60	1000.2	(2.0 %)	24.3
120	1260.5	(2.0 %)	30.6

* Corrected for background

.... contd. next page

TABLE VI (CONTD.)

Radioisotope: L-methionine (methyl-^{14}C)

Immersion period (min)	Surface coverage, θ (mole cm^{-2}) × 10^{10}		
	CPM* (Solutions of copper foils)	2σ	θ
2.0×10^{-3} M methionine; total radioactivity: 500 μC L^{-1}			
0.5	2034.2	(1.5 %)	49.3
2	3150.0	(1.5 %)	76.4
5	2838.2	(1.5 %)	68.8
10	4387.6	(1.0 %)	106.4
2.0×10^{-5} M methionine; total radioactivity: 5 μC L^{-1}			
0.5	33.0	(10 %)	0.8
1	7.5	(15 %)	0.2
2	83.9	(7.0 %)	2.0
5	26.3	(10 %)	0.6
10	95.0	(7.0 %)	2.3
30	79.1	(7.0 %)	1.9
60	84.6	(7.0 %)	2.1

* Corrected for background

remained in the electrolytes after they had been flushed for two hours with purified nitrogen. The difficulty of removing all traces of oxygen may be appreciated if it is realised that, for a nitrogen flow rate of 100 ml min^{-1}, oxygen levels of 1 ppm in the nitrogen stream would have introduced to the electrolytes about 0.7×10^{-10} mole s^{-1} oxygen. It is possible, too, that differences in the prepared copper surfaces were sufficient to make their adsorptive capacities significantly different.

The dependence of the adsorption rates of methionine at copper foils on the bulk concentration of additive was also investigated in solutions flushed with nitrogen, at 2.0×10^{-5} M, 2.0×10^{-4} M, and 2.0×10^{-3} M methionine concentrations in the standard electrolyte, with constant specific activities of the radioisotope. The results, shown in Table VI, indicate that the surface coverages of additives were increased approximately in a proportional manner with increase in the bulk concentrations of methionine from 10^{-5} M to 10^{-3} M.

Desorption experiments also were made in the cell under purified nitrogen. The results, shown in Table VII, indicated that no appreciable exchange process had occurred in a solution containing non-radioactive methionine of equal bulk concentrations in the standard electrolyte after five hours of immersion; in an aerated system most of the

TABLE VII

EXCHANGE OF METHIONINE FROM COPPER FOILS IN SOLUTIONS FLUSHED WITH PURIFIED NITROGEN

Adsorption (30 minutes)

Total methionine concn.: 2.0×10^{-4} M (in standard electrolyte)

Total radioactivity: 50 $\mu C\ L^{-1}$ (L-methionine (methyl-^{14}C))

Desorption

Total methionine concn.: 2.0×10^{-4} M (non-radioactive, in standard electrolyte)

Desorption period (min)	Residual surface coverage, θ (mole cm^{-2}) $\times 10^{10}$		
	CPM*	2σ	θ
	(Solutions of copper foils)		
30	549.0	(3.0 %)	13.3
60	479.2	(3.0 %)	11.6
180	549.0	(3.0 %)	13.3
300	683.5	(3.0 %)	16.6

* Corrected for background

radioactivity would have been exchanged within this period. Comparison of the data in Tables IV and VII show that, after 30 minutes adsorption, the coverages obtained from immersion of foils in the deaerated solutions are 2 - 3 times higher than those obtained with aerated solutions.

Adsorption of cystine on copper

1. Radioisotope estimations

Adsorption of cystine on copper foils from standard electrolyte containing radioactive cystine of 1.0×10^{-4} M concentration occurred at a mean rate of about 1.4×10^{-12} mole cm^{-2} s^{-1}, during the first seven minutes, i.e. essentially the same as that for the adsorption of methionine from similar solutions with about twice the concentration of amino acid (Table VIII, cf. Figure 5). The amount of cystine adsorbed then remained constant temporarily, at about 5.4×10^{-10} mole cm^{-2}, as with methionine, but after a period of about 20 minutes it, too, increased. Comparison with the data of Pradac and Koryta (46) indicates that the adsorption of cystine on copper during the early stages resembled that on platinum more closely than that on gold electrodes.

The amounts adsorbed at longer times are given in Table IX. Neither the adsorption of cystine nor that of methionine was restricted to monolayer coverages. Copper

TABLE VIII

ADSORPTION OF CYSTINE ON COPPER FOILS

Total cystine concn.: 1.0×10^{-4} M (in standard electrolyte)

Total radioactivity: 50 $\mu C\ L^{-1}$ (D,L-cystine-1-^{14}C)

Immersion period $(seconds)^{1/2}$	Surface coverage, θ (mole cm^{-2}) $\times 10^{10}$				
	CPM* (Copper foils)	θ	CPM* (Solutions of copper foils)	2σ	θ
3.2	12.7	1.3	82.8	(5.0 %)	1.0
5.5	18.4	1.8	175.1	(5.0 %)	2.1
7.7	23.2	2.3	117.9	(5.0 %)	1.4
11.0	25.7	2.6	216.5	(5.0 %)	2.6
13.4	33.9	3.4	160.9	(5.0 %)	2.0
15.5	39.4	3.9	297.2	(5.0 %)	3.6
17.3	46.2	4.6	281.3	(5.0 %)	3.4
24.5	54.3	5.4	436.4	(3.0 %)	5.3
30.0	51.1	5.1	-		-
34.6	60.4	6.0	-		-
38.7	52.7	5.3	-		-
42.4	63.5	6.3	-		-
49.0	75.4	7.5	419.9	(3.0 %)	5.1
60.0	88.3	8.8	629.9	(2.0 %)	7.6
73.5	98.3	9.8	-		-
84.9	116.2	11.6	625.2	(3.0 %)	7.6
112.2	161.6	16.1	-		-
134.2	363.2	36.2	-		-
180.0	613.5	61.2	-		-
199.0	1314.5	131.1	-		-
224.5	2023.9	201.9	-		-

* Corrected for background

TABLE IX

ADSORPTION OF CYSTINE ON COPPER FOILS

Total cystine concn.: 1.0×10^{-4} M (in standard electrolyte)

Total radioactivity (when applicable): 50 μC L^{-1}

(D,L-cystine-1-^{14}C)

Immersion period (min)	Surface coverage, θ (mole cm^{-2}) × 10^{10}	
	Radioisotope method	Colorimetric method
30	6.3	-
60	8.8	8.8
90	9.8	9.9
120	11.6	14.7
210	16.1	8.3
300	36.2	15.5
540	61.2	24.8

foils disintegrated completely when they remained for several weeks immersed in solutions of cystine ($\simeq 10^{-1}$ M) in the standard electrolyte in lightly stoppered bottles. At the same time the solutions became green and yellow deposits formed on the foils. Obviously, persistent and considerable chemical reactions occurred.

2. Colorimetric estimations

A photometric method for the estimation of amino acids, using so-called "ninhydrin" reagent (triketo-hydrindene hydrate), has been described with detection limits 0.02 - 0.40 micromole (90). This technique has been modified and applied in an attempt to corroborate the radioisotope estimations of the amounts of cystine adsorbed on copper foils.

Strips of copper foil, 5cm × 20cm, were loosely coiled, cleaned as in the previous adsorption experiments, and immersed for various periods in solutions of L-cystine (1.0×10^{-4} M) in the standard electrolyte. Excess solution adhering to the coils was removed by washing them successively in 3 separate distilled water baths, after which the adsorbed cystine was obtained by shaking them in air with 10.0 ml of a NaOH/acetic acid buffer for 5 minutes. The buffer was prepared by adding glacial acetic acid to 2N NaOH solution until the pH was 10.3. These solutions, and the drainings from two subsequent washes of each coil with

5.0 ml distilled water, were added to 50 ml volumetric flasks. Glacial acetic acid was added to each sample, to bring the pH to 5.36 (about 0.3 ml was required) and the flasks were left to stand, open to the air, for 24 hours. To each flask were then added 1.0 ml of NaCN solution (98 mg L^{-1}) and 5.0 ml "ninhydrin" solution containing 30 g L^{-1} methyl cellosolve (amino acid analysis grade chemicals). The flasks were heated in an oil bath at 100°C for 10 minutes exactly, after which the contents of each flask were immediately diluted to nearly 50 ml with an equi-volume mixture of isopropyl alcohol and distilled water. A deep red colour formed during the heating process, but this was caused to fade by shaking the diluted solutions well to provide good aeration. After cooling, the volumes of the solutions were adjusted to 50.0 ml with the isopropyl alcohol-water mixture and the colour densities determined in 1 cm cuvettes relative to blank samples at 570 mμ in a Perkin Elmer, model 402, UV spectrophotometer. Figure 7 represents the calibration data obtained by additions of 0.1 - 0.9 ml of a 10^{-3} M stock solution. This was prepared by dissolving 1.2015 g L-cystine (B.D.H.) in 100.0 ml H_2SO_4 (approx. 1 N), and adjusting 10.0 ml of this solution to 500.0 ml with distilled water. The cystine calibration gave a colour yield of ≈ 57 %, calculated on the basis of a leucine slope value of 2.94×10^4 (91). The analytical

FIGURE 7

Calibration data for colorimetric estimation of cystine with Triketohydrindene hydrate reagent.

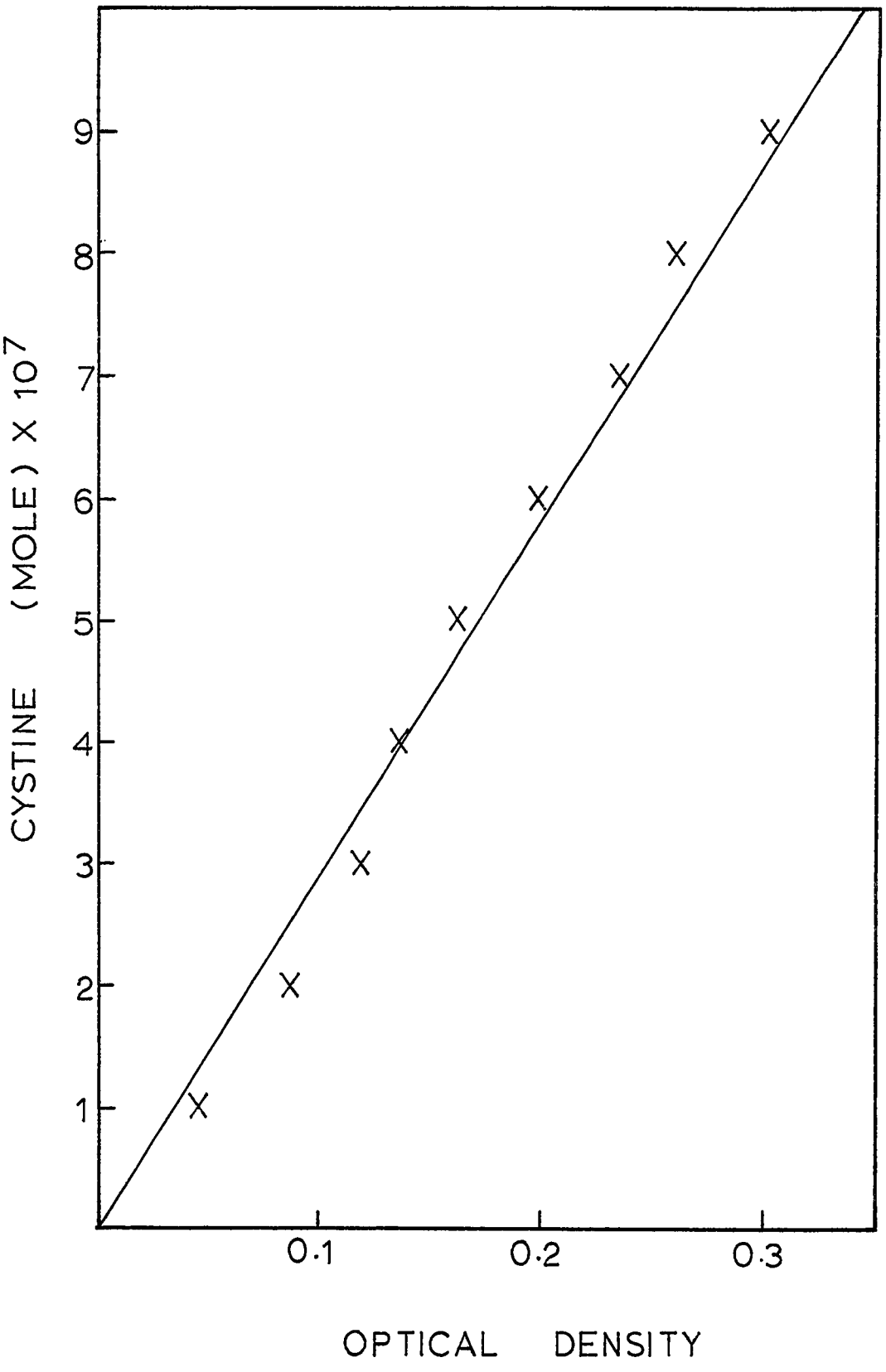
CYSTINE (MOLE) X 10^7
9
8
7
6
5
4
3
2
1
0·1
0·2
0·3
OPTICAL DENSITY

results are compared with those obtained by the radioisotopic technique in Table IX. Although the colorimetric method must be regarded as a highly approximate one, because of the likelihood of incomplete removal and transfer of adsorbed species, the results are in fair agreement with the more sensitive radioisotopic measurements.

Occlusion of cystine and methionine in copper cathodes

As outlined previously, the method and conditions for studying the occlusion of additives on copper foil cathodes, during the passage of current, were similar in all essentials to those used to study their adsorption on open circuit. To obtain meaningful count rates from the foils with occluded additives, it was necessary first to establish the minimum amounts of copper electrodeposit that would provide constant adsorption and back-scattering of the β-rays from the radioisotopes. The data in Table X and Figure 8 illustrate that this was achieved after the passage of 36 coulomb cm^{-2} for the current densities 1.0 A dm^{-2} and 4.0 A dm^{-2}. All subsequent occlusion experiments were therefore made with the passage of this quantity of electricity.

Tables XI - XIII summarize the experimental data for the occlusion of cystine and methionine with various

TABLE X

CHANGE IN COUNT RATE FROM OCCLUDED CYSTINE WITH QUANTITY OF COPPER DEPOSITED

Total cystine concn.: 1.0×10^{-4} M (in standard electrolyte)

Total radioactivity: 50 μC L^{-1} (L-cystine-^{35}S)

Deposition time (min)	CPM* (Copper foils)	
	1.0 A dm^{-2}	4.0 A dm^{-2}
2	405	-
5	984	892
10	1783	1327
15	2259	1447
20	2710	1547
30	3314	-
40	3582	-
50	3495	-
60	3621	-
75	3743	-
90	3915	-

* Corrected for background

FIGURE 8

Change in count rate from occluded cystine with quantity of copper deposited.

1.0×10^{-4} M cystine (in standard electrolyte)

Radioisotope: L-cystine-^{35}S, 50 $\mu C\ L^{-1}$.

◑ Current density - 1.0 A dm^{-2}.

◪ Current density - 4.0 A dm^{-2}.

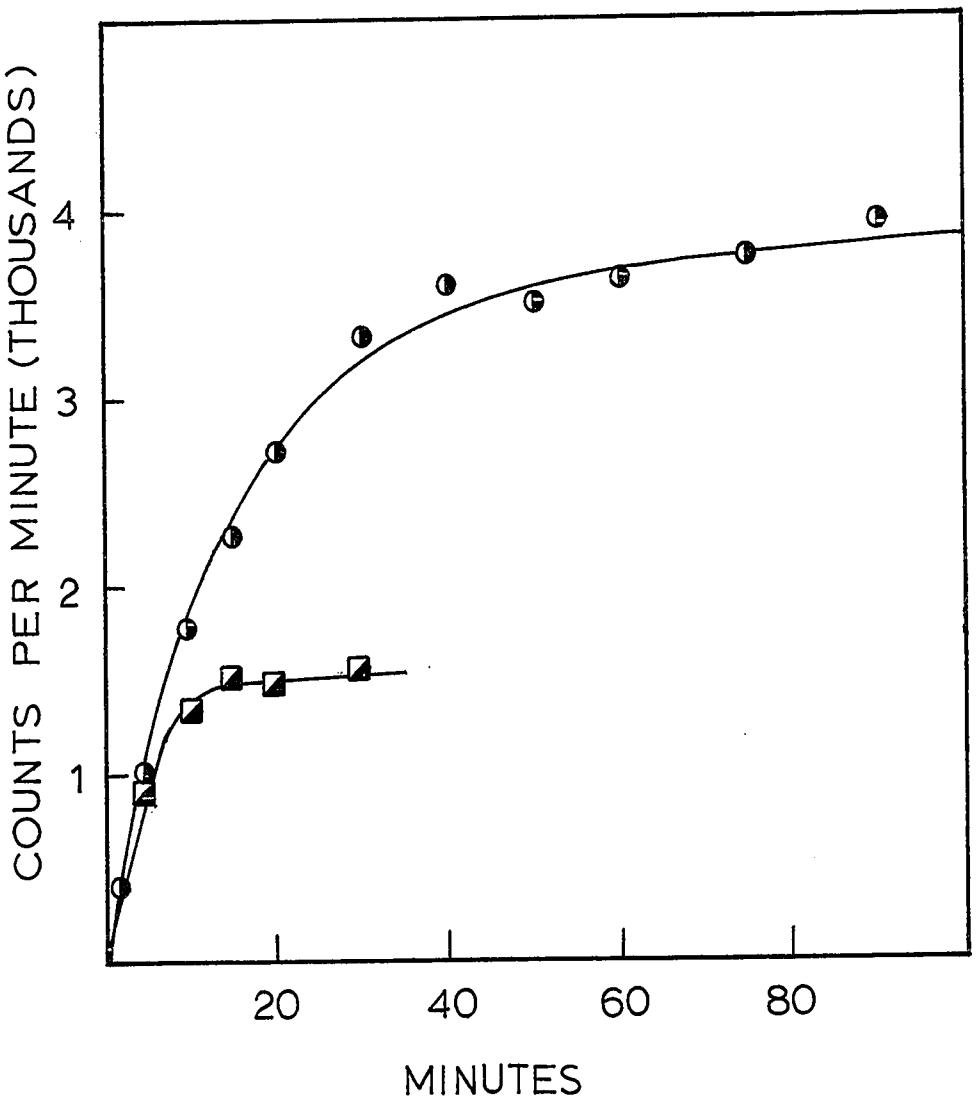
COUNTS PER MINUTE (THOUSANDS)
1
2
3
4
20
40
60
80
MINUTES

TABLE XI

OCCLUSION OF CYSTINE IN ELECTRODEPOSITS AT DIFFERENT CURRENT DENSITIES

Total cystine concn.: 1.0×10^{-4} M (in standard electrolyte)

Total radioactivity: 50 μC L^{-1}

Current density A dm^{-2}	Mean rate of occlusion, C_0 (mole cm^{-2} s^{-1}) $\times 10^{12}$					
	D,L-cystine-1-^{14}C		L-cystine-^{35}S		D,L-cystine-3-^{14}C	
	CPM* (Copper foils)	C_0	CPM* (Copper foils)	C_0	CPM* (Copper foils)	C_0
0.25	5875	9.9	-	-	-	-
0.50	-	-	5841	19.7	-	-
0.75	3593	18.1	-	-	-	-
1.0	3468	23.4	3621	24.4	3329	22.4
1.5	2381	24.1	-	-	-	-
2.0	-	-	2463	32.8	-	-
2.5	1790	30.1	-	-	-	-
3.0	-	-	1783	36.0	-	-
3.5	1499	35.4	-	-	-	-
4.0	-	-	1620	43.6	-	-
4.5	1172	35.5	-	-	-	-
5.0	-	-	1287	43.3	1247	33.6
5.5	1091	40.4	-	-	-	-
6.0	-	-	1222	49.4	-	-

* Corrected for background

TABLE XII

OCCLUSION OF CYSTINE IN ELECTRODEPOSITS AT DIFFERENT CURRENT DENSITIES

Total cystine concn.: 1.0×10^{-4} M (0.5 M $CuSO_4$, no acid)

Total radioactivity: 50 μC L^{-1} (D,L-cystine-1-^{14}C)

Current density (A dm^{-2})	Mean rate of occlusion, C_0 (mole cm^{-2} s^{-1}) × 10^{12}				
	CPM* (Copper foils)	C_0	CPM* (Solutions of copper foils)	2σ	C_0
0.25	6987	11.8	-		-
0.50	4753	16.0	-		-
0.75	4226	21.3	-		-
1.0	3642	24.5	-		-
1.5	3195	32.3	-		-
2.0	2864	38.6	-		-
2.5	2466	41.5	-		-
3.0	2472, 2216	49.9, 44.8	44000	(0.3 %)	44.4
3.5	2079	49.0	37753	(0.5 %)	44.5
4.0	1900, 1733	51.1, 46.7	33530	(0.5 %)	45.2
4.5	1868	56.6	35576	(0.5 %)	53.9
5.0	1545, 1511	52.0, 50.9	29989	(0.5 %)	50.5
5.5	1380	51.1	29001	(0.5 %)	53.8
6.0	1383, 1315	55.9, 53.1	27812	(0.5 %)	56.2
6.5	1370	60.0	29248	(0.5 %)	64.0
7.0	1208	56.9	17260	(0.5 %)	40.7

* Corrected for background

TABLE XIII

OCCLUSION OF METHIONINE IN ELECTRODEPOSITS

AT DIFFERENT CURRENT DENSITIES

Total methionine concn.: 2.0×10^{-4} M (in standard electrolyte)

Total radioactivity: 50 μC L^{-1} (D,L-methionine-2-^{14}C)

Current density (A dm^{-2})	Mean rate of occlusion, C_0 (mole cm^{-2} s^{-1}) $\times 10^{12}$	
	CPM* (Copper foils)	C_0
0.25	1368	4.6
0.50	815	5.5
0.75	384	3.9
1.0	383	5.2
1.5	190	3.8
2.0	236	6.4
2.5	174	5.9
3.0	138	5.6
3.5	186	8.8
4.0	230	12.4
4.5	70	4.2
5.0	178	12.0
5.5	101	7.5
6.0	76	6.1

* Corrected for background

.... contd. next page

TABLE XIII (CONTD.)

Total methionine concn.: 2.0×10^{-4} M (in standard electrolyte)

Total radioactivity: 50 μC L^{-1} (L-methionine (methyl-^{14}C))

Current density (A dm^{-2})	Mean rate of occlusion, C_0 (mole cm^{-2} s^{-1}) × 10^{12}				
	CPM* (Copper foils)	C_0	CPM* (Solutions of copper foils)	2σ	C_0
3.0	242	9.8	5165.2	(1.0 %)	10.4
3.5	202	9.5	5143.3	(1.0 %)	12.1
4.0	247	13.3	5894.2	(1.0 %)	15.9
4.5	274	16.6	5802.2	(1.0 %)	17.6
5.0	311	20.9	6425.4	(1.0 %)	21.6
5.5	151	11.2	2879.3	(1.0 %)	10.7
6.0	135	10.9	2980.7	(1.5 %)	12.0

* Corrected for background

radioisotopes in their molecules. A marked decrease in the ^{14}C or ^{35}S radioisotopic content of deposits occurs with increasing current densities for these additives, as illustrated by the data for cystine in Figure 9. From the relative extents to which cystine molecules with different radioactive contres (D,L-cystine-1-^{14}C, L-cystine-^{35}S, and D,L-cystine-3-^{14}C) were apparently occluded from standard electrolytes that contained cystine in bulk concentrations of 1.0×10^{-4} M, it would seem that at least the $-S-CH_2-CH(COOH)NH_3^+$ fragment of the molecule is trapped stoichiometrically. However, this evidence does not confirm the identity of the occluded species.

An attempt was therefore made to dissolve, in dil. HNO_3, deposits prepared on copper foil from 1.0×10^{-4} M cystine in the standard electrolyte, and to separate any amino acid from the solution by (i) chromatography (92), and (ii) electrophoresis (93). A positive test for the presence of an amino acid was found with "ninhydrin" spray reagent, but neither a quantitative estimate of the amount present, nor a reliable qualitative identification of a specific amino acid was possible by the methods used. The large excess of cupric ion was not removed for the tests and it is possible that these procedures might be more successful if this could be achieved without loss or destruction of the amino acid present. Both cystine and cysteine are known

FIGURE 9

Relation between count rate of occluded cystine and current density, for deposition of copper from electrolyte containing cystine (1.0×10^{-4} M).

Radioactivity: 50 μC L^{-1}.

○ D,L-cystine-1-^{14}C

▨ L-cystine-^{35}S

▲ D,L-cystine-3-^{14}C

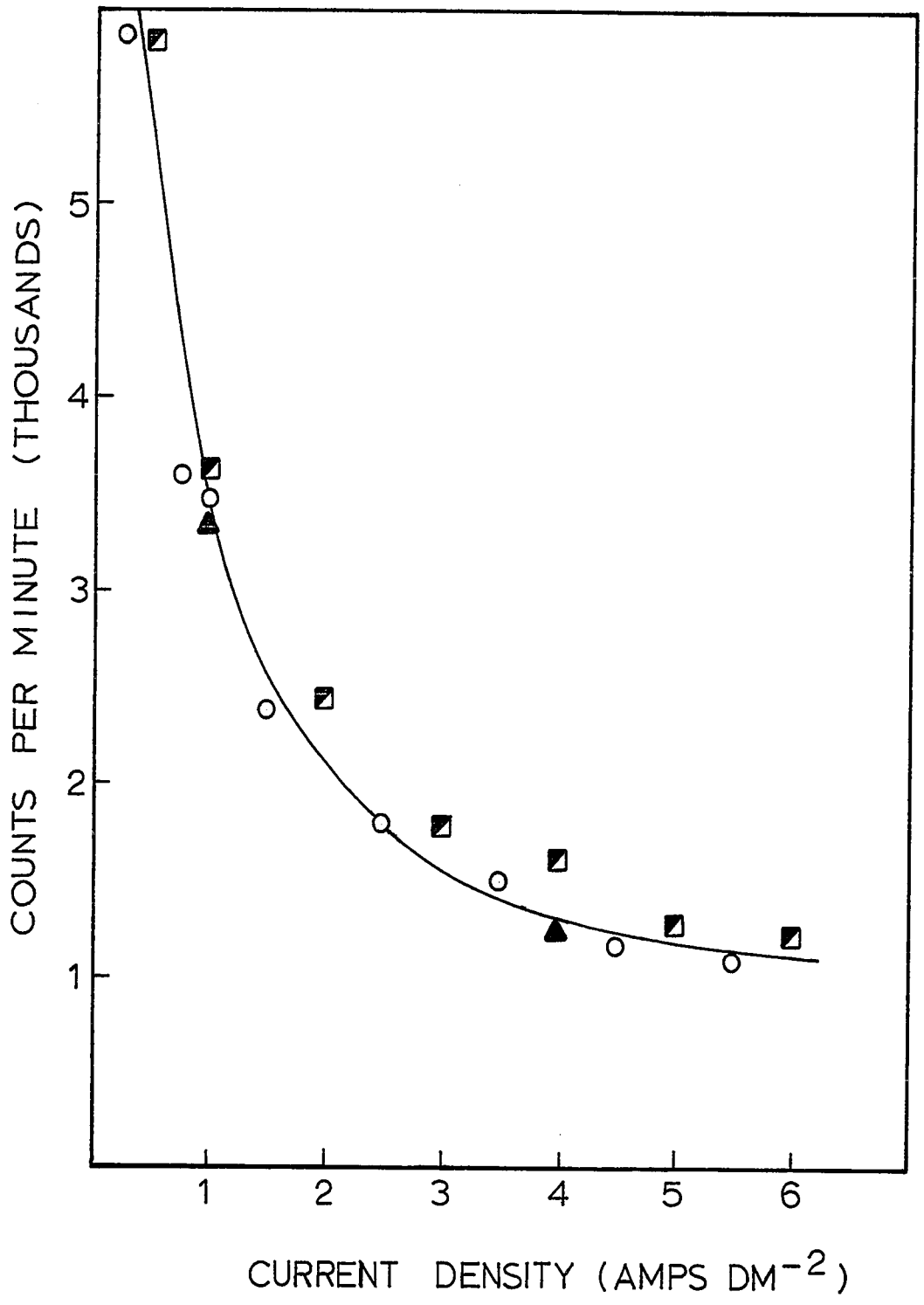
COUNTS PER MINUTE (THOUSANDS)
1
2
3
4
5
1
2
3
4
5
6
CURRENT DENSITY (AMPS DM^{-2})

to oxidise on paper chromatographs (94) in the presence of cupric salts, and this complicates the identification of species and the development of a satisfactory experimental technique. It does seem quite probable, however, that no appreciable degradation of the $-S-CH_2-CH(COOH)NH_3^+$ part of the cystine molecule occurred during its occlusion.

When the mean rates of occlusion were calculated, it was found that the relations between these and current density were markedly different for cystine and methionine. For the current density range investigated, the plot of ln (cystine occluded per second) against ln (current density) is approximately linear with a slope of 0.5 (Figure 10). The amounts occluded at various current density values were similar with and without sulphuric acid in the electrolyte. In corresponding manner, the differences in the initial polarisation maxima, obtained in the presence of cystine and in its absence, are virtually constant at different acid concentrations (42).

The mean rates of occlusion of methionine in the current density range 0.25 - 3.0 A dm^{-2}, shown in Figure 11, were about four times higher than its mean open circuit adsorption rate. With further increase in the current density, the occlusion rates increased until a maximum was reached at about 5 A dm^{-2}. Mechanisms are proposed later for the behaviours of methionine and cystine during their

FIGURE 10

Occlusion of cystine in electrodeposits at different current densities.

1.0×10^{-4} M cystine.

Radioactivity: 50 μC L^{-1}.

O D,L-cystine-1-^{14}C, standard electrolyte

▨ L-cystine-^{35}S, standard electrolyte

● D,L-cystine-1-^{14}C, 0.5 M $CuSO_4$ (no H_2SO_4 added)

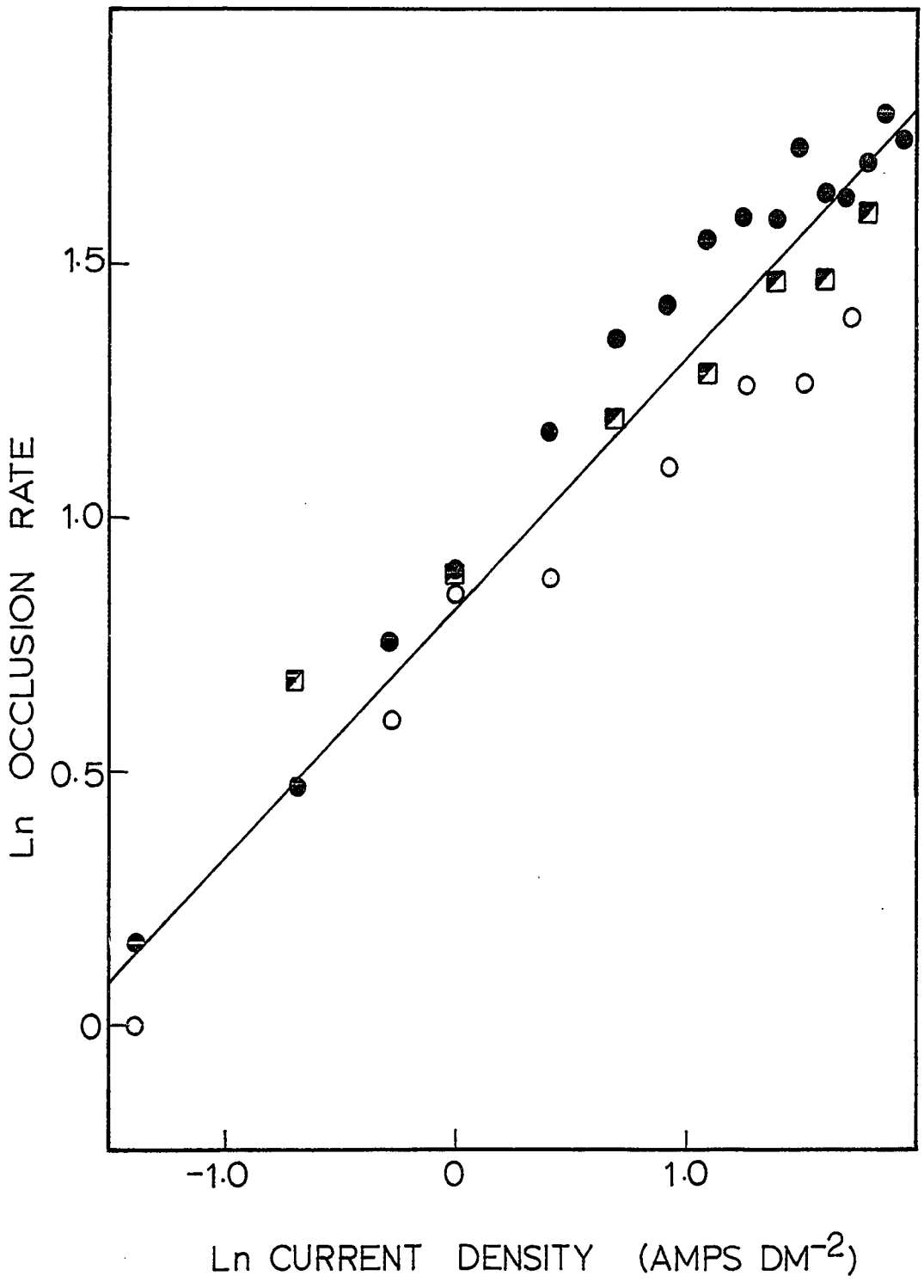
1·5
1·0
0·5
0
Ln OCCLUSION RATE
-1·0
0
1·0
Ln CURRENT DENSITY (AMPS DM^{-2})

FIGURE 11

Occlusion of methionine in electrodeposits at different current densities.

2.0×10^{-4} M methionine (in standard electrolyte)

Radioactivity: 50 μC L^{-1}.

X D,L-methionine-2-^{14}C

○ L-methionine (methyl-^{14}C)

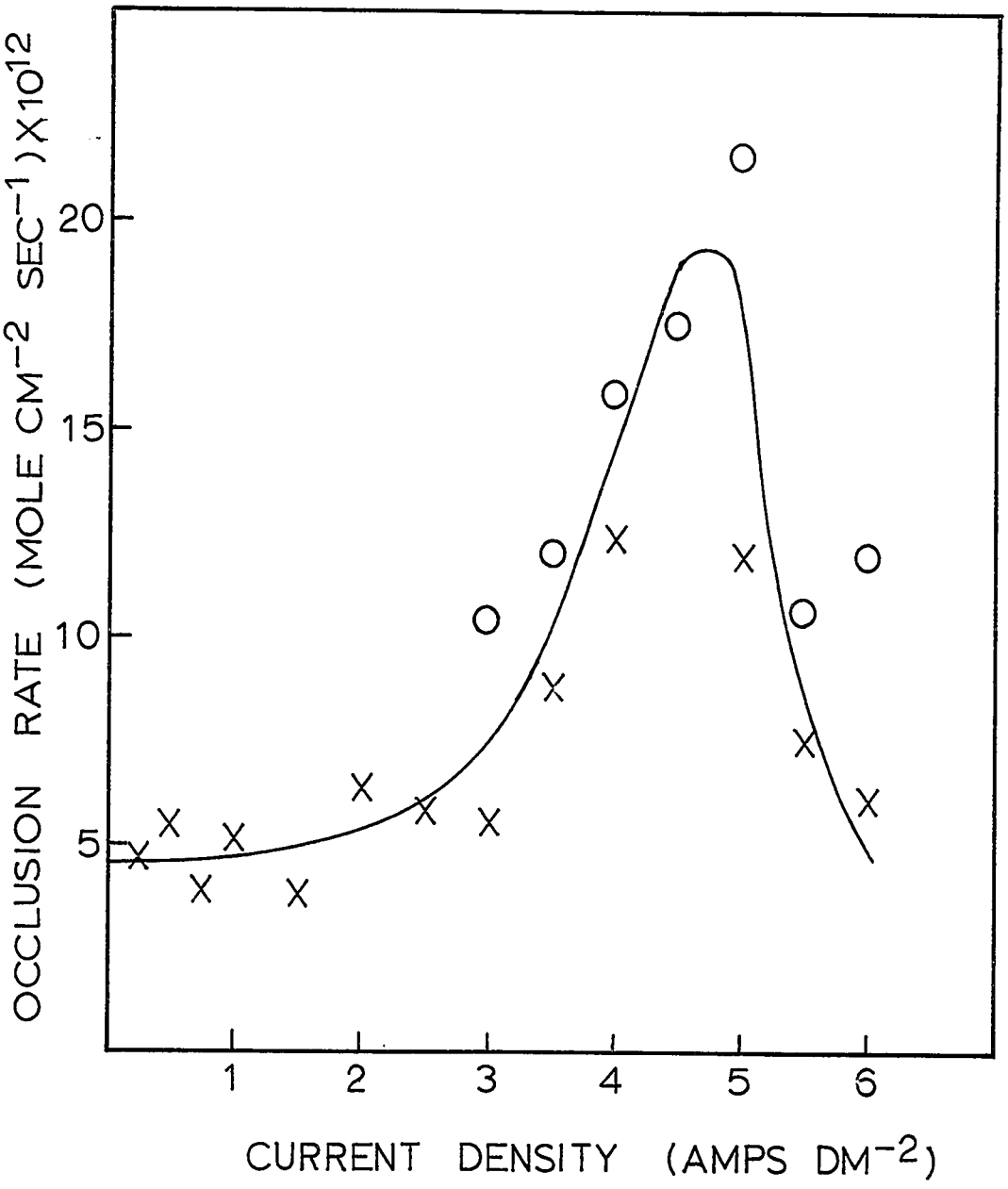
OCCLUSION RATE (MOLE CM^{-2} SEC^{-1}) X 10^{12}
20
15
10
5
1
2
3
4
5
6
CURRENT DENSITY (AMPS DM^{-2})

adsorption and occlusion.

COMPLEXES OF COPPER IONS WITH AMINO ACIDS

It has frequently been suggested that the addition agent effect of an additive during electrodeposition of copper may be attributed to complex formation between the additive and copper ions in the electrolyte (e.g. 95-100). Reference was made earlier to the importance of complexes in the potentiometric behaviour of the cystine-cysteine couple at solid electrodes. Some organic additives behave in a synergic manner with halide, thiocyanate, and cyanide anions (55,101-104). For example, Venkatachalam and Winkler (55) have demonstrated that a surface brightening phenomena may be associated with a 1:1 ratio of cystine: cyanide ion which is occluded into the deposit at a particular cystine concentration and current density. This evidence supports the premise that copper complexes may sometimes have an important addition agent role.

It was decided, therefore, to examine the conditions for complex formation between Cu(II) and Cu(I) ions with cystine and related amino acids and, wherever possible, to determine the infrared spectra of these complexes as an aid to their identifications and to the determinations of their structures.

Cupric-amino acid complexes

Although Cu(II)-cystine had been prepared and analysed as early as 1901 (90), the molecular structure is not known unequivocally. Initial suggestions (105,106) that the complex was monomeric were discounted by Hawkins and Perrin (107), who have proposed that the major species is the dimer, di-μ-cystinato-dicopper(II) di-hydrate. Their analysis establishes stability constants based on the assumption that a non-weighted statistical distribution of complex species exists in equilibrium. In strongly acidic solutions, both the carboxylate and amino groups of dibasic amino acids are protonated. Complexes of the amino acids with cupric ion may then be formed when the protons are titrated from the $-NH_3^+$ groups by additions of base in the presence of cupric ion. With cystine, for example,

$$H^+(^-RSSR^-)H^+ + Cu^{2+} + OH^- \rightleftharpoons H^+(^-RSSR)Cu^+ + H_2O$$

$$H^+(^-RSSR)Cu^+ + H^+(^-RSSR^-)H^+ + OH^- \rightleftharpoons H^+(^-RSSR)Cu(RSSR^-)H^+ + H_2O$$

where $H^+(^-RSSR^-)H^+$ represents the zwitterion form of cystine, $NH_3^+(COO^-)CHCH_2SSCH_2CH(COO^-)NH_3^+$. Thus, the acid dissociation constants for the amino groups, K_{a3} and K_{a4}, will control

the extent of complex formation. Again, for cystine as an example,

$$K_{a3} = [H^+(^-RSSR^-)][H^+]/[H^+(^-RSSR^-)H^+]$$
$$K_{a4} = [(^-RSSR^-)][H^+]/[H^+(^-RSSR^-)]$$

No reliable acid dissociation constants, pK_{a3} and pK_{a4}, were available in the literature for some of the amino acids that were of interest in the present study, and the Speakman method (108) has been applied to determine them.

To discuss this method it may be assumed for simplicity that the dibasic acid may be denoted by H_2A. Then

$$K_{a3} = a_{H^+} \cdot \frac{m_{HA^-}}{m_{H_2A}} \cdot \frac{\gamma_{HA^-}}{\gamma_{H_2A}}$$

$$K_{a4} = a_{H^+} \cdot \frac{m_{A^{2-}}}{m_{HA^-}} \cdot \frac{\gamma_{A^{2-}}}{\gamma_{HA^-}}$$

If y equivalents of strong base, MOH, are added to a solution containing the acid H_2A at molarity x, electrical neutrality requires that

$$m_{H^+} + m_{M^+} = m_{HA^-} + 2m_{A^{2-}} + m_{OH^-}$$
$$= m_{H^+} + y \quad (\text{since } M^+ = y)$$

The initial amount of the acid, x, will represent the ionised and unionised acid present at any instant during the titration, i.e.

$$x = m_{H_2A} + m_{HA^-} + m_{A^{2-}}$$

If
$$z = y + m_{H^+} - m_{OH^-}$$
$$= m_{HA^-} + 2m_{A^{2-}}$$

These several expressions may be combined to give

$$a_{H^+}{}^2 \cdot \frac{z}{2x-z} \cdot \frac{\gamma_{A^{2-}}}{\gamma_{H_2A}} = a_{H^+} \cdot \frac{x-z}{2x-z} \cdot \frac{\gamma_{A^{2-}}}{\gamma_{HA^-}} \cdot K_{a3} + K_{a3}K_{a4}$$

This equation has the form

$$M = NK_{a3} + K_{a3}K_{a4}$$

If, for an acid-base titration, the values of M are plotted against those for N, the graph has a slope which represents K_{a3} and an intercept of $K_{a3}K_{a4}$. The values of M and N may be computed from a knowledge of the number of equivalents of alkali added and the appropriate activities. The activities of undissociated species, γ_{H_2A}, may be taken as unity, and the limiting law of Debye and Hückel used to derive $\gamma_{A^{2-}}$ and

the ratio $\gamma_{A^{2-}}/\gamma_{HA^{-}}$. With the ionic strength, μ, defined by the expression

$$\mu = 0.5\sum_i m_i z_i^2$$

where m_i represents the molality of the ion and z_i is the valence, the limiting law of Debye and Huckel has the well-known general form

$$\log \gamma_i = -Az_i^2\sqrt{\mu}$$

where γ_i is the activity coefficient of the species and A is a constant for the solvent at the specified temperature. For water at 25°, A may be taken as 0.509.

1. Experimental method

The method, apparatus, and experimental conditions described by Hawkins and Perrin (107) were used to make acid-base titrations of the amino acids in the presence of cupric ion, and to determine the pK_{a3} and pK_{a4} values for L-cystine (B.D.H.), D,L-lanthionine (Nutritional Biochemicals Corp.), D,L-homocystine (Pierce Chem. Co.), and D-penicillamine disulphide (Aldrich Chem. Co.). These amino acids were chosen for study because of their closely related molecular structures. They were all used, as supplied, without purification or analyses.

Amino acid solutions were prepared to 2.00×10^{-4} M concentrations, in distilled water that had been out-gassed by boiling, and 50.0 ml portions were taken to yield final concentrations during titrations of 1.00×10^{-4} M. A stock solution of cupric perchlorate (G.Frederick Smith Chem. Co.) was standardized by cation exchange with Dowex 50-X and found to be 2.247×10^{-3} M. Portions (each 5.0 ml) were taken to yield final concentrations of 1.124×10^{-4} M when added to the amino acid solutions. To the mixture of cupric ion and amino acid solutions was added 45.0 ml of stock sodium perchlorate† solution of such concentration that the final ionic strength in the total 100.0 ml volume of the reactants was 0.15. The solutions were then titrated with 0.0981 N NaOH to obtain the cupric complexes. The titrations were made with a Gilmont micrometer burette (2.0 ml total capacity), while stirring the solution with a magnetic stirrer. Each experiment was made under purified nitrogen at 25.0 ± 0.1°C with a fresh salt bridge of ammonium nitrate, sodium nitrate, and agar. For all of these earlier experiments, the pH meter was a Metrohm Herisau, model Compensator E388, calibrated against potassium

---

†Footnote: The sodium perchlorate had been recrystallised from aqueous ethanol and dried in vacuo for 48 hours, prior to preparation of its stock solution.

hydrogen phthalate buffer, pH = 4.01 (25°).

The pK_a titrations were similarly made with 100.0 ml solutions that contained 50.0 ml of the amino acid solution and 45.0 ml of the sodium perchlorate solution, but with 5.0 ml portions of distilled water substituted for the cupric ion solution. The pK_a titration of penicillamine disulphide was made with a 1.00×10^{-3} M solution (instead of 1.00×10^{-4} M as above) ($\mu = 0.15$), in view of the higher solubility of this amino acid.

In later experiments, cupric-amino acid complexes were prepared at various temperatures, for L- and meso-cystine, L- and D,L-homocystine, D,L-lanthionine, and D-penicillamine disulphide. The meso-cystine and L-homocystine were obtained from the Mann Research Lab. Inc., N.Y. and Calbiochem, Los Angeles, respectively. To prepare these complexes portions of $Cu(ClO_4)_2$ solution (3.963×10^{-2} M) were mixed with a solution of amino acid in $HClO_4$ $\left(\frac{N}{I}\right)$ of such volume that the amino acid and cupric ion concentrations in final solution were equivalent. For these experiments, a newly acquired Orion model 701 pH meter with ATC probe, model 07-01-10, was used for determining the pH. Precipitates were collected in a crucible with a fritted disc and washed successively with distilled water, absolute ethanol, and ether.

2. Results

(i) Acid dissociation constants (K_{a3} and K_{a4})

The results of the acid-base titrations are presented in Tables XIV and XV. The pK_a values were calculated by computer programmes, which derived the least-squares gradients and corresponding intercepts for K_{a3} and $K_{a3}K_{a4}$. An example of a programme is shown in Appendix I. The calculated values of pK_{a3} and pK_{a4} for the amino acids used are given in Table XVI. The differences in pK_{a3} and pK_{a4} for cystine and homocystine are those predicted on statistical grounds for consecutive pK_a values of identical, non-interacting groups attached to the same molecule (109),

$$\frac{k_n}{k_{n+1}} = \frac{(N-n)n}{(N-n+1)(n+1)}$$

where k_1, k_2 .... k_n are successive dissociation constants, and N the maximum number of ligands (protons) bound to the molecule. For the four amino acids considered, pK_{a3} and pK_{a4} "overlap", N = 2, n = 1. The theoretically expected difference is therefore $pK_{a4} - pK_{a3} = \log_{10} 4 = 0.60$ (for $K_{a3}/K_{a4} = 1/4$). On this basis, the results for lanthionine and penicillamine disulphide would appear to be anomalous and the behaviour of these additives warrants further investigation.

TABLE XIV

ACID-BASE TITRATIONS FOR COPPER(II)-AMINO ACID COMPLEX FORMATION

Cupric ion concn.: 1.124×10^{-4} M

Amino acid concn.: 1.00×10^{-4} M

$\mu = 0.15$ ($NaClO_4$)

Sodium hydroxide concn.: 0.0981 N

Temperature: 25.0 ± 0.1°C

NaOH (ml)	pH			
	L-cystine	D,L-lanthionine	D,L-homocystine	D-penicillamine disulphide
0	4.271	4.433	4.468	4.328
0.01	4.304	4.482	4.512	4.357
0.02	4.338	4.547	4.594	4.391
0.03	4.372	4.606	4.683	4.422
0.04	4.404	4.658	4.763	4.450
0.05	4.438	4.716	4.839	4.482
0.06	4.470	4.775	4.905	4.516
0.07	4.520	4.834	4.967	4.556
0.08	4.560	4.894	5.036	4.596
0.09	4.598	4.943	5.104	4.632
0.10	4.644	4.996	5.174	4.678
0.11	4.701	5.068	5.247	4.726
0.12	4.765	5.149	5.325	4.788
0.13	4.832	5.224	5.407	4.855
0.14	4.906	5.300	5.488	4.925
0.15	4.995	5.396	5.577	5.018
0.16	5.116	5.516	5.690	5.132
0.17	5.287	5.693	5.833	5.312
0.18	5.548	5.938	6.023	5.611
0.19	5.998	6.370	6.280	6.341
0.20	6.788	6.978	6.741	7.093

TABLE XV

ACID-BASE TITRATIONS FOR pK_{a3} AND pK_{a4} OF

DIBASIC AMINO ACIDS

Amino acid concn.: 1.0×10^{-4} M

$\mu = 0.15$ ($NaClO_4$)

Sodium hydroxide concn.: 0.0981 N

Temperature: 25.0 ± 0.1°C

NaOH (equivalents) $\times 10^4$	pH		
	L-cystine	D,L-lanthionine	D,L-homocystine
0.04903	6.514	6.463	-
0.09806	6.818	6.704	-
0.1471	6.986	6.861	-
0.1961	7.120	6.970	-
0.2451	7.221	7.052	7.262
0.2942	7.306	7.122	7.351
0.3432	7.367	7.178	7.437
0.3922	7.428	7.231	7.494
0.4413	7.487	7.281	7.542
0.4903	7.532	7.330	7.588
0.5393	7.576	7.371	7.632
0.5884	7.618	7.411	7.674
0.6374	7.662	7.448	7.722
0.6864	7.701	7.482	7.755
0.7354	7.734	7.512	7.788
0.7845	7.770	7.540	7.817
0.8335	7.794	7.560	-
0.8825	7.822	7.581	-
0.9316	7.847	7.606	-
0.9806	7.876	7.628	-

.... contd. next page

TABLE XV (CONTD.)

Amino acid concn.: 1.0×10^{-3} M

$\mu = 0.15$ ($NaClO_4$)

Sodium hydroxide concn.: 0.0981 N

Temperature: 25 ± 0.1°C

NaOH (equivalents) $\times 10^3$	pH
	D-penicillamine disulphide
0.2942	7.058
0.3432	7.150
0.3922	7.230
0.4413	7.305
0.4903	7.372
0.5393	7.436
0.5884	7.694
0.6374	7.555
0.6864	7.608
0.7354	7.662
0.7845	7.716
0.8335	7.767
0.8825	7.814

TABLE XVI

CALCULATED pK_{a3} AND pK_{a4} VALUES OF AMINO ACIDS

AMINO ACID (μ = 0.15; 25°)	pK_{a3}	pK_{a4}
L-cystine	8.03	8.62
Literature values (107)	8.03	8.80
D,L-homocystine	8.09	8.67
D,L-lanthionine	8.01	8.09
D-penicillamine disulphide	7.68	9.01

(ii) Complex formation

The pH data for complex formation are illustrated in Figure 12. The values of pH represent the instantaneous readings, as certain values tended to drift slowly, presumably due to precipitation of insoluble species. The Cu(II) complexes of cystine and homocystine are highly insoluble in water. Neutralized Cu(II)-lanthionine solutions gave low yields of a blue precipitate, whereas neutralized Cu(II)-penicillamine disulphide solutions showed no precipitation of insoluble species, even after several days. However, it was possible to obtain crystals of the complex by evaporation of the solvent, as outlined later.

The distributions of polynuclear cupric complexes formed from each of these four amino acids undoubtedly vary, because of steric or other factors, and it is noteworthy that despite the similarity in pK_{a3} and pK_{a4} for cystine and homocystine, their titration curves do not coincide over most of the pH range investigated. Analyses to obtain stability constants for the complexes of the Cu(II)-amino acid systems have not been attempted, owing to the anomalous pK_a values of lanthionine and penicillamine disulphide, and because of possible changes in the equilibria involved when insoluble species are precipitated. Moreover, no physical technique was readily available by which to determine the possible presence, and estimate the concentration of polynuclear species. It may be concluded, however, that all

FIGURE 12

Acid-base titrations for complex formation between cupric ion (1.124×10^{-4} M) and the amino acids (1.00×10^{-4} M): L-cystine (———), D-penicillamine disulphide (— —), D,L-lanthionine (·—·—·), and D,L-homocystine (— — —). (μ = 0.15; temperature: 25.0 ± 0.1°C)

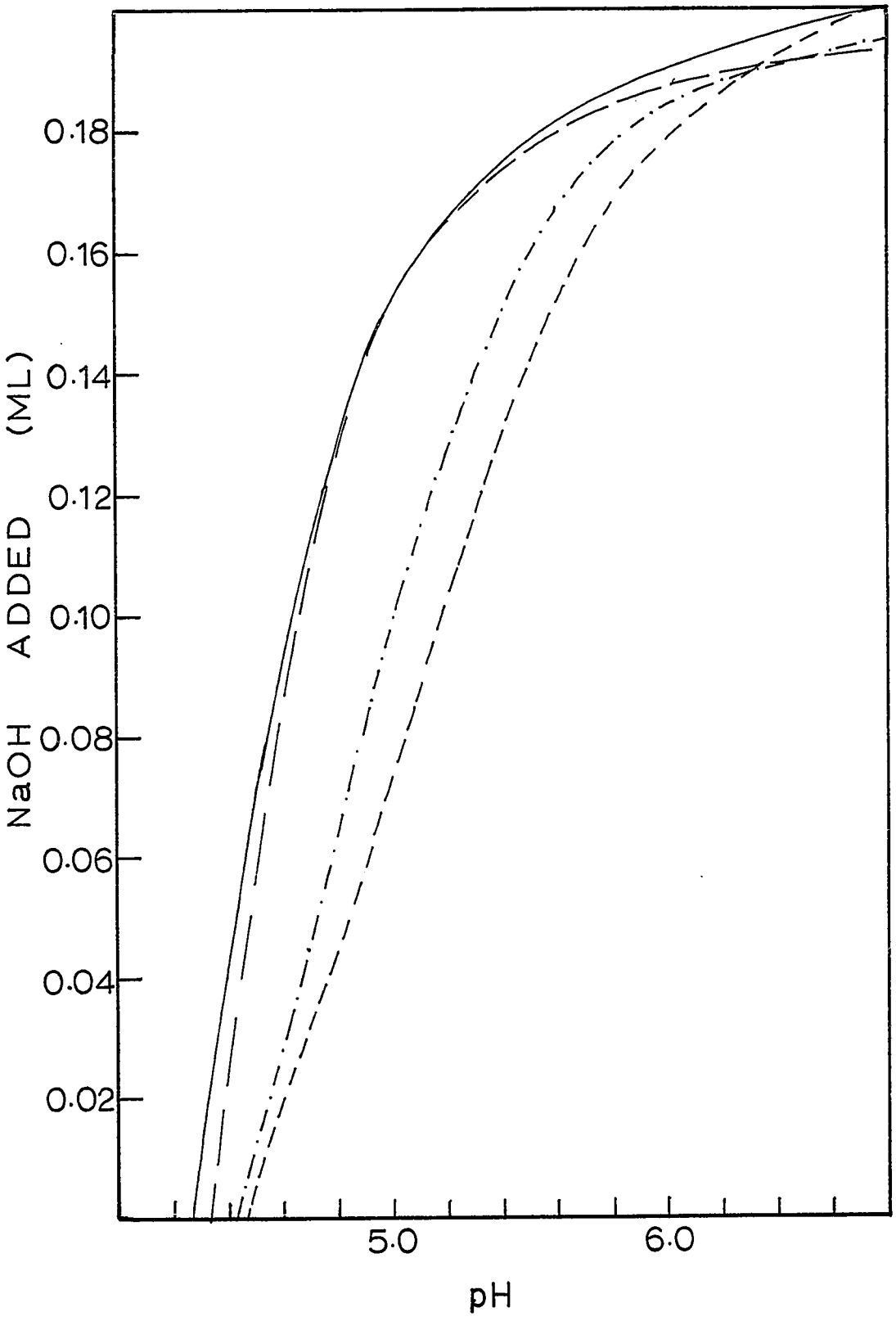
0·18
0·16
0·14
0·12
0·10
0·08
0·06
0·04
0·02
NaOH ADDED (ML)
5·0
6·0
pH

four of the amino acids are likely to exist as their fully protonated forms in the standard electrolyte i.e Cu(II) complex formation at the cathode would be restricted by the acidic conditions.

(iii) Elemental analyses

In Table XVII are found elemental analytical data for complexes prepared at 0° and 100°C of the four amino acids investigated. The analytical data for the insoluble Cu(II)-cystine complex prepared at 0°C correspond reasonably well to an empirical formula $Cu(C_6H_{10}N_2S_2O_4).\frac{1}{2}H_2O$. The water content was confirmed by experiments in which samples were heated at 120°; typically, 258.2 mg of the complex lost 7.6 mg when heated to constant weight. These analyses did not seem to be consistent with published data of Hawkins and Perrin (107) and further studies of this complex were therfore made.

Hawkins and Perrin used a preparative method applicable at higher temperatures, outlined originally by Rây and Bhaduri (105). When the complex was prepared at 100°, analytical data (Table XVII) were in agreement with their empirical formula. It is possible that they isolated a mixture of products. This is suggested by the observation in the present study that, when acidic solutions containing Cu(II) ion and cystine in a 1:1 molar ratio were rapidly brought to pH 7-8 at 5° temperature intervals, the precipitates obtained were light blue-violet (0°-65°), pale blue (65°-75°), grey-blue (75°-90°), and finally

TABLE XVII

ANALYSES† OF Cu(II)-COMPLEXES OF CYSTINE AND RELATED AMINO ACIDS

COMPLEX	Percentages by weight C	H	N	S
Cu(II)-L-cystine (0°) Found	23.43	3.58	9.07	20.40
Yield 98.6 %	23.10	3.63	8.88	20.65
Calcd. for $Cu(C_6H_{10}N_2S_2O_4).1/2H_2O$	23.18	3.57	9.01	20.63
Cu(II)-L-cystine (100°) Found	22.88	3.78	8.70	19.97
Calcd. for $Cu(C_6H_{10}N_2S_2O_4).H_2O$	22.53	3.78	8.76	20.05
Cu(II)-meso-cystine (0°) Found	21.99	3.17	8.70	20.89
Yield 99.3 %				
Cu(II)-D-penicillamine disulphide (pseudomorphic form) Found	29.36	5.52	6.95	15.55
	29.21	6.12	6.85	15.35
Calcd. for $Cu(C_{10}H_{18}N_2S_2O_4).3H_2O$	29.15	5.87	6.80	15.56
Cu(II)-L-homocystine (0°) Found	28.42	4.56	8.14	18.63
Yield 98.4 %	28.14	4.58	7.93	18.96
Calcd. for $Cu(C_8H_{14}N_2S_2O_4).1/2H_2O$	28.35	4.46	8.27	18.92

.... contd. next page

TABLE XVII (CONTD.)

COMPLEX	Percentages by weight C	H	N	S
Cu(II)-D,L-homocystine (100°) Found	24.90	4.69	6.64	14.93
Cu(II)-D,L-lanthionine (0°) Found Yield 58.1 %	25.03	4.38	9.41	7.89
Calcd. for $Cu(C_6H_{10}N_2SO_4).H_2O$	25.04	4.20	9.74	11.14

† All C,H,N, and S microanalyses were made by the Schwarzkopf Microanalytical Lab., N.Y.

pale green (100°). The weight yields remained constant within about ±5 %. Similarly, at 100° homocystine complexes of Cu(II) gave a green coloured, insoluble precipitate and penicillamine disulphide a greenish solution of complexes.

The marked instability of the disulphide group of cystine towards alkali in the presence of certain heavy metal ions is well known (90,110). At the higher temperatures, it is likely that the disulphide groups of cupric complex species suffered base hydrolyses. Danehy and Hunter (111) have proposed that the most likely initial step in the alkaline decomposition of cystine and penicillamine disulphide, by aqueous sodium hydroxide ($\frac{N}{1}$) at 35.2°C, is direct nucleophilic attack by hydroxyl ion on the disulphide groups. Such a mechanism yields products according to the Schiller-Otto stoichiometry, i.e. 75 % thiol, 25 % sulphinic acid. The hydrolyses of disulphides in the presence of metal ions are complex (112,113), and vary with the nature of the disulphide and the metal ion. Under certain conditions, Cecil and McPhee (113) found the reaction to be first order in respect of both the disulphide and the metal ion. To examine the possible interconversion of complexes formed at different temperatures, 50.0 mg of the green Cu(II)-cystine complex formed at 100°C was dissolved in 10.0 ml $HClO_4$ solution ($\frac{N}{1}$) at room temperature, left 48 hours and then neutralized to pH 7.0. The light blue-violet

complex characteristic of a preparation at room temperature was recovered in 75 % yield (identity confirmed by infrared spectrum). It is conceivable, especially in view of the elemental analyses, that the green compound is a mixed complex of Cu(II) ion with both cysteine and cysteine sulphenic acid. The mass balance could then be described by the equations,

$$2RSSR + 2Cu(II) + 2H_2O \xrightarrow{\Delta, OH^-} 2(RSHCu(II)RSOH) \quad \text{(green)}$$

$$2(RSHCu(II)RSOH) \longrightarrow 2Cu(II) + 3RSH + RSO_2H$$

$$6RSH + 1.5\ O_2 \longrightarrow 3RSSR + 3H_2O$$

$$3Cu(II) + 3RSSR \longrightarrow 3(RSSRCu(II))$$

However, it should be noted that sulphenic acids are usually quite unstable (114,115,116) and that cysteine sulphenic acid has never been isolated. No attempt has been made by the author to isolate and identify the pure components of these high-temperature, green compounds but they might provide a preparative route to unstable sulphenic acids. The green soluble cupric complex of penicillamine disulphide that is formed at 100°C is possibly amenable to crystallisation and this would permit x-ray determination of its structure from a single crystal of the material.

As noted previously, the molecularity of the Cu(II)-cystine complex has not been ascertained. Its insolubility

hampers the application of most of the appropriate experimental techniques. Perhaps the molecularity could be checked by a study of the kinetics of formation, but equipment suitable for very fast reactions would be needed (cf. ref. (117)) and was not available. There are also other uncertainties in the characterisation of these cupric species that should not be underestimated. Thus, in Table XVII many of the analytical data do not permit even the assignments of empirical formulae with assurance, since non-stoichiometric analyses may result from the presence of polynuclear species or free amino acid in the precipitate. Water molecules may also be present, either hydrogen bonded in the polycrystalline solids, or bonded to the metal ion as aquo ligands (118).

(iv) Infrared spectra of complexes

The infrared spectrum of the Cu(II)-cystine complex formed at 0°C was obtained in the region from 4000-250 cm^{-1} and is shown in Figure 13, in comparison with a spectrum for cystine of equivalent molar amount in KBr discs i.e. 0.311 mg and 0.240 mg in 210 mg KBr, respectively. Infrared spectra of the copper complexes, described in this section, were measured with Perkin-Elmer spectrometers; a model 337 instrument was used for Nujol mulls, and a model 521 instrument for KBr discs, of the complexes. Calibration spectra were taken with polystyrene film and atmospheric

FIGURE 13

Infrared spectra of Cu(II)-complexes (in KBr discs).
Full line: Light blue-violet needles of Cu(II)-cystine complex formed at 0°C.
Dotted line: L-cystine.

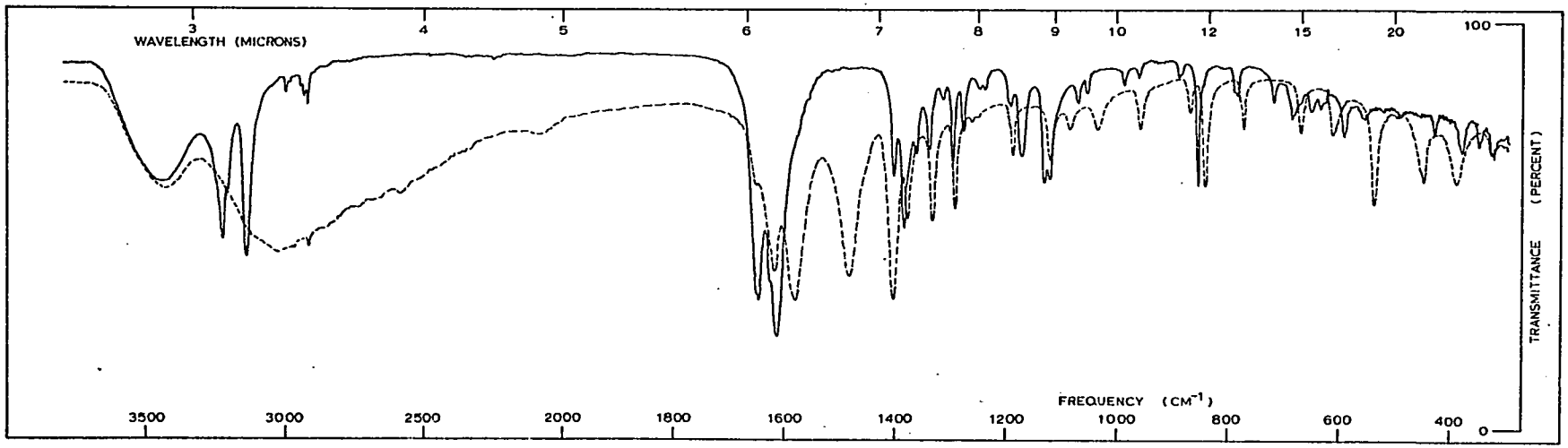
WAVELENGTH (MICRONS)
3
4
5
6
7
8
9
10
12
15
20
100
TRANSMITTANCE (PERCENT)
0
FREQUENCY (CM⁻¹)
3500
3000
2500
2000
1800
1600
1400
1200
1000
800
600
400

water vapour. Peak positions of the spectra of complexes are considered to be reproducible to at least ±5 cm^{-1}.

Herlinger, Wenhold, and Long (120) have catalogued the copper ligand stretching frequencies for copper amino acid complexes, the structures of which are known from x-ray determinations, and have suggested vibrational criteria to distinguish between cis and trans configurations. For trans complexes asymmetric stretching modes are predicted at circa 470 cm^{-1} for ν(Cu-N) and at circa 330 cm^{-1} for ν(Cu-O), but for cis complexes two stretching modes, asymmetric and symmetric, are predicted for each linkage. If the Cu(II)-cystine complex formed at 0°C were a monomer, the complex with meso-cystine might well be a cis geometric isomer, as follows:

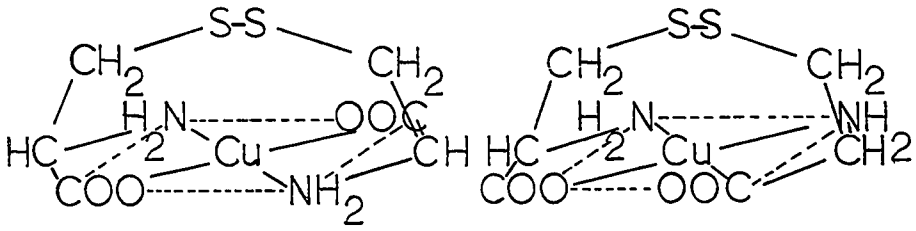

L- or D-cystine, trans meso-cystine, cis

The infrared spectrum of the Cu(II)-meso-cystine complex formed at 0°C was indistinguishable with the

resolution used from that for the Cu(II)-L-cystine complex formed at the same temperature. However, this statement should be qualified by adding that the extent and rate of racemisation was not established for the conditions used in preparation of the complexes. The racemisation rate is not expected to be high at 0° (85).

Table XVIII contains empirical assignments for the Cu(II)-L-cystine complex formed at 0°C, mostly based on the Urey-Bradley force-field analysis of Condrate and Nakamoto (121) for trans square-planar coordination of metal glycino complexes. In Figure 14, the spectral region that was chosen to apply the vibrational criteria of Herlinger et al is shown for Cu(II)-L-cystine complex formed at 0°C, measured with 4.0 mg of the complex in 200mg KBr disc. It is tentatively proposed from these data that the complex is bonded in cis configuration with cupric ions, as long-chain polynuclear molecules.

The form of the spectrum for the region shown in Figure 14 is remarkably similar to that observed by Herlinger et al for Cu(II)-bis(L-isoleucine).H_2O and that for Cu(II)-bis(D,L-phenylalanine).H_2O complexes (120). The authors assigned cis configurations to both of these complexes on the basis of their infrared spectra. It is of interest to note that Cu(II)-bis(D,L-phenylalanine).H_2O exists as blue-violet, needle-like crystals (vide infra).

TABLE XVIII

INFRARED SPECTRA OF L-CYSTINE AND CUPRIC-L-CYSTINE COMPLEX FORMED AT 0°C

L-cystine (cm^{-1})	Cu(II)-L-cystine (cm^{-1})	Tentative assignment
3440 s	3450 s	Coordinated H_2O
3030 s,br	3235 s	NH_2 asym. str.
-	3215 s,sh	
-	3148 s	NH_2 sym. str.
-	3008 w	CH_2 sym. str.
-	2925 w	CH_2 sym. str.
2090 w,br	-	SH str.
1654 m,sh	1654 s,sh	
1621 s	1650 s	NH_2 scissoring
-	1629 s,sh	
1584 s	1617 s	C=O asym. str.
1485 s	-	NH_3^+ sym. str.
1407 s	1406 m	CH_2 scissoring
1382 m	1387 s	C-O sym. str.
-	1365 m	
1337 m	1341 m	
-	1317 w	CH_2 wagging
1295 m	1300 m	
-	1281 m	
1264 w	1250 w	
1253 w	1242 w	
1191 m	1195 w	CH_2 twisting

.... contd. next page

TABLE XVIII (CONTD.)

L-cystine (cm^{-1})	Cu(II)-L-cystine (cm^{-1})	Tentative assignment
-	1175 m	C-N str.
-	1134 m	NH_2 twisting
1125 m	1124 m	
1088 w	1073 w	
1038 w	1057 w	NH_2 wagging
-	992 w	
962 m	964 w	C-C str.
873 w	892 w	CH_2 rocking
845 s	857 s	C-S str.?
775 m	788 m	C=O in plane
-	722 m	
673 m	689 m	NH_2 rocking
-	654 m	C=O out-of-plane
615 m	636 w	C=O out-of-plane
608 w,sh	-	
540 m	594 w	C=O out-of-plane
-	558 w	Ring defn., C-C-N bend? (122)
-	523 w	
497 w	494 w	Cu-N asym. str.
452 m	431 m	Cu-N sym. str.
392 m	382 m	Out-of-plane ring defn.
-	352 m	Cu-O asym. str.
325 m	325 m	Skeletal defn.
-	281 w	Cu-O sym. str.

s - strong, m - medium, w - weak, br - broad, sh - shoulder

FIGURE 14

Infrared spectrum of Cu(II)-L-cystine complex formed at 0°C (in KBr disc). Metal-ligand assignments are indicated by asterisks.

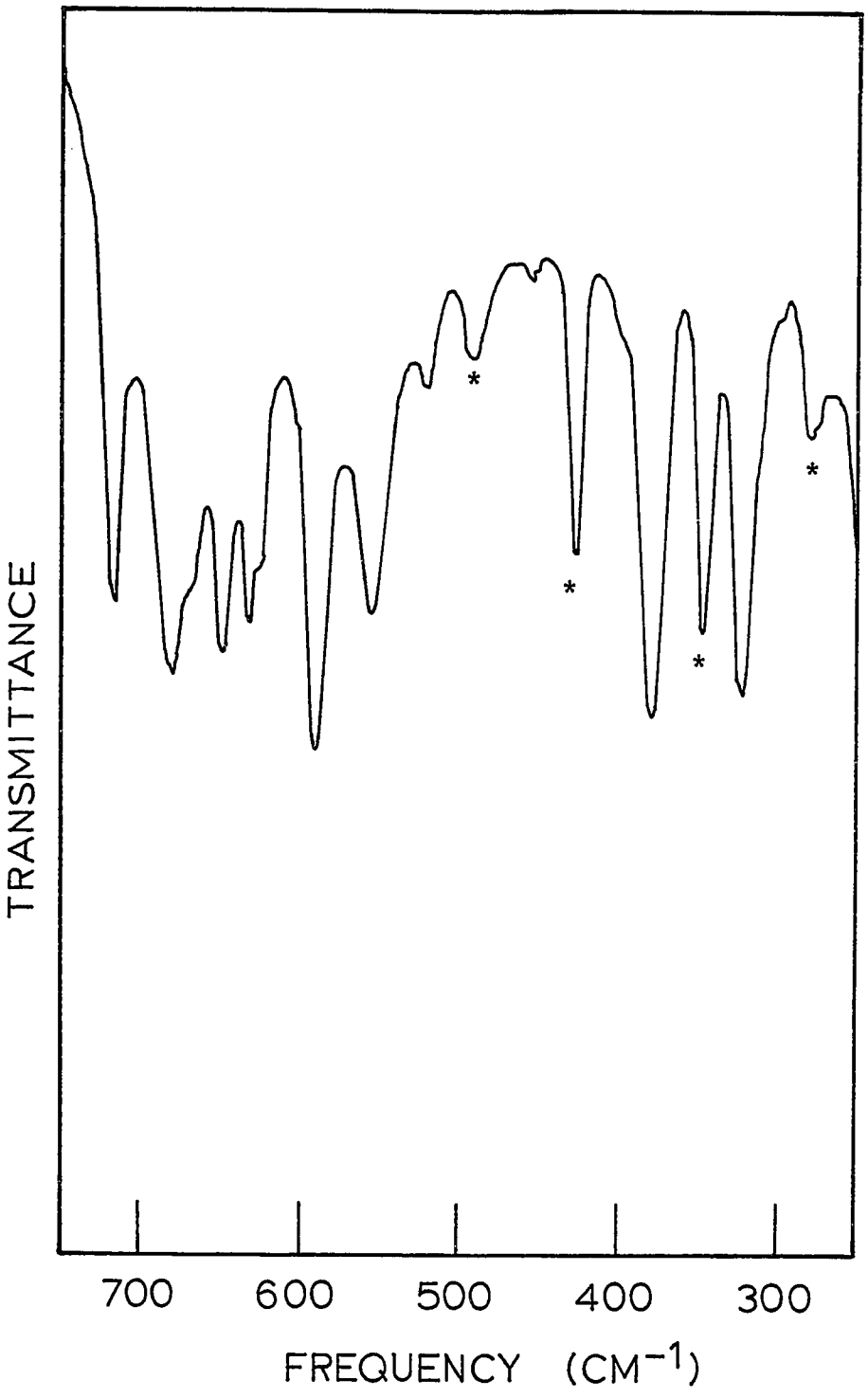
TRANSMITTANCE
700
600
500
400
300
FREQUENCY (CM⁻¹)

The cis geometrical isomerism of Cu(II)-bis(L-isoleucine). H_2O has been confirmed by the x-ray diffraction method (120). Herlinger et al have reiterated that stabilisation of the relatively unusual cis configuration may depend on a first-coordination-sphere interaction with a single water molecule, leading to an extensive hydrogen-bonding network and efficient packing. They suggest further, that such factors may be more important for formation of the isoleucine complex than energy terms arising from the difference in chelate ring geometries. It is reasonable, too, that the packing variations of molecular units is ultimately reflected in the morphology of these crystals. Thus, although Hawkins and Perrin may be correct in their supposition that the major solution species of Cu(II)-cystine is a dimer, the molecularity and geometrical isomerism of solid-state species can depend on other factors e.g. hydrogen bonding, the "twist" of the chelate molecule, etc..

It would be interesting to apply the infrared vibrational criteria to the cupric complexes of L-homocystine and meso-homocystine prepared at 0°C, as these may be able to form fully chelated trans and cis monomers, respectively, because of the longer carbon chain length of homocystine compared with that of cystine. The analyses for Cu(II)-homocystine complexes formed at 100°C generally revealed a lower sulphur content than that anticipated from comparison

with the cystine complex formed at the same temperature, and desulphuration of the disulphide group in the homocystine complexes might be suspected.

Figure 15 contains the spectrum of the green Cu(II)-L-cystine complex formed at 100°C, obtained with 1.0 mg in a 200 mg KBr disc. A strong band in the spectrum of the complex formed at 0°C, at 857 cm^{-1}, which conceivably could be associated with the disulphide group, is reduced in intensity in the complex formed at 100°C, and a new strong band appears in the spectrum at 1102 cm^{-1}. No assignments were attempted for this compound, since no spectrum was available for another compound that might serve as a basis for comparison, nor were the analytical data adequate for confident characterization of it.

For spectra of metal complexes with large organic chelate molecules, not only have band assignments to be made on an empirical basis in most cases, but the conditions under which the solid, polycrystalline KBr discs permit spectra to be made can also introduce difficulties. The complications involved in the differentiation of geometrical isomers by infrared spectroscopy have been discussed by Hawkins (119). He points out, for example, that intramolecular interactions, on the basis of which criteria for isomer selection are made, are often of magnitude similar to intermolecular crystal effects. In addition, hydrogen

FIGURE 15

Infrared spectrum of green Cu(II)-L-cystine complex formed at 100°C (in KBr disc).

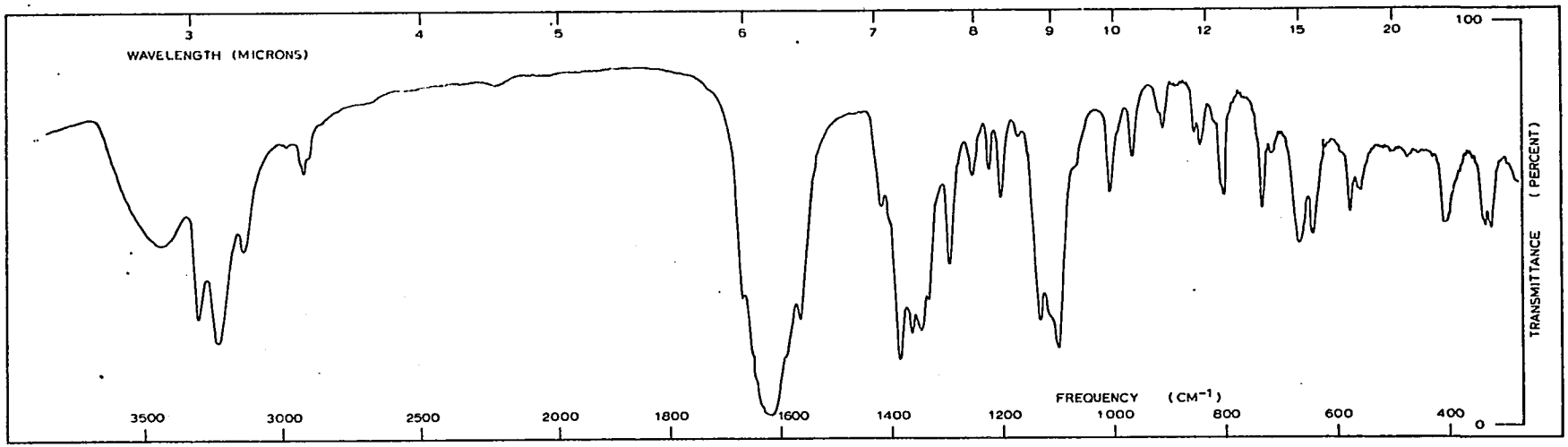
WAVELENGTH (MICRONS)
3
4
5
6
7
8
9
10
12
15
20
100
TRANSMITTANCE (PERCENT)
0
FREQUENCY (CM⁻¹)
3500
3000
2500
2000
1800
1600
1400
1200
1000
800
600
400

bonding or other interactions, can also cause shifts in the frequencies of some modes, and peak assignments become correspondingly more difficult to make on an empirical basis. Nevertheless, attempts must be made to evaluate the extent of problems such as these in the application of infrared spectroscopy and progress will only be made with a part theoretical-part empirical approach.

(v) Cu(II) complexes of penicillamine disulphide[†]

It was mentioned earlier that it was possible to obtain crystals of the soluble Cu(II)-penicillamine disulphide complex by evaporation of the solvent. To obtain these crystals, 296.4 mg of D-penicillamine disulphide was dissolved in about 50 ml of distilled water, and an equivalent amount of freshly precipitated cupric hydroxide was added. The resulting deep blue solution, after filtration, was allowed to evaporate from an open dish at room temperature. If a film or cloudiness developed during evaporation, the solution was again filtered. Royal blue crystals were finally deposited. These effloresced in the atmosphere to form extremely brittle, blue pseudomorphic

---

[†]Footnote: Cu(II)-penicillamine disulphide complexes have not been previously described in the literature. They may be of interest in the treatment of Wilson's disease. A brief discussion of this aspect of their chemistry is presented in Appendix II.

crystals, but the change was sufficiently slow (≃ 150 min) that crystals of the unstable hydrate could be suspended in toluene and their density determined on a Berman specific gravity balance calibrated with calcite crystals.

Elemental analyses of the pseudomorphic form, shown in Table XVII, were consistent with an empirical formula $[Cu(C_{10}H_{18}N_2S_2O_4).3H_2O]$. The weight loss to constant weight of the unstable hydrate was 7.83 % at room temperature. If the loss is assumed to be due entirely to loss of water molecules, this corresponds to an empirical formula of $[Cu(C_{10}H_{18}N_2S_2O_4).5H_2O]$. Some of the water molecules may be bonded in the square-planar configuration to cupric ions as aquo ligands, because steric effects caused by the methyl groups prevent chelation by the amino or carboxylate groups.

Some preliminary x-ray measurements were made on the unstable hydrate crystals and on the pseudomorphic form of the complexes. X-ray geometrical data are summarized in Table XIX. The crystal morphology of the unstable hydrate may be illustrated as follows:

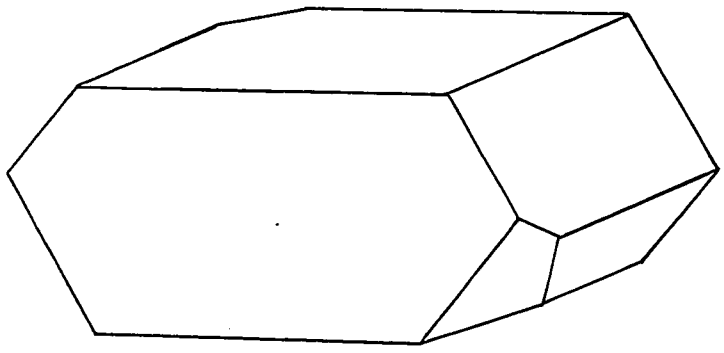

TABLE XIX

SUMMARY OF X-RAY DIFFRACTION DATA OF

CUPRIC-PENICILLAMINE DISULPHIDE COMPLEXES

Unstable hydrate, emp. formula $Cu(C_{10}H_{18}N_2S_2O_4).5H_2O$

a = 1.551 ± 0.008 nM

b = 1.994 ± 0.060 nM

c = 1.224 ± 0.014 nM

β = 92°8'

ρ meas. = 1.54(2)

ρ calc. = 1.57(6)

z = 8

Monoclinic, space group A2 (from morphology). Data were collected by zero-level Precession photographs, and zero- and first-level Weissenberg photographs. Single crystal mounted along c-axis in glass tube under saturated solution. Radiation-Cu(Ni filter).

Pseudomorph, emp. formula $Cu(C_{10}H_{18}N_2S_2O_4).3H_2O$

a = 1.488 ± 0.036 nM

b = 1.862 ± 0.080 nM

c = 1.232 ± 0.020 nM

Orthorhombic, "space group" Pnmm. Data were collected by zero- and upper-level Precession photographs with various crystal alignments. Radiation-Mo(Zr filter).

Electron microscope photographs of the Cu(II)-cystine crystals prepared at 0°C, and those of the pseudomorphic form of Cu(II)-penicillamine disulphide are shown in Figure 16. The almost unique fibrous morphology of the Cu(II)-cystine complex has prompted several studies (106,123). Kahler et al have estimated the height and width of the fibres to be equal at 8.5 ± 0.5 nM (106). They concluded that the fibres are formed because the solid complex comprises a linear chain, polymeric structure. Although the x-ray photographs of the Cu(II)-penicillamine disulphide pseudomorph reveal powder-like diffraction bands for the reciprocal lattice net a*b* (Figure 17), which could be indicative of a bundle of fibre needles, the electron microscope photographs show that the morphology is quite unlike that of the Cu(II)-cystine crystals. Partially randomized molecules and plate-like crystallites would seem to be generated in the dehydration and transformation to the pseudomorphic form.

Cuprous-amino acid complexes

The formation of cuprous cysteinate has been used as an analytical determination for the cysteine and cystine contained in wool hydrolysates (90,124), from which it is precipitated by the reaction of either cysteine or cystine with excess cuprous chloride. An alternative preparation

FIGURE 16

Electron microscope photographs of copper complexes.
Top: Light blue-violet needles of Cu(II)-L-cystine complex formed at 0°C. Magnification: × 6730.
Lower: Pseudomorphic form of Cu(II)-D-penicillamine disulphide complex. Magnification: × 5830.

FIGURE 17

X-ray diffraction photographs of copper complexes.
Top: Unstable hydrate of Cu(II)-D-penicillamine disulphide complex. 0-level reciprocal lattice net, a*c*.
Lower: Pseudomorphic form of Cu(II)-D-penicillamine disulphide complex. 0-level reciprocal lattice net, a*b*.

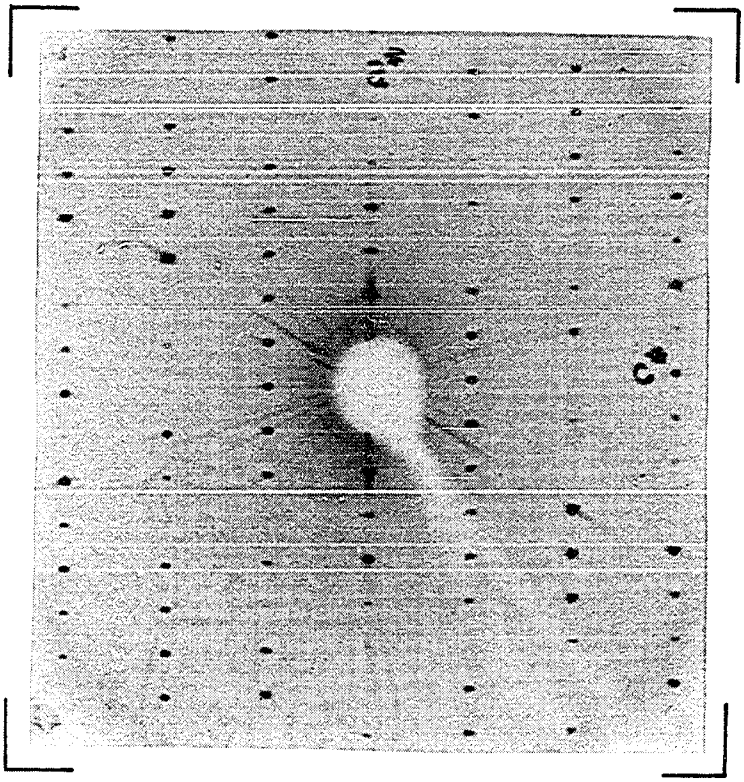

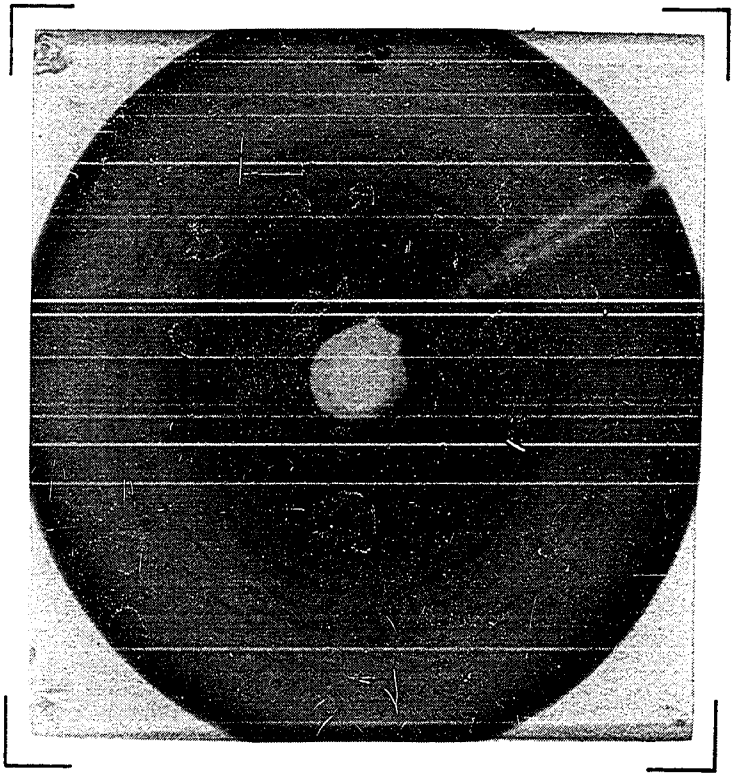

has been described by Swan (125), who suggested that ascorbic acid would reduce cupric copper to cuprous rapidly and irreversibly and that the equilibrium could be displaced owing to the precipitation of cuprous cysteinate, insoluble at pH 4. The reactions are

$$2Cu^{2+} + C_6H_8O_6 \longrightarrow 2Cu^{+} + C_6H_6O_6 + 2H^{+}$$

$$RSSR + 4Cu^{+} \rightleftharpoons 2RSCu + 2Cu^{2+}$$

Cu(I)-cysteinate species have been investigated by the polarographic method (126). Again, as for the Cu(II)-cystine complexes, the insolubility and the possibility of the formation of polynuclear complexes, cf. (127), complicate any structural analyses.

Cysteine has three possible coordination sites - the carboxylate, the amino, and the sulphydryl groups. In strongly acidic media (pH<2), these should all be protonated. However, metal ion complexes can form by chelation with amino acid molecules and anions, in which one or several sulphur atoms act as donor ligands (128,129,130). Mixed Cu(II) and Cu(I) complexes should also be possible, by analogy with the complex $(AgCuMt_2)ClO_4$, where Mt = methionine (129). It was necessary, therefore, to examine the reactivity of Cu(I) with potential ligands in 1M H_2SO_4.

1. Preparation of complexes

Cuprous cysteinate was prepared by the procedure described by Swan. The preparation required that all solutions be deaerated and handled in a glove-bag under nitrogen. L-cystine (0.240 g) was dissolved in 50 ml NH_4OH $(\frac{N}{1})$ and the pH was adjusted to about 9-10 by addition of acetic acid. Ascorbic acid (0.5 g) was added, followed by a solution of $CuSO_4.5H_2O$ (0.500 g) in 50 ml distilled water. A deep brown intermediate formed and disappeared to give a yellow-brown solution. With acidification to pH ≃ 4-5 with acetic acid, cream-coloured cuprous cysteinate was precipitated. When the cuprous-cysteinate precipitate and solution were poured into excess 1M H_2SO_4, a gelatinous yellow precipitate formed. This was filtered off and vacuum dried overnight. When the preparation was repeated with a copper ion:methionine molar ratio of 1:1, a clear, pale green solution was obtained without formation of a precipitate.

2. Elemental analyses

Analyses of the yellow precipitate, obtained from the above preparation, gave: C 11.07 %, H 3.78 %, N 6.40 %, S 21.29 %. The copper content, estimated by E.D.T.A./murexide titrations, was 16.8 % (131). No empirical formula can be suggested from the analytical data and the preparative method probably requires further examination and development.

The nitrogen:carbon ratio of 1.5:3 found analytically was higher than that expected for ligands of cysteine alone (1:3), and it is possible that the yellow solid contained ammonium cations, sulphate anions, and water molecules, as well as Cu(I) ion and cysteine ligands. The yellow compound darkened on its surface when exposed to air, as did the original cream-coloured cuprous cysteinate complex.

POLARISATION STUDIES

Polarisation measurements are frequently made to investigate the behaviour of organic compounds as addition agents during the electrodeposition of metals. They are often applied in combination with other experimental methods and usually require relatively simple apparatus. The polarisation produced by an additive has frequently been thought to depend most directly on the extent to which the surface of the electrode is covered by the additive. However, the effects of coverage on reactions at uncovered portions of the surface may be slight (as with certain reactions on mercury) or may be unpredictable and highly complex e.g. in electrocrystallisation processes (19). As a consequence, the major applications of polarisation data have been to determine the amount of a given addition agent present in an electrolyte (e.g.(98)), rather than as a means

of assessing the role or efficacy of the additive. Nevertheless, the sensitive response of polarisation values to the presence of additives made it of particular interest in the present study to examine the polarisations produced by cystine and methionine during copper deposition, in relation to the radioisotopic data reported previously for the extents of their occlusion in the deposits, and to their characteristics as complexing agents with cupric and cuprous ions.

Apparatus and method

Polarisation measurements were made in a vertical cell with a Luggin probe, similar in design to a cell which has been described previously (55), but constructed entirely from glass and teflon. A schematic, self-explanatory diagram of it is shown in Figure 18.

Additive solutions of required concentrations were prepared in standard electrolyte as solvent. The additives used were D,L-lanthionine and D-penicillamine disulphide (Aldrich Chem. Co.), L-cystine and D,L-methionine (Fisher Scientific Co.), D,L-selenocystine (Sigma Chem. Co.), and D,L-homocystine (Pierce Chem. Co.).

Directly prior to each experiment, disc cathodes of polycrystalline copper plate were cleaned with emery paper,

FIGURE 18

Schematic diagram of cell for polarisation measurements.

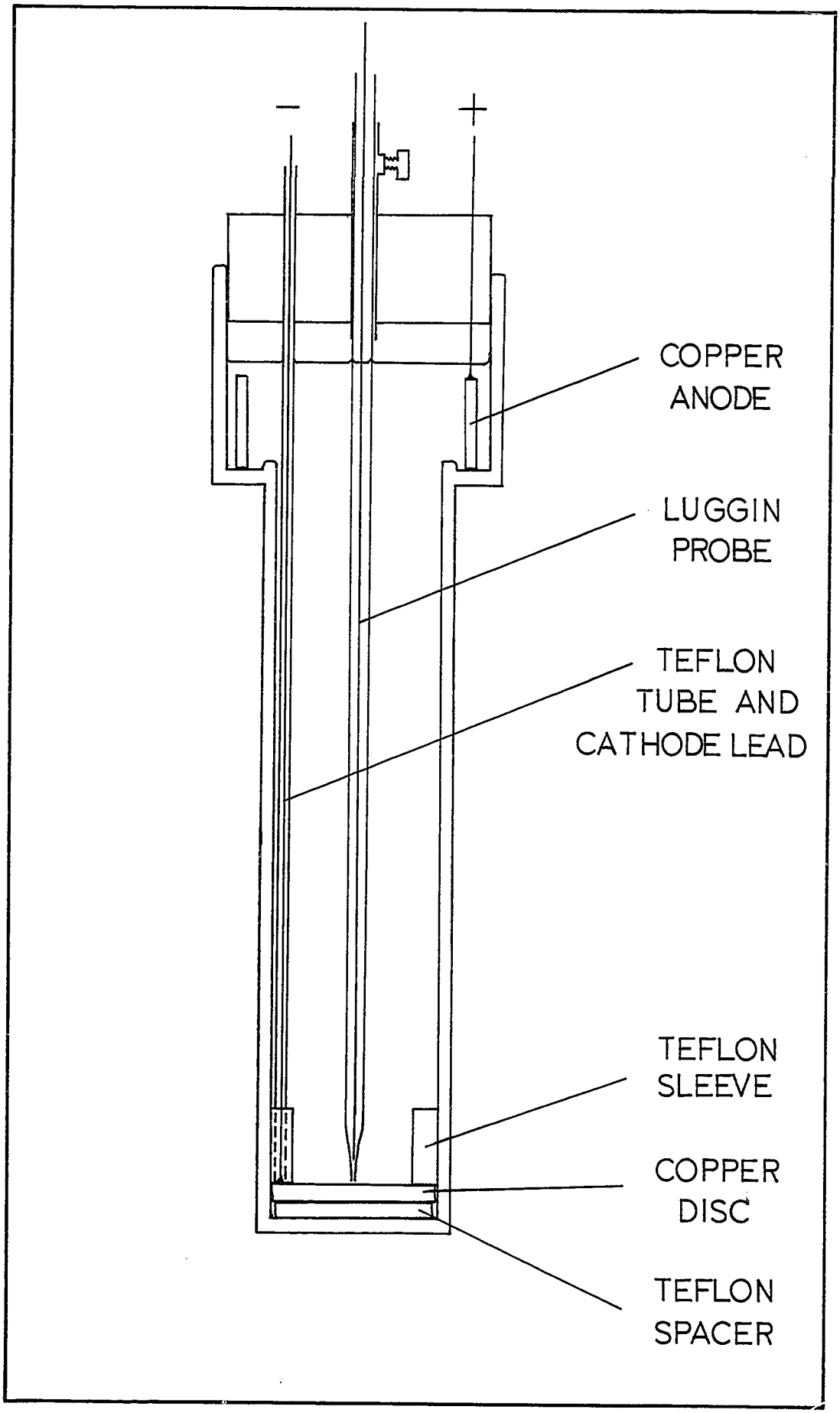
−
+
COPPER
ANODE
LUGGIN
PROBE
TEFLON
TUBE AND
CATHODE LEAD
TEFLON
SLEEVE
COPPER
DISC
TEFLON
SPACER

etched, and electropolished (anodically) with a D.C. potential of 6V for 20 minutes. Then followed thorough washes with 10 % orthophosphoric acid, triple distilled water, and finally standard electrolyte. Polarisation figures represent the so-called steady-state values, obtained after 60 minutes of galvanostatic deposition at a particular current density.

In another series of experiments, cathodic substrates were prepared by deposition from the pure standard electrolyte. The conditions employed were 2.0 A dm^{-2} for 60 minutes on polycrystalline copper discs which had been etched, as outlined earlier, and washed in standard electrolyte. The polarisation values were recorded after 10 minutes of deposition at current densities progressing from the lowest to the highest, 0.25-5.0 A dm^{-2}.

Cathodic overpotential measurements were made with a conventional circuit and potentiometer (Gray Instruments, model no.9302). No corrections were made for resistance polarisation, on the assumption that these should cancel to a good approximation when $|\Delta\eta|$ values are derived (62). All depositions were conducted at 25.0 ± 0.1°C. After each experiment the cathodes were washed in warm tap water, rinsed with acetone to prevent tarnishing, and quickly dried. They could then be stored in a desiccator until required for microscopic examinations, without depreciation of their

surface brightnesses.

Results

Tables XX-XXII summarize the overpotentials measured with a series of sulphur-containing amino acid additives for copper deposition on electropolished and electrodeposited substrates. In the current density range 0.50-3.5 A dm^{-2}, the polarisation values for deposition from the standard electrolyte without additives were slightly higher on the electropolished than the electrodeposited substrates. On the electrodeposited substrates, the overpotential at 2.0 A dm^{-2} was 107 ± 10mV and the least-squares Tafel slope, b, for current densities 0.50-2.0 A dm^{-2} was calculated to be 51 ± 3mV. These values are in reasonable accord with the published results of 105 ± 5mV and 52 ± 1mV, respectively (61,62).

An interesting aspect of the polarisation-current density data on electropolished substrates is the relative effectiveness of these amino acid additives to increase the overpotentials above those for the pure standard electrolyte, i.e. to affect $|\Delta\eta|$. The order was: lanthionine > cystine > homocystine > methionine > penicillamine disulphide. Addition of selenocystine to the standard electrolyte had relatively little effect on the overpotentials, but evidence

TABLE XX

STEADY STATE POLARISATION VALUES FOR STANDARD ELECTROLYTE: ELECTROPOLISHED SUBSTRATES

Min	Cathodic polarisation (mV)							
	Current density (A dm^{-2})							
	0.5	1.0	1.5	2.0	2.5	3.0	3.5	4.0
1	47.9	85.1	114.6	120.0	147.6	157.6	162.5	181.9
2	47.8	80.2	114.3	116.7	142.4	155.2	164.1	181.4
5	44.4	84.7	113.8	123.7	144.4	159.1	167.4	181.1
10	42.3	86.3	114.8	124.7	144.8	157.3	164.8	179.6
15	43.1	83.9	115.2	124.2	143.8	161.7	164.0	177.5
20	43.7	86.7	115.0	124.5	142.6	161.5	164.8	177.8
25	44.2	88.6	114.8	124.5	141.6	160.8	164.4	176.8
30	44.5	90.2	114.8	124.6	141.0	160.2	164.3	176.0
40	45.3	92.3	114.0	124.3	140.2	156.1	164.2	176.4
50	46.0	93.7	115.5	124.4	139.8	157.1	163.6	173.8
60	46.7	94.1	116.4	124.4	139.7	157.0	163.6	173.3
Steady state values	46	94	116	124	140	157	164	174

TABLE XXI

STEADY STATE POLARISATION VALUES WITH ADDITIVES PRESENT:

ELECTROPOLISHED SUBSTRATES

Additive in standard electrolyte (5.0×10^{-4} M)	Cathode polarisation (mV) for C.D. ($A\ dm^{-2}$) of:			
	1.0	2.0	3.0	4.0
L-cystine	160	226	380	400
D,L-methionine	172	224	282	330
D,L-homocystine	209	249	314	342
D,L-lanthionine	173	320	342	448
D,L-selenocystine	86	124	180	242
D-penicillamine disulphide	73	129	194	194
No additive	94	124	157	174

TABLE XXII

POLARISATION VALUES WITH ADDITIVES PRESENT:

ELECTRODEPOSITED SUBSTRATES

A : No additive

B : Cystine (1.0×10^{-4} M)

C : Methionine (2.0×10^{-4} M)

D : Lanthionine (1.0×10^{-4} M)

E : Penicillamine disulphide (1.0×10^{-4} M)

Current density (A dm^{-2})	Cathodic polarisation (mV)				
	A	B	C	D	E
0.25	20	-	60	29	29
0.50	36	81	100	64	35
0.75	52	-	138	101	41
1.0	65	109	164	135	46
1.5	87	146	201	190	55
2.0	107	185	231	239	66
2.5	129	229	264	273	78
3.0	149	263	290	299	89
3.5	168	289	315	325	101
4.0	187	311	334	348	112
4.5	204	332	353	369	124
5.0	224	352	372	390	137

of decomposition to selenium was found, as mentioned earlier.

Cystine, homocystine, and penicillamine disulphide each have in their structures a disulphide linkage which is capable of two-electron reduction under certain conditions, and their chemical reactivities and behaviour are similar. Their relative effectiveness as cathode polarizers is paralleled roughly by their relative solubilities in water, but the significance of this observation is undoubtedly limited by the concomitant intervention of other factors, such as steric effects, the extent of complex formation with ions and the relative solubilities of these complexes, the relative strengths with which particular functional groups may be adsorbed on the copper surface, or any depolarisation tendencies that the additives may possess. Depolarisation is a term applied to compounds which are able to diminish the deposition overpotential at a particular current density. It is believed that they achieve this by facilitating electron transfer to the discharging metal ions or by changing the mean outer Helmholtz plane potential, ψ_1 (26,132).

Table XXIII shows the $|\Delta\eta|$ values for deposition on electrodeposited substrates in the presence of the additives cystine, methionine, and lanthionine. As the current density was increased from 0.25 to 5.0 A dm^{-2}, $|\Delta\eta|$ values increased for each of these additives until a current density of about 3 A dm^{-2} was reached, beyond which they remained

TABLE XXIII

RELATIONS BETWEEN CURRENT DENSITY, CHANGES IN POLARISATION, AND CALCULATED SURFACE COVERAGES FROM RADIOISOTOPE AND POLARISATION DATA

$|\Delta\eta|$ in mV; C_0 in (mole cm^{-2} s^{-1}) $\times 10^{12}$;

θ fractional coverage

Current density (A dm^{-2})	Cystine (1.0×10^{-4}M)			Methionine (2.0×10^{-4}M)			Lanthionine (1.0×10^{-4}M)	
	$\|\Delta\eta\|$	θ	C_0	$\|\Delta\eta\|$	θ	C_0	$\|\Delta\eta\|$	θ
0.25	-	-	9.9	40	0.54	4.6	9	0.16
0.50	45	0.59	19.7	64	0.72	5.5	28	0.42
0.75	-	-	18.1	86	0.82	3.9	49	0.62
1.0	44	0.58	23.4	99	0.86	5.2	70	0.75
1.5	59	0.69	24.1	114	0.89	3.8	103	0.87
2.0	78	0.78	32.8	124	0.91	6.4	132	0.93
2.5	100	0.86	30.1	135	0.93	5.9	144	0.94
3.0	114	0.89	36.0	141	0.94	5.6	150	0.95
3.5	121	0.91	35.4	147	0.94	8.8	157	0.95
4.0	124	0.91	43.6	147	0.94	12.4	161	0.96
4.5	128	0.92	35.5	149	0.95	4.2	165	0.96
5.0	128	0.92	43.3	148	0.95	12.0	166	0.96

approximately constant to the highest current densities used. Included in the table also are data for surface coverages calculated by application of the blocking theory, which will be discussed shortly.

POLAROGRAPHY OF CYSTINE

It was of interest to observe the reduction behaviour of cystine at a dropping mercury electrode to determine whether cysteine was likely to be reduced to the sulphide ion at potentials more positive than the hydrogen ion wave. It was also of incidental interest to measure the diffusion coefficient of cystine. Accordingly, polarographs were obtained with a Cambridge General Purpose Polarograph at sensitivity 1/15, coupled to a Sargent recorder, model SRG. Solutions were deaerated 30 minutes with purified nitrogen, and Triton-X100 was used as a maximum suppressor. Potentials were measured in a two compartment cell with a coarse frit and an agar-saturated K_2SO_4 salt bridge in contact with a saturated calomel electrode (SCE) of large surface area. The Ilkovic equation was applied to the mean diffusional current, $\tilde{i}_d$, of the cystine/cysteine wave after correction for the residual current,

$$\tilde{i}_d = \frac{6}{7} i_{max} = 0.627nFD^{1/2}m^{2/3}t^{1/6}c$$

where the flow rate of mercury, m = 0.001788 g s^{-1}; the mean drop time, t = 3.97 s^{-1}; Hg column height 79.3 cm; and c is the bulk concentration of depolarizer, mole cm^{-3}. The constancy of this form of the Ilkovic equation is of the order ± 5 % (89,133).

Curve 1 of Figure 19 represents the polarograph obtained at 25.0 ± 0.1°C for L-cystine at a concentration of 1.00×10^{-3} M in 0.1 M perchloric acid containing 0.005 % Triton-X100. From the data, the diffusional coefficient of cystine was evaluated by assuming a two-electron reduction per molecule, as $D = 7.9 \times 10^{-6}$ cm^2 s^{-1} (at -1.2V vs. SCE) and $E_{1/2}$ = -0.970V vs. SCE. No reduction currents could be detected for degradation of cysteine at potentials more positive than the hydrogen ion wave. It has been proposed that cystine may be reduced electrolytically and occluded in copper electrodeposits as CuS (134,135). On the other hand, Lahousse and Heerman (57) considered that experimental proof was still lacking for the desulphuration of cystine and methionine on the surface of copper during its deposition. If electrolytic degradation of cystine molecules to sulphide occurred at low over-potentials during copper electrodeposition, by rupture of C-S bonds, the potential required would be lower than that for hydrogen ion discharge and this is untenable on the basis of the polarographic results. No reduction currents

FIGURE 19

Dropping mercury electrode polarographs for L-cystine (1.00×10^{-3} M) in $HClO_4$ (0.1 M) - Curve 1; and L-cystine (5.00×10^{-4} M) + Cu^{2+} (5.00×10^{-4} M) in $HClO_4$ (0.1 M) - Curve 2. Temp. 25.0 ± 0.1°C.

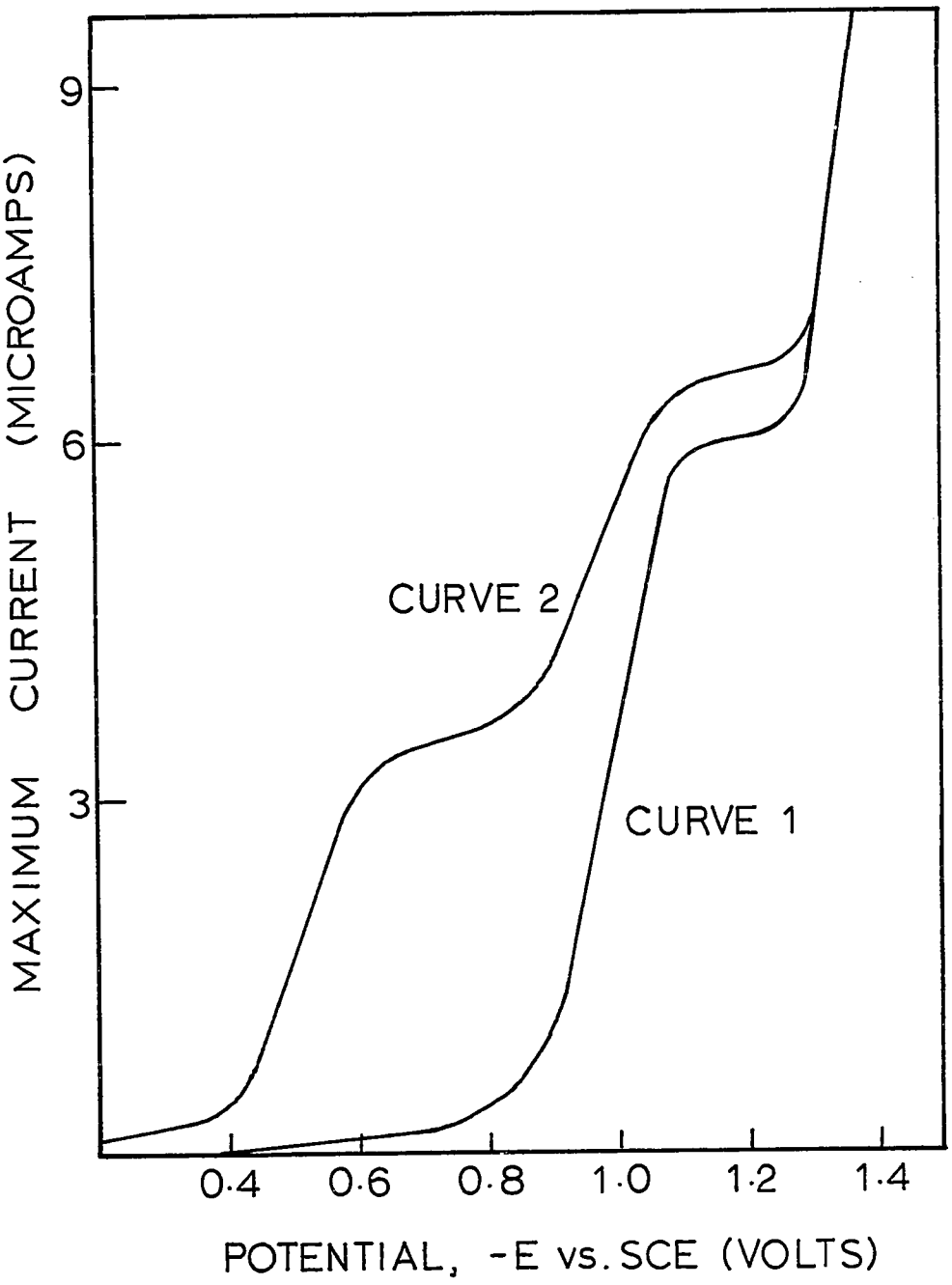
MAXIMUM CURRENT (MICROAMPS)
9
6
3
CURVE 2
CURVE 1
0·4
0·6
0·8
1·0
1·2
1·4
POTENTIAL, -E vs. SCE (VOLTS)

could be detected for the reduction of either D,L-methionine or D,L-lanthionine at potentials more positive than the hydrogen ion wave. Both of these latter additives were examined in 0.1 M $HClO_4$ supporting electrolyte at concentrations 1.00×10^{-3} M.

Curve 2 of Figure 19 was obtained at 25.0 ± 0.1°C with 5.00×10^{-4} M L-cystine in the presence of 5.00×10^{-4} M Cu^{2+} (added as $CuSO_4$) in 0.1 M $HClO_4$ containing 0.05 % Triton-X100. The two distinct waves for cystine and cupric ion demonstrate that no measurable complex formation had occurred at this pH between cupric ion and cystine.† The limiting current of cystine is nearly equal to that for cupric ion for equivalent concentrations, particularly in the absence of any maximum suppressor, cf. (136). The half wave potential of the cupric ion reduction wave was found to be -0.513V vs. SCE, in reasonable agreement with the value quoted by Kolthoff and Okinaka (137), $E_{1/2}$ = -0.516 V vs. SCE; with $D_{Cu^{2+}} = 8.5 \times 10^{-6}$ cm^2 s^{-1} ($Cu(ClO_4)_2$). Viscometer measurements have yielded $D_{Cu^{2+}} \simeq 8.6 \times 10^{-6}$ cm^2 s^{-1} ($CuSO_4$), (138).

†Footnote: Acid-base equilibria of cupric ion-cystine complex formation could be studied by the polarographic method, but the treatment of data suffers from the problems of acid-base titration methods, since similar assumptions usually have to be made for the choice of species to include in the postulated equilibria.

MORPHOLOGIES OF ELECTRODEPOSITS

It was pointed out previously that a variety of morphological forms generally appear in an electrodeposit from purified electrolytes as the current density is increased. Deposits have been prepared from electrolytes containing amino acid additives (at concentrations $\simeq 10^{-4}$ M) to observe the resulting morphologies, and possibly to relate these to the polarisation changes that an additive may cause at different current densities. Accordingly, electrodeposits were made in the presence of strong and weak cathode polarizers and examined by optical microscopy. Photographs of deposits were taken with a polaroid camera on a Vickers Projection microscope[†] and with a 35 mm camera on a standard microscope.

Experimental observations

Table XXIV summarizes the gross effects of cystine (a strong polarizer) and penicillamine disulphide (a weak polarizer), added to the standard electrolyte, upon the morphologies of deposits prepared on electropolished

---

[†]Footnote: The author is grateful to Dr. W.M.Williams, Metallurgical Engineering Dept., McGill, for the use of equipment.

TABLE XXIV

MORPHOLOGIES OBSERVED ON ELECTROPOLISHED SUBSTRATES

Amino acid (5.0×10^{-4} M) in the standard electrolyte.
Deposition time - 60 minutes.

Deposition C.D. ($A\ dm^{-2}$)	Penicillamine disulphide	Cystine
1.0	Layers; some pyramids, steps, cubes	Hillocks; small nodules
2.0	Cubes; some steps, pyramids	Rough nodules, some large
3.0	Fairly amorphous; some columnar growths	"
4.0	Fine cubic structure; amorphous layers	Deep nodular growths, even sized and large

substrates.

Figure 20-A,B illustrates the nodular growths obtained on electropolished substrates with 0.5×10^{-4} M cystine as additive, at current densities of 3.0 and 4.0 A dm^{-2}, respectively (cf. Table XXIV, 5.0×10^{-4} M cystine additive). The photographs of Figure 20 were taken at undetermined magnification. Clearly, the surface density of large nodules was increased at the higher current density and it is interesting to note that nodules are formed on a substrate that originally was smooth.

Cathodic overpotentials and the morphologies of the resulting deposits formed on electropolished substrates in the presence of penicillamine disulphide were not markedly different from those obtained in the absence of an additive (Table XXI). The variations in growth types with current densities paralleled roughly those obtained by Bockris et al (30) on electropolished {100} faces of copper single crystals. The overpotential always seemed to be a better indication than the current density of the type of growth to be expected. For example, Figure 21-A illustrates the deposit formed after 60 minutes at 3.0 A dm^{-2} on an electrodepcsited substrate when the overpotential, η, was 85 mV with penicillamine disulphide present (1.0×10^{-4} M). The morphology comprised large angular forms with smaller, stepped pyramids. At the same current density in the absence of

FIGURE 20

A. Additive: cystine, 0.5×10^{-4} M in the standard electrolyte.
Current density: 3.0 A dm^{-2} on electropolished substrate for 60 minutes. Magnification: undetermined.

B. Additive: cystine, 0.5×10^{-4} M in the standard electrolyte.
Current density: 4.0 A dm^{-2} on electropolished substrate for 60 minutes. Magnification: undetermined.

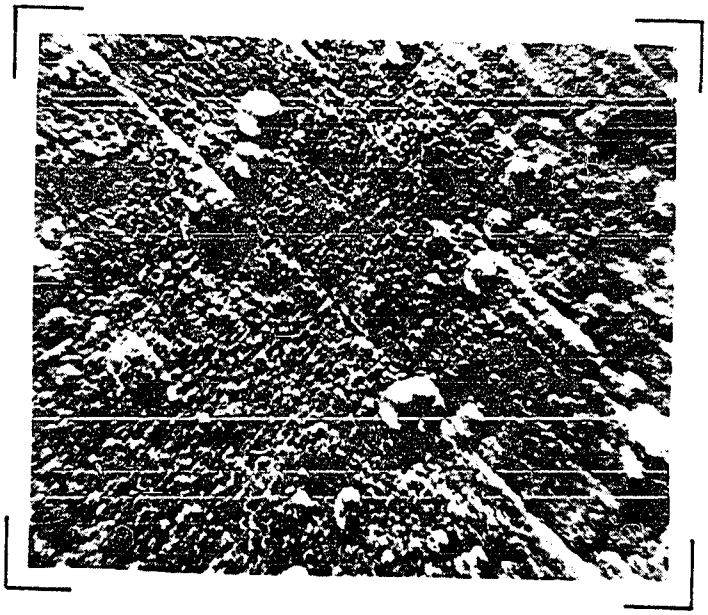

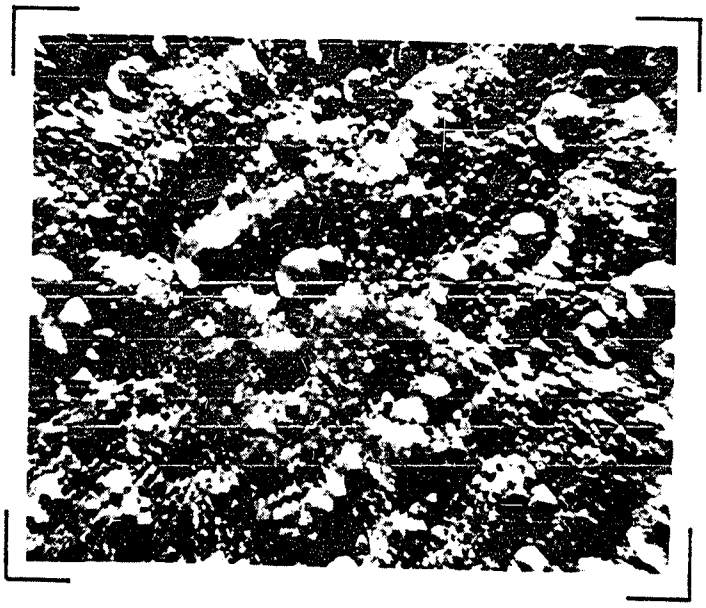

FIGURE 21

A. Additive: penicillamine disulphide (1.0×10^{-4} M)
in the standard electrolyte.
Current density: 3.0 A dm^{-2}, on electrodeposited substrate
for 60 minutes. Magnification: × 400.

B. No additive: standard electrolyte.
Current density: 2.0 A dm^{-2}, on etched, polycrystalline
substrate for 60 minutes. Magnification: × 400.

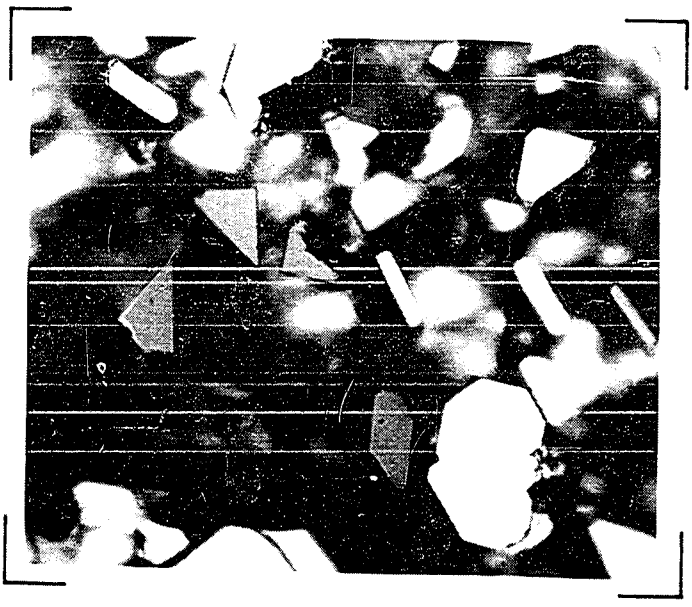

additive, with $\eta \simeq 150$ mV, the deposit consisted mainly of blocks and cubes, whereas pyramidal forms were again observed at lower current densities of 1.0 A dm^{-2}, when $\eta < 100$ mV.

Figure 21-B shows the regular and varied forms of crystallites produced by deposition from the pure standard electrolyte on etched, polycrystalline copper substrates. Their sizes were mostly in the range $\simeq 10 - 50\mu$, which was similar to the range for the grain sizes of the substrate copper. It is probable that certain substrate grains are able to develop preferentially, depending on the applied overpotential. Preferred nucleation has been observed, for example, on certain of the crystallographic faces of polycrystalline silver (139). At current densities in excess of 4 A dm^{-2} the morphologies of copper deposits became polycrystalline (cf. (140)) and eventually, with further increase of the current density, non-adherent and amorphous.

Depositions on electrodeposited substrates, with cystine and lanthionine as additives, developed nodule-like growths (Figure 22-A,B). Shanefield and Lighty (70) obtained similar growth hillocks in copper electrodeposits when they added traces of gelatin to highly purified copper perchlorate solutions. Lanthionine, the most effective cathode polarizer of the additives studied, quickly

FIGURE 22

A. Additive: cystine, 1.0×10^{-4} M in the standard electrolyte.
Current density: 3.0 A dm^{-2} on electrodeposited substrate for 60 minutes. Magnification: × 400.

B. Additive: lanthionine, 1.0×10^{-4} M in the standard electrolyte.
Current density: 3.0 A dm^{-2} on electrodeposited substrate for 60 minutes. Magnification: × 400.

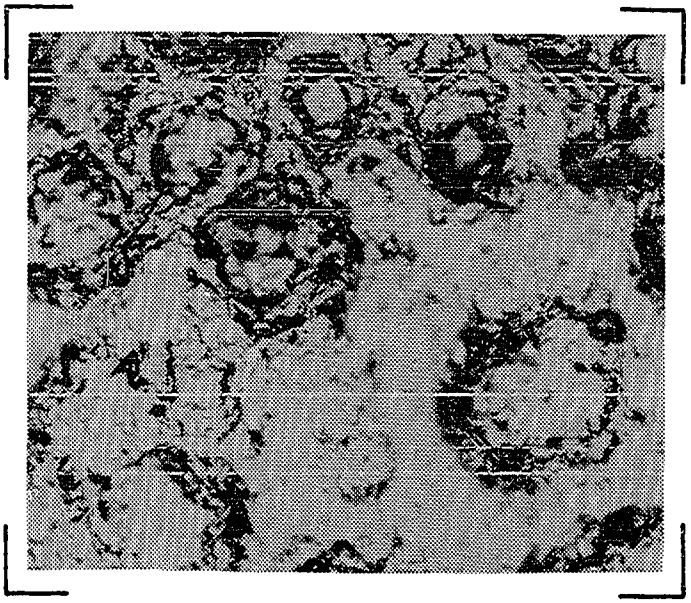

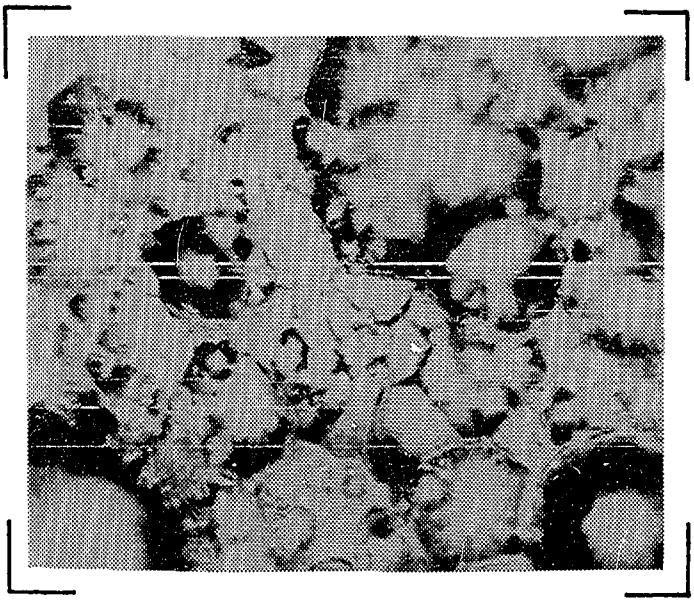

obliterated the recognisable crystallite shapes or morphological forms and produced a bubble-like morphology with smooth, rounded nodules, shown in Figure 22-B.

DISCUSSION

Several aspects of the present study would seem to require additional comment, explanation, and perhaps speculation:

(i) The consistent appearance of well-defined, morphological forms of copper deposits as the current density was increased.

(ii) Adsorption of additives on copper foils increased with time to reach an initial plateau value, followed by further increases (Figure 5). No desorption of radioactive methionine occurred from foils when they were immersed in the aerated standard electrolyte (Table IV), but an exchange process did occur when similarly prepared foils were immersed in aerated solutions of methionine in the standard electrolyte (Table V). The initial adsorption rate of methionine was higher from solutions that had been flushed with purified nitrogen (Table VI) and, conversely to the behaviour in aerated solutions, the exchange reaction of

adsorbed methionine did not occur from foils when they were immersed in deaerated methionine solutions in the standard electrolyte (Table VII).

(iii) The mean rates of occlusion during copper deposition for cystine and methionine additives were found to vary in a different manner over the current density range 0.25 - 6.0 A dm^{-2} (Figures 10,11).

(iv) The surface coverages of methionine and cystine, calculated from $|\Delta\eta|$ values by application of the blocking theory, increased with increase of the current density from 0.25 to 3.0 A dm^{-2}, and then remained fairly constant with $\theta > 90$ % at the higher current densities (Table XXIII).

MORPHOLOGIES OF COPPER DEPOSITS

The point of morphological interest on which particular comment seems desirable is the commonly observed appearance of pyramidal forms during the electrocrystallisation of copper, for the initiation of which no satisfactory model or explanation has yet been proposed. The shape of the pyramids varies with the substrate epitaxy, e.g. tetragonal on {100} (76), triangular and hexagonal on {111} (84), and they usually appear in a range of current densities slightly higher than that at which layer-type

growth predominates. On reflection, the writer has come to the opinion that, if the discharge of cations were considered to occur randomly at all sites of a crystal face, and the incorporation of an ad-atom into the metal lattice also occurs in more or less random manner (cf. (76)), an increase in the deposition rate might be expected to lead to nucleation of simple pyramid formation, and that these might be able to grow preferentially in certain circumstances. The description to be outlined is purely qualitative, as yet, but might perhaps lend itself to more quantitative treatment in the future.

For simplicity, cubic "brick" atoms may be considered to arrive at, and to be incorporated into an ideal cubic lattice, illustrated in Figure 23. Provided that each ad-atom is eventually located in an atomic "monolayer in formation" (MIF) on the substrate, flat crystal faces must result. Once a monolayer is partially formed however, cations which arrive at the lattice cannot distinguish successive layers and may deposit as atoms at sites upon the MIF or on remaining available substrate sites. A reasonable assumption might then be that cations arriving at sites on the MIF may "step-down", by diffusional processes as ad-atoms, to become part of the MIF, provided they do not arrive at sites where they are coordinated with an adjacent atom already deposited on the MIF, such that they are bonded

FIGURE 23

Illustration of lattice model for pyramid initiation.

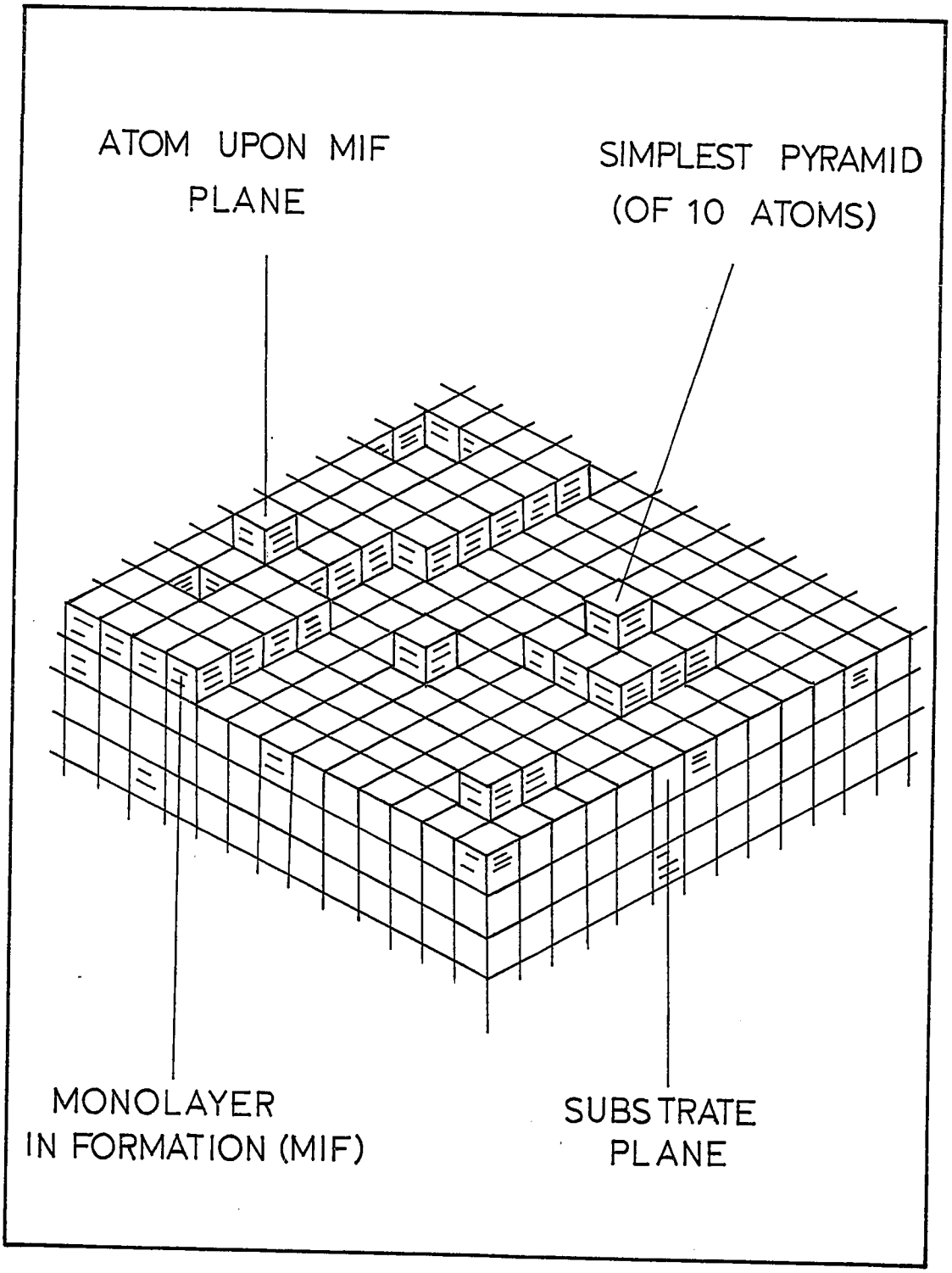
ATOM UPON MIF PLANE
SIMPLEST PYRAMID (OF 10 ATOMS)
MONOLAYER IN FORMATION (MIF)
SUBSTRATE PLANE

by at least one vertical and one lateral bond. If higher level "pile-ups" are neglected, a steady state deposition would correspond to discharge of cations to the extent of about 50 % on substrate sites and the remainder on sites created by the MIF. Many of these latter arrivals would "step-down" to be incorporated into the MIF.

As the rate of deposition is increased, the lifetime of a given ad-atom discharged on a MIF array of 3 × 3 atoms, should eventually become approximately equal to the time for another atom to arrive at a site adjacent to it on the array, and "step-down" of the given atom to the MIF would be prevented. This would result in initiation of the simplest form of three-dimensional growth, a pyramid comprising 3 × 3 atoms in one layer and 2 adjacent atoms upon this array. If, however, the MIF is completed before the group can itself expand to become a three-dimensional unit upon that MIF, the upper atoms become indistinguishable from those of the next MIF to form. On a completely random basis, the mean time for a second atom to arrive adjacent to an atom on a 3 × 3 (cubic) array would be roughly one-eigth of the mean arrival time per site. Once the simplest pyramids (nuclei) can form, it is possible that cations arriving at their inclined faces will be discharged and incorporated into the lattice without further diffusion and the subsequent growth of the pyramid is assured.

This latter suggestion is supported by the measurements for the horizontal growth rate of pyramids, referred to earlier, in which the experimental growth rate represents about 28 atoms $site^{-1}$ s^{-1} and the growth rate calculated for random discharge at an ideal (100) lattice plane about 20 atoms $site^{-1}$ s^{-1}. If the epitaxy of the inclined faces of the pyramids provided a more favourable site for deposition than the epitaxy of the substrate crystal plane, the pyramids may be expected to grow preferentially.

For simple models, such as the one described above, it may prove possible to determine the relation between the random arrival rate and the surface diffusion terms that define the condition for initiation of a pyramid, e.g. by computer simulation techniques (141).

ADSORPTION OF CYSTINE AND METHIONINE ON COPPER

Proposed mechanism for adsorption

If it is assumed that the increase in the surface concentration of radioactive methionine, shown in Figure 5, is only diffusion dependent, the diffusion coefficient, D, may be calculated from the expression

$$M_t = 2c_0 (Dt/\pi)^{1/2}$$

in which M_t is the amount of additive that diffuses to a plane surface on which its initial concentration is zero from a semi-infinite medium of bulk additive concentration, c_0 (mole cm^{-3}). The derivation of this expression is given in Appendix III. The diffusion coefficient, D, is assumed to be constant and unaffected by any potential gradients or conditions of electrodeposition. The value so obtained from the data of Figure 5 for the condition at which the plateau is first reached, $D = 1.3 \times 10^{-8}$ cm^2 s^{-1}, is smaller by at least an order of magnitude than values expected for aqueous media ($\simeq 10^{-6}$ cm^2 s^{-1}). As with the time dependence of surface tension (142), a low value of D estimated in this way is an indication of some kind of surface activation barrier or chemical reaction. In general, for the situation where diffusion and a chemical reaction together determine the concentration adjacent to the surface, the behaviour approaches that for ideally rapid diffusion only if the diffusion rate is very much faster than that of any chemical reaction that may take place at the surface. This suggests that the rate of methionine adsorption depends on a diffusion process which is modified or controlled by a chemical reaction, although not necessarily at the surface.

The rates at which methionine is adsorbed on, and exchanged from copper foils immersed in the standard electrolyte containing the additive have been found to be

sensitive to the presence of dissolved oxygen in the electrolyte. This indicates that some readily oxidizable species, presumably Cu(I) might be involved in some way in the adsorption and exchange processes. The presence of Cu(I) in the electrolyte, in the presence of metallic copper, is readily explained by the well-known equilibrium,

$$Cu(0) + Cu(II) \rightleftharpoons 2Cu(I)$$

$$K \simeq 1.8 \times 10^{-8} \text{ g . ion } L^{-1}, \; p_{O_2} = 0.208 \text{ atm., } 25° \quad (143)$$

The Cu(I) ions may then be oxidized to Cu(II) ions by reaction with oxygen dissolved in the electrolyte. Since the extent of complex formation between Cu(I) ions and the amino acid additive would depend on the concentration of Cu(I) ions, it would ultimately depend on the concentration of oxygen in the solution. Similarly, since cuprous cysteinate is known to be sensitive to oxidation on exposure to air, it is likely that any complexes that may form between Cu(I) and cysteine may be sensitive to oxidation by oxygen dissolved in the electrolyte. The same is probably true of Cu(I)-methionine complexes. Accordingly, as the Cu(I) ions diffuse into the bulk electrolyte from the copper surface where they are formed, and encounter molecules of the additive, they may react to form an insoluble or slightly soluble complex which might be readily adsorbed on the

electrode. This adsorbed species might remain as such on the metal surface, but it might be reoxidized by oxygen dissolved in the electrolyte to Cu(II) ions and additive molecules. These might then either react again with Cu(I) ions or diffuse into the bulk electrolyte. Clearly, such a process should operate to decrease gradually the radioactivity due to a radioisotopic species adsorbed on a copper surface, when the metal with the adsorbed additive is immersed in an aerated electrolyte containing non-radioactive additive.

On the other hand, when foil samples with adsorbed radioactive additive were placed in aerated solutions of standard electrolyte containing no additive, no significant desorption was found to occur (Table IV). This may be explained if, despite oxidation of some adsorbed cuprous complexes by dissolved oxygen, the supply of Cu(I) ions at the electrode is sufficient to ensure that any additive molecules liberated when the oxidations occur are immediately complexed again and readsorbed.

The plateau regions of Figures 5 and 6 presumably represent conditions for equal rates of opposing processes. In general, steady state conditions might be established if, and when, the rate of adsorption of complex species were reduced or increased, while the rate of desorption or exchange were correspondingly increased or reduced. However,

the complexity of the system as a whole discourages any attempt at present to be specific about the manner in which such a steady state may be achieved. Among the many possible reactions that may be mentioned are the formation of Cu(I) ions and their oxidation both in the adsorbed layer and in solution, the formation of Cu(I) complexes with cystine and cysteine, heterogeneously and homogeneously, the corresponding oxidations of such complexes, etc.. Only a most exhaustive study of the stoichiometry, equilibria, and kinetics of these many possible reactions would allow their relative contributions to the adsorption, desorption, and exchange processes to be assessed.

The data for adsorption of methionine shown in Table VI, indicate that the extent to which additive is adsorbed increases proportionally with the concentration of additive, for the concentrations 10^{-5} M to 10^{-3} M. These results might indicate that no limit was reached for the production of Cu(I) ions. On the other hand, it is possible that Cu(I)-methionine complex and methionine itself are adsorbed on the copper surface, but only the complex is capable of undergoing an exchange process as a result of oxidation by dissolved oxygen. The residual radioactivity would then correspond to the retention of adsorbed methionine in the uncomplexed state (Figure 6). Thus, the production of Cu(I) ions need not necessarily limit the rate

of adsorption of radioactive additive from high bulk concentrations, if uncomplexed amino acid adsorbs to any significant extent. As a further possibility, the residual radioactivity at the surface of a copper foil during the exchange experiments in aerated electrolyte might have simply become buried by a layer of non-radioactive additive species that continues to collect at the cathode during the exchange process.

A means of testing the validity of the exchange mechanism, suggested above, might be to observe the chemiluminescence of electron transfer reactions from -SH of copper complexes to oxygen molecules, with a sufficiently sensitive photomultiplier arrangement. The long-time chemiluminescence (4 - 10 minutes) that accompanies the occurrence of similar electron transfer reactions has been used analytically to study the influence of different catalytic promoters on electron donors of biological interest, e.g. cysteine, glutathione (144).

OCCLUSION OF CYSTINE AND METHIONINE ON COPPER

Proposed mechanism of occlusion

The current density limits used in the present studies, 0.25 - 6.0 A dm^{-2}, represent theoretical lattice

growth rates of 4 and 173 copper layers per second respectively, if it is assumed that the current efficiency was 100 %[†] and that an ideal lattice plane of 1 cm^2 contains 1.8×10^{15} atoms ({111} packing density) for low and 1.1×10^{15} atoms ({110} packing density) for high current density conditions (82). If the adsorption rate for the radioisotopic species is small compared with the rate of copper deposition, the surface density of adsorbed species at any instant during deposition will be much less than that corresponding to monolayer coverage. The decrease in radioisotopic contents of deposits with increasing current densities may be attributed to such a reduction in the surface density of the radioisotopes, as the species may be assumed to be adsorbed at an essentially constant rate, while the rate of deposition increases with current density. Indeed, it seems likely that, except perhaps at very low current densities, the rate of occlusion during electrodeposition from solutions with low additive concentrations should be controlled by the maximum rate of adsorption of the addition agent for open circuit conditions. Actually, the observed rates for occlusion of methionine, $\simeq (4 - 6) \times 10^{-12}$ mole cm^{-2} s^{-1}, were several times higher than the mean open circuit

---

[†]Footnote: In this c.d.range, current efficiences are ≃ 98 % or better, for deposition from acid copper sulphate electrolytes (20).

adsorption rate, ≃ 1.4×10^{-12} mole cm^{-2} s^{-1} (measured in the time scale 10 - 400 secs), but convection currents (streaming) at the vertical cathode, or other effects might contribute to the transport of additional additive to the cathode e.g. transference, mechanical trapping, less interference by oxygen, etc.. Ideally, the adsorption rate should be measured for the time scale during which each new layer of copper is deposited, ≃ 5 - 250 msecs..

Maximum adsorption of organic additives at an electrode, without accompanying electrodeposition processes, generally occurs at potentials in the vicinity of the potential of zero charge (cf. Introduction) of the particular system. Hence the maximum in the mean occlusion rate of methionine shown in Figure 11 could reflect a dependence of methionine adsorption on the potential at the electrode during electrodeposition. The current density range of the peak is not broad and it occurred at about 5 A dm^{-2}, for which current density the determined overpotential was -372 mV, or ≃ -0.05 V vs. NHE (Table XXII). By comparison, it is interesting to note the maximum adsorption of additive on copper without concurrent deposition, e.g. napthalene (145), is known to occur in a small potential range and the value of the PZC for copper (H_2SO_4 electrolyte) has been placed in the potential range 0.0 to -0.2 V vs. NHE (145).

If it is valid to interpret the experimental results

of Figure 11 to indicate that adsorption of methionine on copper in the presence of metal deposition processes is potential dependent, the author knows of no other example of such a variation in the behaviour of an additive with deposition current densities. It would be interesting, therefore, to measure the occlusion rates of an organic compound whose potential-adsorption isotherm characteristics have been studied at polarized copper electrodes. It should be borne in mind, perhaps, that sulphate ions are probably adsorbed from acid copper sulphate electrolytes at copper electrodes and may compete with other species for available surface (146,147).

As the overpotential is made increasingly negative during deposition of copper in the presence of cystine, a potential may be reached eventually at which cystine is reduced at the copper electrode by a direct charge-transfer reaction,

$$RSSR + 2H^{+} + 2e \underset{k_2}{\overset{k_1}{\rightleftharpoons}} 2RSH$$

Leyko (47) has verified experimentally that cystine may be reduced to cysteine at a copper electrode. If the reversible reaction is fast relative to diffusion or subsequent reaction of cysteine, then

$$[\text{cysteine}] = \sqrt{K[\text{cystine}]} \qquad (\text{for } [H^+] \text{ constant})$$

In the presence of an additive with only minimal influence on the rate of deposition of copper, it may be assumed that the Tafel relation is obeyed

$$\eta = a - b \ln i$$

where η is the overpotential for the copper deposition reaction (formally negative for cathodic reactions), a and b are constants, and i is the current density. Correspondingly, for the reversible reduction of cystine to cysteine, as above, electrochemical rate theory gives, for the forward reaction,

$$k_1 = A_1 \exp[-\alpha\eta nF/RT],$$

and for the reverse reaction,

$$k_2 = A_2 \exp[(1-\alpha)\eta nF/RT]$$

From these relations,

$$K = k_1/k_2 = \text{const.} \exp[-\eta nF/RT]$$

where A_1 and A_2 are constants, α is a transfer coefficient for the charge-transfer reaction, and n is the number of electrons of the faradaic reduction. Thus, ln i should be linearly related to ln K. If [cystine] ≃ constant, the value of [cysteine] will vary in an approximately linear way with $K^{1/2}$ as the potential is decreased (becomes more negative). If the cysteine formed at the electrode then reacts rapidly with cupric ion according to the equilibrium,

$$4RSH + 2Cu^{2+} \rightleftharpoons RSSR + 2RSCu + 4H^{+}$$

the major species occluded may be a Cu(I)-cysteinate complex. It may be recalled that Miller and Teva (52) similarly contend that cysteine reacts rapidly with mercury electrodes and becomes adsorbed as a complex cysteinate species.

From the foregoing, it appears that the variation found experimentally for the mean occlusion rates, calculated as cystine, from bulk concentration 1.0×10^{-4} M in the standard electrolyte, (from Figure 10: occlusion rates ≃ $(11 - 54) \times 10^{-12}$ mole cm^{-2} s^{-1}, at current densities 0.25 - 6.0 A dm^{-2}, respectively) can be interpreted by electrochemical rate theory if cystine is rapidly and reversibly reduced to cysteine. The observed increase in occluded cystine confirms, of course, that the limiting rate of diffusion in support of occlusion was not achieved in the

current density range and with the bulk concentration of cystine (1.0×10^{-4} M) used in the study.

RELATION BETWEEN MEASURED AND CALCULATED EXTENTS OF COVERAGE BY CYSTINE AND METHIONINE

In Table XXIII are recorded the occlusion rates observed experimentally for cystine and methionine in the standard electrolyte, together with the corresponding values for their coverage, θ, calculated from the expression given by the site-blocking theory,

$$\theta = 1 - \exp[-\Delta\eta/b]$$

The coverages calculated from the observed $|\Delta\eta|$ values increased with increase of the deposition current density. For deposition in the presence of cystine at the current densities 0.50 and 5.0 A dm^{-2}, θ was calculated to be 0.59 and 0.92, respectively. The corresponding occlusion rates, were 19.7×10^{-12} and 43.3×10^{-12} mole cm^{-2} s^{-1}. At the same current densities for deposition in the presence of methionine, θ was calculated to be 0.72 and 0.95, while the occlusion rates were relatively lower than those for cystine, at 5.5×10^{-12} and 12.0×10^{-12} mole cm^{-2} s^{-1}.

It seems reasonable to assume that the total

quantities of these additives adsorbed at the copper electrodes are occluded into the deposits during deposition i.e. the rates of occlusion are directly proportional to the coverages. In support of this premise, it may be noted that both cystine and methionine additives are strongly adsorbed and have mean rates of occlusion that are higher than their experimentally determined rates of adsorption. Moreover, at a current density of 1 A dm^{-2}, about 30 layers of new copper are deposited per second, a rate of deposition that seems likely to ensure the occlusion of all the additive in the immediate vicinity of the surface. Indeed, the term "surface" may have little conceptual significance under conditions of such rapid crystal growth.

If, as above, the rates of occlusion be accepted as directly proportional to the coverages due to adsorption, there appears to be little, if any, relation between the coverages estimated from the occlusion rates determined experimentally by the radioisotope technique and those calculated from the blocking theory. A simple order of magnitude calculation will serve to illustrate the nature of the discrepancy. The area associated with a cysteinate complex at mercury has been estimated to be $\simeq 0.16$ nM^2 (52). At a current density of 1.0 A dm^{-2}, the experimental rate of occlusion of cystine into a copper cathode was estimated to be $\simeq 23.4 \times 10^{-12}$ mole cm^{-2} s^{-1}, on the assumption that the

area of the electrode was given by its geometrical area; the actual area will be somewhat larger than the geometrical area, and the rate of occlusion per unit area correspondingly less than this figure. If it is assumed that each cystine molecule is able to block $\simeq 0.32\ nM^2$ of the copper electrode as cysteinate complex (cystine $\equiv$ 2 cysteine) and that at 1.0 A dm^{-2} about 30 new copper layers are deposited per second, the theoretical surface coverage can be roughly estimated as

$$\simeq \frac{0.32}{10^{14}} \times \frac{23.4}{30} \times 10^{-12}\ N_0 \simeq 0.001$$

where N_0 is Avogadro's number. The Tafel slope in the presence of cystine additive at 1.0 A dm^{-2} was approximately parallel to that for the pure standard electrolyte, a necessary criterion for the application of the blocking theory (61,62).

The corresponding figure for a continuously maintained coverage, calculated fron the $|\Delta\eta|$ value (Table XXIII) by the blocking theory, was $\theta = 0.58$ i.e. 2 - 3 orders of magnitude larger than that observed experimentally. In addition, besides predicting far higher coverages than those estimated from occlusion rates, the coverages calculated from the blocking theory for methionine fail to reflect the maximum that was found in the occlusion rates

for this additive (Figure 11).

From investigations by faradaic impedance measurements, Hampson and Latham (148) have placed the fraction of sites that are active on copper electrodes, at equilibrium in nitrate electrolyte, at only $\simeq 1.3 \times 10^{-3}$ to 10^{-4} of the total surface. If only a restricted number of sites are available for discharge of cations, preferential adsorption of an additive at these active sites would cover only a small fraction of the total surface area, yet correspond to the development of the relatively high overpotentials measured. A blocking theory that assumes the total surface to be available would require very high calculated surface coverages to be compatible with comparable overpotential values.

The failure of coverages calculated from $|\Delta\eta|$ values to correspond to those estimated from occlusion rates may indicate that the overpotential increments should not be associated with the gross surface coverages by additives during electrocrystallisation processes. It was pointed out earlier that profound modifications to morphologies of electrodeposits may result from the presence of cystine as an additive in the electrolyte, and examples of such changes were illustrated. The disruptions introduced to the crystal lattices by adsorbed or occluded additives undoubtedly change the nature of nucleation sites available for electro-

crystallisation, and this may modify the charge-transfer overpotentials for the copper deposition reaction, without appreciable change to the Tafel slope.

Examples of this behaviour are found in the overpotential data for copper deposition at different crystallographic faces of single crystals in electrolytes without additives. The effects of the substrate epitaxy on η values are large. For example, at a current density of 1.0 A dm^{-2}, the overpotential values (in millivolts) during deposition found by Hayashi et al (84), were as follows: in 0.5 M $Cu(ClO_4)_2$ - 1 M $HClO_4$, $\eta(100) \simeq 85$; $\eta(111) \simeq 65$; $\eta(110) \simeq 15$; in 0.5 M $CuSO_4$ - 0.5 M H_2SO_4, $\eta(100) \simeq 70$; $\eta(111) \simeq 60$; $\eta(110) \simeq 40$; cf. (148). If the presence or occlusion of an additive were to change the epitaxy of a proportion of the crystallites, e.g. from (110) to (111), the data cited above for deposition on single crystal faces indicate that large overpotential increments might result.

A second and perhaps more important feature of the modifications to deposit morphologies which may lead to sizable increases in $|\Delta\eta|$ values should be considered. Lanthionine, the most effective polarizer, produced the smoothest deposit morphologies, as determined by optical microscopy. If by its action, a large decrease in the area of the electrode surface occurred, from what it would have been at a similar current density in the absence of additive,

the actual current density would be higher and the overpotential increased correspondingly. This behaviour also would explain the observation that the overpotential always seemed to give a better indication than the current density of the growth type to be expected; the current density values recorded were necessarily based on geometrical areas, whereas true current densities should be estimated from true surface areas, i.e. taking into account the surface morphology. The blocking theory does not take these effects into account.

It should be emphasized, perhaps, that the conclusions outlined above may be applicable only for the additives and experimental conditions used in the present study. Extensive similar studies would be necessary to determine whether they are valid with other additives and experimental conditions.

APPENDIX I

FORTRAN IV COMPUTER PROGRAMME FOR

pK_a TITRATIONS

```
      ACID DISSO CONSTS FOR AMINO ACIDS
      DIMENSION X(100), Y(100),XC(100),YC(100),D(100)
      DIMENSION P(100),B(100),H(100)
      REAL M
      L=20
      DO 71 I=1,L
      READ (5,77) P(I),B(I)
77    FORMAT (F12.6,E12.4)
      H(I)=0.1**P(I)
      X(I)=H(I)*(0.000100-B(I))*0.1628/(0.6352*(0.000200-B(I))
      Y(I)=H(I)**2*B(I)*0.1628/(0.000200-B(I))
71    CONTINUE
      SUMX=0.
      SUMY=0.
      SUMXY=0.
      SUMXX=0.
      DO 30 I=1,L
      SUMX =SUMX + X(I)
      SUMY =SUMY + Y(I)
 5    SUMXX =SUMXX +X(I)**2
      SUMXY =SUMXY +X(I)*Y(I)
30    FN=L
      M = (FN*SUMXY-SUMX*SUMY)/(FN*SUMXX-(SUMX)**2)
      C = (SUMXX*SUMY-SUMX*SUMXY)/(FN*SUMXX-(SUMX)**2)
      DSQ = 0
      DO 40 I=1,L
      YC(I) = M*X(I) + C
      D(I) = Y(I) - YC(I)
      DSQ = D(I)**2 + DSQ
      DEL = FN*SUMXX - (SUMX)**2
      SIGM = SQRT(ABS(DSQ/DEL))
      SIGC = SQRT((SIGM**2)*(SUMX*SUMX)/FN)
      T = C/M
      PR1 = -ALOG10(M)
      PR2 = -ALOG10(T)
      WRITE (6,73) P(I),B(I),X(I),Y(I),YC(I),D(I),H(I)
73    FORMAT (F12.6,6E12.4)
40    CONTINUE
      WRITE (6,14) SIGM,SIGC,M,C
14    FORMAT (1H0,10X,4E12.4)
      WRITE (6,75) PR1,PR2
75    FORMAT (1H0,10X,2F8.4)
      STOP
      END
```

APPENDIX II

TREATMENT OF WILSON'S DISEASE WITH PENICILLAMINE

Wilson's disease (hepatolenticular degeneration) is a rare, inherited disease in which abnormal amounts of copper accumulate in the liver, kidneys, brain, and cornea, perhaps as a result of a deficiency or absence of a specific copper-concentrating enzyme system in the liver, which leaves the metal more readily available to diffuse into other tissues. D-penicillamine has proved to be an effective therapeutic agent, and it is believed that its action relies on its ability to complex with and thereby remove the excess (stored) body copper. In addition, penicillamine has been administered for lead and mercury poisoning, and for cystinuria (150).

These applications have prompted a number of studies of the complex formation between penicillamine and various metal ions (e.g. (151,152,153)). However, for such equilibria, complicated distributions of polynuclear species are possible (cf. (127)) and assumptions are necessary to calculate stability constants for certain experimental conditions. McCall et al (154) were unable to detect copper complexes with D-penicillamine, although zinc complexes were found, in the urine of patients with Wilson's disease

to whom the drug had been administered. They concluded that the effect of penicillamine on copper metabolism was likely to be secondary to the formation of cuprous mercaptide.

One interesting aspect of the present study is the high solubility of Cu(II)-penicillamine disulphide complexes, compared with those of either cystine or homocystine. If, in the course of its drug function, D-penicillamine or Cu(I)-penicillamine complexes were to become oxidized, the solubility of the Cu(II) complexes with the disulphide might ensure the continued removal of the excess copper, and perhaps other metal ions, from their particular location in the body. The high solubility of penicillamine disulphide and certain of its complexes with metal ions is intriguing and no explanation can be offered. Indeed, the relative solubilities of metal-penicillamine complexes, compared with those of other sulphur-containing amino acid complexes, may be important to the efficacy of penicillamine in drug usage.

APPENDIX III

LINEAR DIFFUSION TO A PLANAR ELECTRODE

A solution of Fick's second law of diffusion in one dimension

$$\frac{\partial C}{\partial t} = D \frac{\partial^2 C}{\partial x^2}$$

is given by

$$C = \frac{A}{t^{1/2}} e^{-x^2/4Dt}$$

where A is a constant. The total quantity of material diffusing in a semi-infinite column of unit cross-sectional area may be written

$$G = \int_0^\infty C \, dx$$

Substituting the expression for C in this equation and solving for A leads to an expression which represents the concentration distribution of an amount of material, G, originally deposited at the x = 0 plane. After a time, t,

$$C = \frac{G}{(\pi Dt)^{1/2}} e^{-x^2/4Dt}$$

Adsorption from a bulk solution of essentially constant concentration has an initial state defined by

$$\begin{matrix} c = c_0, & x > 0 \\ c = 0, & x = 0 \end{matrix} \qquad t = 0$$

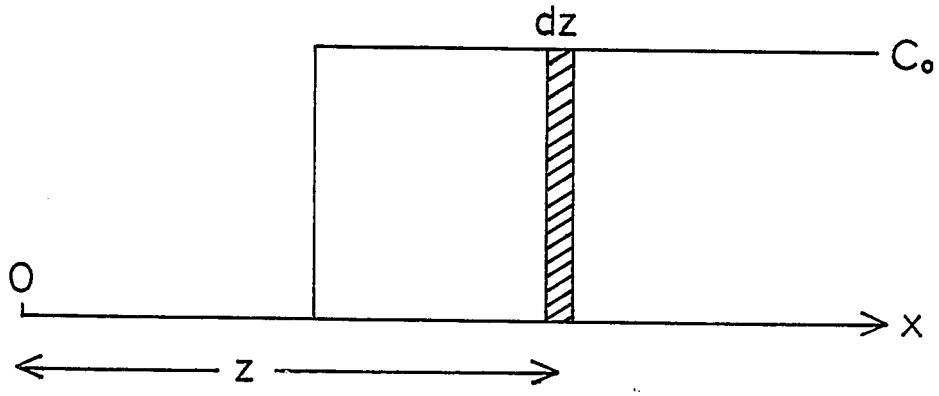

At the point O in the diagram, the concentration due to an element, dz, at distance z and after time t is $c_0(\pi Dt)^{-1/2}\, dz\, e^{-z^2/4Dt}$. The concentration distribution which arises as a result of the boundary condition, $c = 0$, $x = 0$, $t > 0$, is obtained by integrating all the available elements, and

$$c(x,t) = c_0(\pi Dt)^{-1/2} \int_x^\infty e^{-z^2/4Dt}\, dz = 2\pi^{-1/2} c_0 \int_{x/2(Dt)^{1/2}}^\infty e^{-u^2}\, du$$

where $u = z/2(Dt)^{1/2}$. This expression is written usually

as the error function complement,

$$c(x,t) = c_0 \text{ erfc } x/2(Dt)^{1/2}$$

The expression for the total quantity of material, M_t, removed from the system or adsorbed at $x = 0$ after time t is obtained from the flux at the boundary $x = 0$; from Fick's first law,

$$F = -D \left(\frac{\partial c}{\partial x}\right)_{x=0} = -D \frac{\partial}{\partial x} \{c_0 \text{ erfc } x/2(Dt)^{1/2}\}_{x=0}$$

$$= Dc_0(Dt\pi)^{-1/2}$$

Thus, $M_t = \int_0^t F \, dt = 2c_0(Dt/\pi)^{1/2}$.

CONTRIBUTION TO KNOWLEDGE

1. Open circuit adsorption rates of methionine and cystine from aerated acid copper electrolytes have been measured at copper foils with a radioisotopic technique. For cystine (1.0×10^{-4} M bulk concentration) and methionine (2.0×10^{-4} M bulk concentration) additives, the mean adsorption rates in the time scale 5 - 400 seconds were similar and approximately 1.4×10^{-12} mole cm^{-2} s^{-1} (based on geometrical areas). The amino acid surface concentrations reported for the adsorption of cystine were confirmed by colorimetric analyses with Triketohydrindene hydrate reagent.

2. The adsorption, desorption, and exchange rates for methionine on copper foils were found to be sensitive to the presence of oxygen. This indicates that oxidizable compounds, such as cuprous ion complexes, may be the major species involved in the adsorption mechanism.

3. For copper deposition current densities of 0.25 - 3.0 A dm^{-2}, the mean occlusion rate of methionine (2.0×10^{-4} M) was roughly four times that expected from the net forward adsorption rate of 1.4×10^{-12} mole cm^{-2} s^{-1}. The approximation was made that all additive that was adsorbed

became irreversibly occluded into the electrodeposits.

4. The mean occlusion rates of methionine in the current density range, 0.25 - 6.0 A dm^{-2}, exhibited a maximum at about 5 A dm^{-2}. At this current density the overpotential was in the general vicinity of the potential of zero charge for polarized copper electrode systems. The additive adsorptivity, therefore, was interpreted to be potential-dependent during the process of concurrent deposition of copper.

5. According to occlusion measurements with various radioisotope centres, the cystine molecule was apparently occluded into deposits in a wholly stoichiometric manner. Electrolytic degradation to sulphide appeared to be improbable.

6. Radioactive cystine occluded at rates $\simeq (11 - 54) \times 10^{-12}$ mole cm^{-2} s^{-1} (calculated as cystine) for deposition current densities of 0.25 - 6.0 A dm^{-2}, respectively. This variation may be accounted for by electrochemical rate theory if cystine is assumed to be reduced rapidly and reversibly to cysteine and occluded as a cuprous complex into the electrodeposits. Similar occlusion rates were found for cystine additive from a copper sulphate

(0.5 M) electrolyte without added sulphuric acid.

7. A diffusion coefficient for cystine (1.00×10^{-3} M) at a dropping mercury electrode in 0.1 M $HClO_4$ (25°), with Triton-X100 (0.005 %) as maximum suppressor, was calculated from the Ilkovic equation to be $D = 7.9 \times 10^{-6}$ cm^2 s^{-1} (at -1.2 V vs. SCE).

8. Calculation of the electrode surface coverages, based on the amounts of additives adsorbed and occluded into the deposits, have indicated that the limiting diffusional rates for the additives were not achieved in these experiments.

9. Surface coverages were calculated from the overpotential increments, $|\Delta\eta|$, obtained in the presence of methionine and cystine additives, from application of the simple site-blocking theory. The results differed by 2 to 3 orders of magnitude from those calculated from the occlusion data, when the deposition rate of new layers was taken into account. It is suggested that profound changes in the morphologies of deposits formed in the presence of strong polarizers may cause modifications to the epitaxy or the (true) area of substrates during electrocrystallisation, and these effects may increase

quite largely the overpotential for copper ion deposition at a particular experimental current density.

10. A simple mechanism whereby pyramidal forms in metal electrodeposits may be initiated is described. Deposition at random lattice sites is assumed and pyramidal forms become possible as the current density is increased when, at a certain deposition rate, the surface diffusion processes to the monolayer-in-formation are too slow to prevent stabilisation and growth of the simplest 3-dimensional nuclei.

11. The Speakman method has been applied to determine the pK_{a3} and pK_{a4} values for several dibasic amino acids. The results obtained were: L-cystine 8.03 and 8.62; D,L-homocystine 8.09 and 8.67; D,L-lanthionine 8.01 and 8.09; and D-penicillamine disulphide 7.68 and 9.01, respectively.

12. Cu(II)-cystine complex formed at 0°C was prepared and analysed. The empirical formula was derived as $Cu(C_6H_{10}N_2S_2O_4).\frac{1}{2}H_2O$. The infrared spectrum of the complex has been recorded and given empirical assignments based on model calculations for similar metal-glycino complexes. The solid complex was postulated to contain

cis isomers from application of infrared vibrational criteria to distinguish geometrical isomers of similar bis(amino acid)-copper(II) complexes. At higher temperatures of preparation (75° - 100°), a different complex species resulted that possibly contained the chelates cysteine and cysteine sulphenic acid.

13. An unstable complex, Cu(II)-penicillamine disulphide pentahydrate was isolated and preliminary x-ray diffraction data obtained. The monoclinic cell dimensions were found to be: a = 1.551(8) nM, b = 1.994(60) nM, and c = 1.224(14) nM, β = 92°8'; $\rho_{meas.}$ = 1.54, $\rho_{calc.}$ = 1.58, z = 8, space group A2.

14. Unstable Cu(II)-penicillamine disulphide pentahydrate dehydrated to a pseudomorphic form with an empirical formula $Cu(C_{10}H_{18}N_2S_2O_4).3H_2O$ and with disorder about the c axis. The unit cell was found to be orthorhombic with: a = 1.488(36) nM, b = 1.862(80) nM, and c = 1.232(20) nM. Electron microscope photographs have revealed that the pseudomorphic form of the complex was not comprised of fibre needles comparable with those of the Cu(II)-cystine complex formed at 0°C.

BIBLIOGRAPHY

1. W.H.Safranek, "Modern Electroplating", 172 (F.A.Lowenheim, Ed.), John Wiley & Sons, Inc [1963]
2. T.E.Thorpe, "Humphry Davy", Cassell and Co. Ltd. [1896]
3. H.Jacobi, British Patent 8610 [1840]
4. H.J.Sand, Brit. Assoc. Adv. of Science, 4th. Report, 346 [1921]
5. R.C.Snowdon, Trans. Am. Electrochem. Soc. 7 143 [1905]
6. A.G.Betts, Trans. Am. Electrochem. Soc. 8 76 [1905]
7. W.Blum, Colloid Symp. Monograph, 301 [1928]
8. H.Schneider, A.J.Sukava, and W.J.Newby, J. Electrochem. Soc. 112 568 [1965]
9. A.J.Sukava, H.Schneider, D.J.McKenney, and A.T.McGregor, J. Electrochem. Soc. 112 571 [1965]
10. M.Ya.Popereka, "Internal Stresses in Electrolytically Deposited Metals", 191, transl. available from U.S. Dept. of Commerce (TT68-50634)
11. J.O'M.Bockris and A.K.N.Reddy, "Modern Electrochemistry", 1221, Plenum Press [1970]
12. E.Raub and K.Müller, "Fundamentals of Metals Deposition", 105, Elsevier Publishing Corp. [1967]
13. A.Bewick and H.R.Thirsk, "Modern Aspects of Electrochemistry, No.5", 291 (J.O'M.Bockris and B.E.Conway, Eds.),

Plenum Press [1969]

14. J.O'M.Bockris and G.A.Razumney, "Fundamental Aspects of Electrocrystallisation", Plenum Press [1967]
15. V.Klapka, Coll. Czech. Chem. Comm. 35 899 [1970]
16. Ch.Schnittler, Electrochim. Acta 13 469 [1968]
17. Z.A.Tkachik, K.M.Gorbunova, and E.S.Sevast'yanov, Sov. Electrochem. 5 319 [1969]
18. L.H.Jenkins and R.B.Durham, J. Electrochem. Soc. 117 1506 [1970]
19. O.Kardos and D.G.Foulke, "Advances in Electrochemistry and Electrochemical Engineering, vol. 2", 145 (C.W.Tobias, Ed.) Interscience Publ. [1962]
20. S.S.Kruglikov, "Electrochemistry 1965", 95, transl. available from U.S. Dept. of Commerce (TT70-50034)
21. H.Fischer, "Elektrolytische Abscheidung und Elektrokristallisation von Metallen", Springer-Verlag [1954]
22. N.Ibl, Ph.Javet, and F.Stahel, Electrochim. Acta 17 733 [1972]
23. K.J.Vetter, "Electrochemical Kinetics", Academic Press [1967]
24. B.E.Conway, "Theory and Principles of Electrode Processes", Ronald Press Co. [1965]
25. E.Gileadi (Ed.), "Electrosorption", Plenum Press [1967]
26. B.B.Damaskin, O.A.Petrii, and V.V.Batrakov, "Adsorption of Organic Compounds on Electrodes", Plenum Press [1971]

27. S.E.Beacom and B.J.Riley, J. Electrochem. Soc. 108 758 [1961]

28. A.T.Vagramyan and Z.A.Solev'ev, "Methods for Studying Electrodeposition of Metals", Moskva, Izdatel'stvo AN SSSR [1960]

29. B.Ke, J.J.Hoekstra, B.C.Sison, and D.Trivich, J. Electrochem. Soc. 106 382 [1959]

30. A.Damjanovic, M.Paunovic, and J.O'M.Bockris, J. Electroanal. Chem. 9 93 [1965]

31. E.Gileadi, L.Duic, and J.O'M.Bockris, Electrochim. Acta 13 1915 [1968]

32. G.Grube and V.Ruess, Z. Elektrochem. 27 45 [1921]

33. A.K.Graham, Trans. Am. Electrochem. Soc. 52 157 [1927]

34. H.Kersten, J. Phys. Chem. 35 3644 [1931]

35. R.Taft and H.E.Messmore, J. Phys. Chem. 35 2585 [1931]

36. P.Jacquet, Compt. rend. 194 456 [1932]

37. H.Fischer, Kolloid Z. 106 50 [1944]

38. W.H.Gauvin and C.A.Winkler, J. Electrochem. Soc. 99 447 [1952]

39. B.I.Parsons and C.A.Winkler, Can. J. Chem. 32 581 [1954]

40. Yu.V.Lyzlov, T.A.Mechkovskaya, and A.G.Samartsev, Z. Fiz. Khim. 31 2720 [1957]

41. E.A.Ollard, "Introductory Electroplating", 145, Robert Draper Ltd. [1969]

42. A.J.Sukava and C.A.Winkler, Can. J. Chem. 33 961 [1955]

43. A.Jogarao, S.Gurnviah, and K.P.Iyer, Metal Finishing 64 82 [1967]

44. R.S.Nikitina and O.A.Suvarovo, Sov. Electrochem. 3 580 [1967]

45. A.Bernotas, J.Bubelis, and J.Matulis, Mater. Respub. Konf. Elektrokhim. Litov SSR, 8th., Vilnyus, 56 [1966]

46. J.Pradac and J.Koryta, J. Electroanal. Chem. 17 167, 177, 185 [1968]

47. W.Leyko, Bull. de la Soc. des Sciences et des Lettres de Lodz, Classe III, vol. III, 14 1 [1952]

48. D.B.Cater and I.A.Silver, "Reference Electrodes", 489 (D.J.G.Ives and G.J.Janz, Eds.) Academic Press [1969]

49. H.Borsook, E.L.Ellis, and H.M.Huffman, J. Biol. Chem. 117 281 [1937]

50. P.C.Jocelyn, Eur. J. Biochem. 2 327 [1967]

51. W.Stricks and I.M.Kolthoff, J. Am. Chem. Soc. 73 1723, 1728 [1951]

52. I.R.Miller and J.Teva, J. Electroanal. Chem. 36 157 [1972]

53. R.S.Saifullin, F.I.Nadeeva, L.N.Akulolva, and E.P.Zentsova, Elektron. Obrab. Mater. 2 31 [1968]

54. S.M.Kochergin and L.L.Khonina, J. Appld. Chem. USSR 35 877 [1962]; ibid. 36 642 [1963]

55. S.Venkatachalam and C.A.Winkler, J. Electrochem. Soc. 115 591 [1968]

56. T.B.Lloyd, M.R.Lauver, and F.Hovorka, J. Electrochem.

Soc. 94 431 [1948]

57. G.Lahousse and L. Heerman, Bull. des Soc. Chim. Belges 80 125 [1971]

58. J.Llopis, J.M.Gamboa, and L.Arizmendi, C.I.T.C.E. 8th. Meeting, Madrid 1956, 123, Butterworths [1958]

59. O.Volk and H.Fischer, Electrochim. Acta 5 112 [1961]

60. S.S.Kruglikov, Yu.D.Gamburg, and N.T.Kudryavtsev, Electrochim. Acta 12 1129 [1967]

61. A.K.P.Chu and A.J.Sukava, J. Electrochem. Soc. 116 1188 [1969]

62. R.O.Loutfy and A.J.Sukava, J. Electrochem. Soc. 118 216 [1971]

63. A.Aramata and P.Delahay, J. Phys. Chem. 68 880 [1964]

64. L.L.Shreir and J.W.Smith, J. Electrochem. Soc. 99 64, 452 [1952]

65. H.Seiter, H.Fischer, and H.Albert, Electrochim. Acta 2 97 [1960]

66. H.J.Pick, G.G.Storey, and T.B.Vaughan, Electrochim. Acta 2 165 [1960]

67. S.C.Barnes, G.G.Storey, and H.J.Pick, Electrochim. Acta 2 195 [1960]

68. R.Piontelli, G.Poli, and G.Serravalle, "Transactions of the Symposium on Electrode Processes", 67 (E.Yeager, Ed.) John Wiley & Sons [1961]

69. M.Fleischmann and H.R.Thirsk, "Advances in Electro-

chemistry and Electrochemical Engineering, vol. 3", 123 (P.Delahay and C.W.Tobias, Eds.) Interscience Publ. [1963]

70. D.Shanefield and P.E.Lightly, J. Electrochem. Soc. 110 973 [1963]
71. S.C.Barnes, J. Electrochem. Soc. 111 296 [1964]
72. E.Budevski, W.Bostanoff, T.Witanoff, Z.Stoinoff, A.Kotzewa, and R.Kaishev, Electrochim. Acta 11 1697 [1966]
73. R.Kaishev and E.Budevski, Contemp. Phys. 8 489 [1967]
74. G.Eichkorn and H.Fischer, Z. phys. Chem. 61 10 [1968]
75. H.Fischer, Plating 56 1229 [1969]
76. L.H.Jenkins, J. Electrochem. Soc. 117 630 [1970]
77. H. Seiter and H.Fischer, Z. für Elektrochem. 63 249 [1959]
78. J.O'M.Bockris and A.Damjanovic, "Modern Aspects of Electrochemistry, vol. 3", 224 (J.O'M.Bockris and B.E.Conway, Eds.) Butterworths [1964]
79. M.Volmer and T.Erdey-Gruz, Z. phys. Chem. 157A 165 [1931]
80. M.Volmer, "Kinetik der Phasenbildung", (K.F.Bonhoeffer, Ed., Die Chemische Reaktion, vol. IV) Steinkopff, Leipzig [1939]
81. B.E.Conway and J.O'M.Bockris, Proc. Roy. Soc. London A248 394 [1958]; Electrochim. Acta 3 340 [1961]
82. N.A.Pangarov, J. Electroanal. Chem. 9 70 [1965]
83. R.F.Strickland-Constable, "Crystallisation", Academic Press [1968]

84. T.Hayashi, S.Higuchi, H.Kinoshita, and T.Ishida, J. Electrochem. Soc. Japan 37 64 [1969]

85. J.C.Andrews, J. Biol. Chem. 102 263 [1933]

86. P.Mader, J.Volke, and J.Kuta, Coll. Czech. Chem. Comm. 35 552 [1970]

87. F.Feigl, Anal. Chim. Acta 24 501 [1961]

88. R.E.Huber and R.S.Criddle, Arch. Biochem. Biophys. 122 164 [1967]

89. L.Meites, "Polarographic Techniques", Interscience Publ. [1965]

90. J.P.Greenstein and M.Winitz, "Chemistry of the Amino Acids", J.Wiley & Sons, Inc. [1961]

91. H.Rosen, Arch. Biochem. Biophys. 67 10 [1957]

92. G.Zweig and J.R.Whitaker, "Paper Chromatography and Electrophoresis, vol. 1", Academic Press [1967]

93. P.J.Peterson and G.W.Butler, J. Chromat. 8 70 [1962]

94. A.A.Albanese and M.Lein, Science 110 163 [1949]

95. G.Fuseya and M.Nagano, Trans. Am. Electrochem. Soc. 51 [1927]

96. E.Bertorelle, I.Bellobono, A.Scarati, and C.Bernasconi, Tech. Proc. Ann. Conv. Am. Electroplater's Soc. 46 64 [1959]

97. Ph.Javet, N.Ibl, and H.E.Hintermann, Electrochim. Acta 12 781 [1967]

98. J.K.Prall and L.L.Shreir, Trans. Inst. Met. Fin. 41 29 [1964]

99. J.Matulis and L.Valentelis, Liet. TSR Mokslu. Acad. Darbai, Ser.B, 3 17 [1957]

100. United States Patent 3,377,174 [April 9, 1968]

101. L.Mandelcorn, W.B.McConnell, W.Gauvin, and C.A.Winkler, J. Electrochem. Soc. 99 84 [1952]

102. R.C.Turner and C.A.Winkler, Can. J. Chem. 30 507 [1952]

103. V.P.Galushko and Yu.M.Loshkarev, Zh. Fiz. Khim. 39 1185 [1965]

104. M.A.Loshkarev, Yu.M.Loshkarev, A.A.Kazarov, and L.P.Snetkova, Coll. Czech. Chem. Comm. 33 486 [1968]

105. P.Rây and A.Bhaduri, J. Ind. Chem. Soc. 27 297 [1950]

106. H.Kahler, B.J.Lloyd, and M.Eden, J. Phys. Chem. 56 768 [1952]

107. C.J.Hawkins and D.D.Perrin, Inorg. Chem. 2 843 [1963]

108. J.C.Speakman, J. Chem. Soc. 855 [1940]

109. F.R.N.Gurd and P.E.Wilcox, "Advances in Protein Chemistry, vol. XI", 316 (M.L.Anson, K.Bailey, and J.T.Edsall, Eds.) Academic Press [1956]

110. T.F.Lavine, J. Biol. Chem. 117 309 [1937]

111. J.P.Danehy and W.E.Hunter, J. Org. Chem. 32 2047 [1967]

112. N.A.Rosenthal and G.Oster, J. Soc. Cosmet. Chem. 5 286 [1954]

113. R.Cecil and J.R.McPhee, Biochem. J. 66 538 [1957]

114. D.S.Tarbell and D.P.Harnish, Chem. Rev. 49 1 [1951]

115. J.Reid Shelton and K.E.Davis, J. Am. Chem. Soc. 89 718 [1967]

116. B.C.Pal, M.Uziel, D.G.Doherty, and W.E.Cohn, J. Am. Chem. Soc. 91 3634 [1969]

117. A.F.Pearlmutter and J.Stuehr, J. Am. Chem. Soc. 90 858 [1968]

118. H.C.Freeman, "The Biochemistry of Copper", 77 (J.Peisach, P.Aisen, and W.E.Blumberg, Eds.) Academic Press [1966]

119. C.J.Hawkins, "Absolute Configuration of Metal Complexes", chapt. 8, Wiley-Interscience [1971]

120. A.W.Herlinger, S.L.Wenhold, and T.V.Long, J. Am. Chem. Soc. 92 6474 [1970]

121. R.A.Condrate and K.Nakamoto, J. Chem. Phys. 42 2590 [1965]

122. M.Tsuboi, T.Takenishi, and A.Nakamura, Spectrochim. Acta 17 634 [1961]

123. D.Otto, G.Ferenc, and M.Tamas, Magyar Kémiai Folyóirat 68 1 [1962]

124. S.D.Rossouw and T.J.Wilken-Jorden, Biochem. J. 29 219 [1935]

125. J.M.Swan, Aust. J. Chem. 18 411 [1965]

126. H.Hamaguchi and Y.Kamemoto, J. Chem. Soc. Japan 81 346 [1960]

127. D.D.Perrin and I.G.Sayce, J. Chem. Soc.(A) 53 [1968]

128. H.Shindo and T.L.Brown, J. Am. Chem. Soc. 87 1904 [1965]

129. C.A.McAuliffe, J.V.Quagliano, and L.M.Vallarino, Inorg. Chem. 5 1996 [1966]

130. P.Hemmerich, 15 ref. (118)

131. G.Schwarzenbach and H.Flaschka, "Complexiometric Titrations", 256, Methuen and Co. [1969]

132. A.J.Sukava and C.A.Winkler, Can. J. Chem. 34 128 [1956]

133. D.R.Crow, "Polarography of Metal Complexes", Academic Press [1969]

134. V.N.Lebedeva, Sov. Electrochem. 3 1305 [1967]

135. G.R.Johnson and D.R.Turner, J. Electrochem. Soc. 109 798, 918 [1962]

136. I.M.Kolthoff and C.Barnum, J. Am. Chem. Soc. 63 520 [1941]

137. I.M.Kolthoff and Y.Okinaka, J. Am. Chem. Soc. 81 2296 [1959]

138. L.A.Woolf and A.W.Hoveling, J. Phys. Chem. 74 2406 [1970]

139. T.Kilner and A.Plumtree, J. Electrochem. Soc. 115 929 [1968]

140. J.Bebczuk de Cusminsky, Electrochim. Acta 15 73 [1970]

141. G.H.Gilmer and P.Bennema, J. Appld. Phys. 43 1347 [1972]

142. A.F.H.Ward and L.Tordai, J. Chem. Phys. 14 453 [1946]

143. D.Schab and K.Hein, Neue Hütte 15 461 [1970]

144. J.Stauff and F.Nimmerfall, Z. Naturforsch B 24 852 [1969]

145. J.O'M.Bockris, M.Green, and D.A.J.Swinkels, J. Electrochem. Soc. 111 743 [1964]

146. D.Armstrong, N.A.Hampson, and R.J.Latham, J. Electroanal. Chem. 23 361 [1969]

147. J.O'M.Bockris and B.E.Conway, J. Chem. Phys. 28 707 [1958]

148. N.A.Hampson and R.J.Latham, Trans. Far. Soc. 66 3131 [1970]

149. K.Ekler and C.A.Winkler, Can. J. Chem. 33 1756 [1955]

150. L.S.Goodman and A.Gilman (Eds.), "The Pharmacological Basis of Therapeutics, 4th. Edn.", The Macmillan Company [1970]

151. E.J.Kuchinskas and Y.Rosen, Arch. Biochem. Biophys. 97 370 [1962]

152. D.A.Doornbos and J.S.Faber, Pharm. Weekblad 99 289 [1964]

153. J.J.Vallon and A.Badinand, Bull. Soc. Pharm. Marseilles 15 253 [1967]

154. J.T.McCall, N.P.Goldstein, R.V.Randall, and J.B.Gross, Am. J. Med. Sci. 254 13 [1967]